SERC High Performance Computing Usage Annual Reports 2022–2024

Supercomputer Education and Research Centre
Indian Institute of Science
Bangalore - 560012

Table of Contents

1. SERC High Performance Computing (HPC) Facilities

The Supercomputer Education and Research Centre (SERC) at IISc has been at the forefront of providing high performance computing (HPC) facilities to the academic and research community of Indian Institute of Science (IISc) and beyond. SERC has been providing more than four decades of high-end computing support to the academic and research community. The Centre hosts 24/7 supercomputing facilities and services including supercomputers of Petaflop capacities for traditional HPC (High performance computing), deep learning and AI based applications, HPC software and about 4 Petabytes of storage. With *PARAM Pravega*, DGXH100, and advanced visualization resources, SERC enables researchers to perform large-scale simulations, data analysis, and AI/ML workloads.

Currently, the centre houses multiple HPC systems including **Param Pravega**, one of India's most powerful supercomputers, along with dedicated visualization and storage servers. Our Pram Pravega supercomputer system has served about 23 departments, 170 research groups and 650 users of the Institute in various fields including aerospace, astrophysics, brain research, chemistry, civil engineering, climate modelling, combustion, CFD, computational and data sciences, computer science, condensed matter physics, computational nano electronics, earth sciences, electronics system engineering, geophysics, hydrology, large eddy simulations, inorganic and physical chemistry, materials research, mechanical engineering, microbiology and cell biology, molecular biophysics, molecular dynamics, materials physics, plasma physics, process modelling, planetary sciences, quantum modelling of materials, turbulent flows, etc. In addition to IISc users, 23 research groups of 19 Institutes from outside IISc and across the country have been using Param Pravega for their research needs, making Param Pravega a truly National supercomputing installation for research. These research efforts have resulted in at least 164 publications by IISc researchers and at least 31 publications from researchers external to IISc in high impact journals. These works have also resulted in generation of software in multiple domains, and notable awards, including the prestigious ACM Gordon Bell Award in SC 2023.

The HPC infrastructure at SERC is continuously upgraded to meet the growing computational demands of the academic and research community.

Param Pravega:

Commissioned in 2022, Param Pravega is one of the fastest supercomputers in an academic Institution in India. With a peak performance of **3.3 Petaflops**, the system is built on a hybrid architecture comprising CPU and GPU nodes. The system has 428 regular nodes of 48-core Intel Xeon Cascade Lake 8268 2.9 GHz processors, for a total of 20,544 cores, with 192 GB RAM and 480 GB local SSD, 156 high-memory nodes of 48-core Intel Xeon Cascade Lake 8268 2.9 GHz processors, for a total of 7488 cores, with 768 GB RAM and 480 GB local SSD, and 40 GPU nodes with each node consisting of Intel Xeon G-6248 2.5 GHz processors and 2 Nos. of NVIDIA V100 GPUs. The system has 4 PetaBytes of usable storage space, and the

nodes are interconnected using fat-tree toplogy with a BullSequana XH200 Mellanox HDR Infiniband interconnection.

Param Pravega is extensively used for large-scale simulations, data-intensive tasks, and AI/ML applications. Researchers from IISc and collaborating institutions leverage Param Pravega for domains such as climate modeling, fluid dynamics, computational chemistry, materials science, and deep learning and others.

DGX H100 Systems:

SERC also hosts **NVIDIA DGX H100 systems**, designed specifically for Artificial Intelligence and Machine Learning research. These systems provide exceptional performance for training and inference of large-scale deep learning models. With advanced GPU architecture, high-bandwidth interconnects, and optimized AI software stacks, the DGX H100 accelerates research in areas such as natural language processing, computer vision, data analytics, and generative AI.

Visualization and Data Servers:

SERC maintains dedicated high-memory visualization servers that assist researchers in post-processing and analyzing large datasets generated by simulations. These servers provide powerful graphics capabilities and interactive environments for scientific visualization.

Storage Infrastructure:

The HPC ecosystem is supported by a robust, high-capacity storage infrastructure with petabytes of space for long-term data storage and efficient high-speed data access. This ensures seamless workflow between compute and visualization servers.

2. Usage in 2022-2024

The High-Performance Computing (HPC) facilities at SERC have witnessed extensive usage during the period **2022–2024**. Researchers from diverse departments at IISc, as well as collaborating institutions, have leveraged the **PARAM Pravega**, **DGX H100 systems**, and visualization servers for computationally intensive projects.
Over this period, the HPC systems in SERC have been used with the following statistics over 2022-24.

- More than **300 active users** from about **70 faculty groups** across IISc and collaborating institutions.
- Usage by **24 departments** spanning **6 divisions** of IISc.
- Execution of over **5,00,000 jobs** on PARAM Pravega, DGX-H100 and other systems.
- **650+ million CPU core hours and 1+ million GPU node hours**.
- Research with SERC HPC resources have yielded at least **30 PhD thesis**.
- Running **large-scale simulations** in climate science, materials discovery, fluid dynamics, and astrophysics.

- Conducting **data-intensive studies** in computational biology, genomics, and health informatics.
- Enabling **artificial intelligence and machine learning research**, including deep learning, natural language processing, and computer vision.
- Supporting **multi-disciplinary collaborations** across science, engineering, and technology domains.

The systems together supported more than **twenty-three thousand jobs each month**, with resource utilization of 92-97% at all times. Collectively, these efforts contributed to a large number of **peer-reviewed publications, doctoral theses, and collaborative projects**, underscoring the critical role of SERC's HPC ecosystem in advancing research and innovation.

Following are the various domain areas of research carried out on Param Pravega.

1. Aerospace Engineering
2. Astrophysics
3. Chemical Engineering
4. Civil Engineering
5. Climate Change
6. Combustion
7. Computational Fluid Dynamics
8. Computational Fluid-Structure Interactions
9. Computational Materials Science
10. Condensed Matter Physics
11. Computational Nanoelectronics
12. Data-driven methods
13. Earth Sciences
14. Geophysics
15. Hydrology
16. Large Eddy Simulations
17. Materials Engineering
18. Materials Physics
19. Mathematical models for cardiac tissue
20. Membrane Biophysics, Protien-Membrane Interactions, Membrane Assisted Protein Folding
21. Molecular dynamics
22. Ocean Modeling
23. Plasma Physics
24. Process Modeling
25. Planetary Science
26. Quantum Modeling of Materials
27. Turbulent Flows

Number of Users			
	2022	**2023**	**2024**
DGX-1	23	23	15
DGX H100	-	-	19
RNC	140	116	104
Param Pravega	Not available	Not available	258
Total	158	132	318

Number of Faculty Groups			
	2022	**2023**	**2024**
DGX-1	14	13	11
DGX H100	-	-	11
RNC	47	44	41
Param Pravega	Not available	Not available	68
Total	56	52	88

Total Number of Jobs				
	2022	**2023**	**2024**	**Total**
DGX-1	3,239	2,942	1,375	7,556
DGX H100	-	-	2,505	2,505
RNC	80,045	61,997	204,343	346,385
Param Pravega	36,845	51,582	71,425	159,852
Total	120,129	116,521	279,648	516,298

CPU and GPU Job Share (%)						
	2022		**2023**		**2024**	
	CPU	**GPU**	**CPU**	**GPU**	**CPU**	**GPU**
DGX-1	0.00%	100.00%	0.00%	100.00%	0.00%	100.00%
DGX H100	-	-	-	-	0.00%	100.00%
RNC	94.61%	5.39%	93.19%	6.81%	95.04%	4.96%
Param Pravega	Not Available	Not Available	Not Available	Not Available	83.26%	16.74%

Number of CPU Core Hours				
	2022	**2023**	**2024**	**Total**
DGX-1	0.00	0.00	0.00	0.00
DGX H100	-	-	0.00	0.00
RNC	12,653,148.44	14,576,054.29	12,684,415.41	39,913,618.14
Param Pravega	212,135,407.20	217,968,217.00	194,390,875.52	624,494,499.72
Total	224,788,555.64	232,544,271.29	207,075,290.93	664,408,117.86

Number of GPU Node hours				
	2022	**2023**	**2024**	**Total**
DGX-1	34,347.53	40,968.72	16,554.36	91,870.61
DGX H100	-	-	9,500.43	9,500.43
RNC	39,139.82	38,475.92	23,893.87	101,509.61
Param Pravega	385,672.60	517,609.00	491,925.85	1,395,207.45
Total	459,159.95	597,053.63	541,874.50	1,598,088.09

Following departments in IISc use Param Pravega.

1. Aerospace Engineering
2. Biochemistry
3. Center for Atmospheric and Oceanic Sciences
4. Center for Brain Research
5. Center for infrastructure, Sustainable Transportation & Urban Planning
6. Centre for Nanoscience Engineering
7. Chemical Engineering
8. Civil Engineering
9. Computational and Data Sciences
10. Computer Science and Automation
11. Earth Sciences
12. Electrical Engineering
13. Electronics and Communications Engineering
14. Electronics Systems Engineering
15. Inorganic and Physical Chemistry
16. Interdisciplinary Center for Water Research
17. Materials Engineering
18. Materials Research Centre
19. Mechanical Engineering
20. Molecular Biophysics Unit

21. Organic Chemistry
22. Robert Bosh Centre for Cyberphysical Systems
23. Solid State and Structural Chemistry Unit

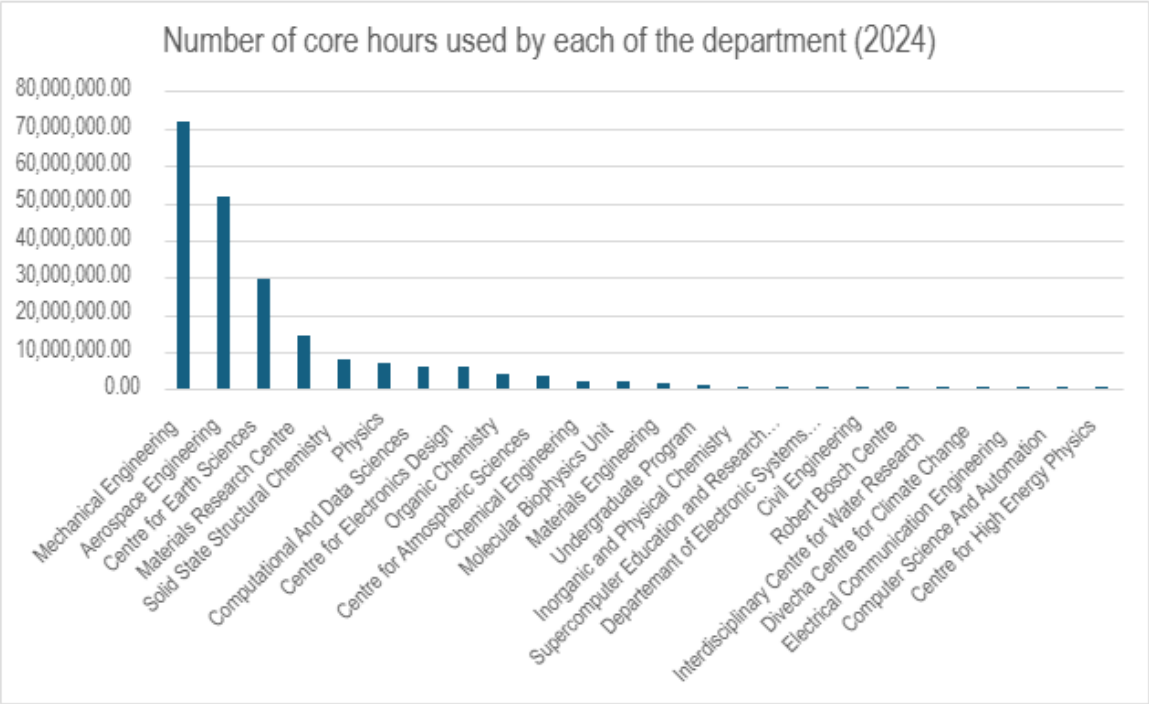

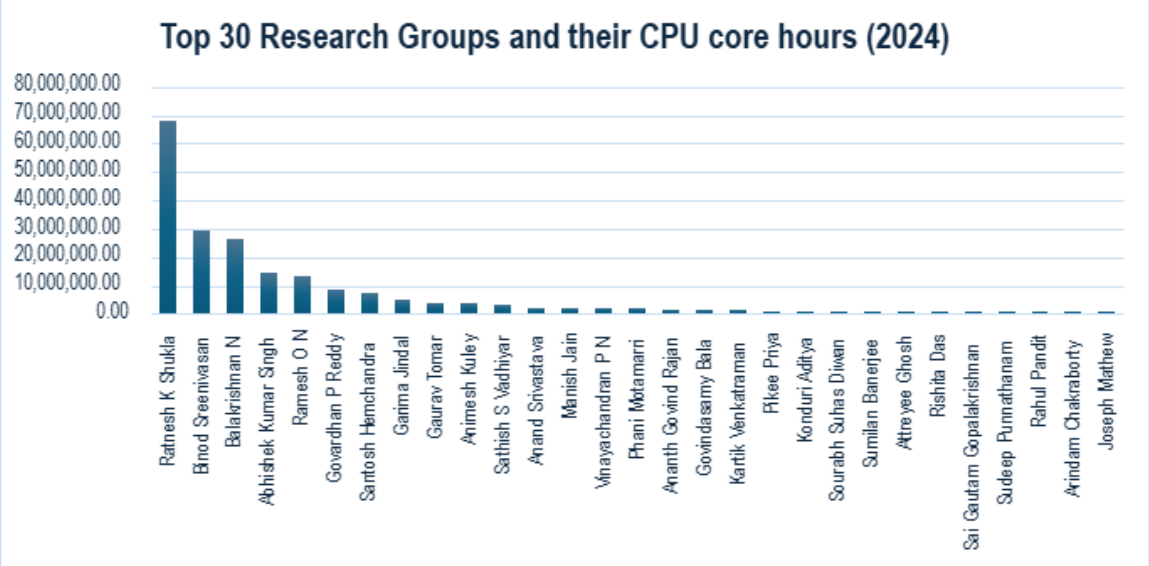

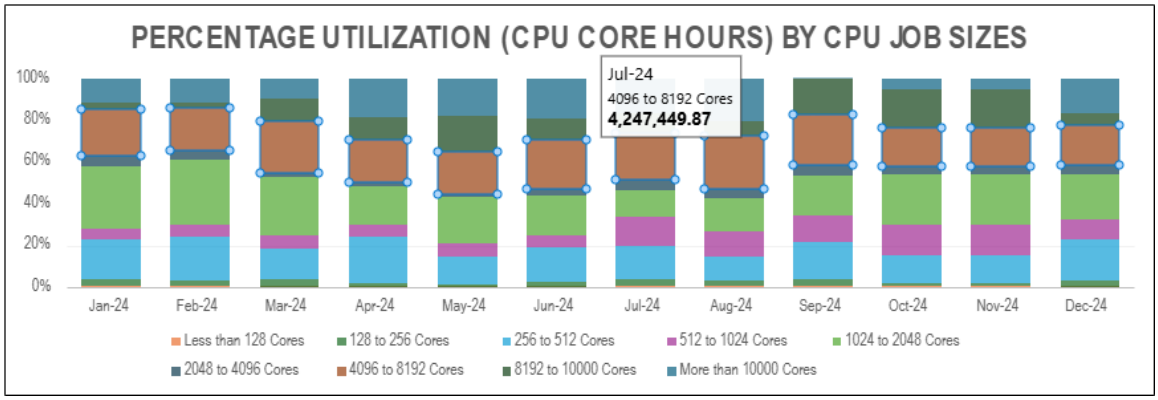

3. IISc's Scientific Applications on SERC HPC Usage

During **2022–2024**, the HPC facilities at SERC were extensively utilized by researchers across IISc for a wide range of **scientific and engineering applications**. The availability of PARAM Pravega, DGX H100 systems, visualization platforms, and large-scale storage enabled projects requiring **massive computational power and data handling capabilities**.

The applications broadly covered:

- **Climate science and Earth system modeling** – long-term simulations of climate variability, monsoon predictability, carbon cycle feedbacks, and ocean–atmosphere interactions.
- **Aerospace and mechanical engineering** – high-fidelity simulations of turbulence, combustion, aerodynamics, and propulsion systems.
- **Materials science and chemistry** – density functional theory (DFT) calculations, molecular dynamics, phase transition studies, and nanomaterials research.
- **Computational biology and life sciences** – biomolecular simulations, genomics, protein folding, and drug discovery applications using GPU-accelerated codes.
- **Physics and astrophysics** – plasma turbulence, galaxy formation, black hole accretion models, and geodynamo simulations.
- **Artificial intelligence and machine learning** – training of large language models, deep learning for computer vision and NLP, generative AI, and data-intensive analytics on DGX H100 systems.

These diverse applications underscore the **central role of SERC's HPC ecosystem** in enabling IISc's research community to address grand scientific challenges, produce high-impact publications, and contribute to national and global scientific progress.

The following sections give details of the usage of **HPC** for various computational science problems.

3.1 Department of Aerospace Engineering (AE)

3.1.1 Prof. Joseph Mathew's Lab

3.1.1.1 Problem areas:

The evolution of isolated and collections of hairpin vortices are studied using Direct Numerical Simulation (DNS) for a Reynolds number of 1500. The multiple hairpin vortices are arranged on a circle. This configuration is a simplified model to understand late stages of transition in round jets as multiple hairpins are ejected in the wake of an unstable vortex ring during transition. The evolution shows that a process called viscous vortex reconnection occurs and for capturing this grids of sizes up to 210 million were used. Depending upon the vorticity directions, we see complex interactions with neighbouring hairpins leading to a series of reconnections and formation of smaller scales. Simulations were performed using Incompact3d, an open source parallelized incompressible Navier-Stokes equation solver. For computing spatial derivatives sixth order compact finite differences are used, while for time marching third-order Runge-Kutta method is used.

3.1.1.2 SERC's resources:

These simulations were performed on Param Pravega. For a single run 480 CPU cores were used for 12-24 hours depending on the evolution time.

3.1.1.3 Parallelization strategies employed:

Incompact 3d uses a 2D pencil decomposition of the computational domain and for this it uses the open source 2DECOMP&FFT library. The communication between different parts of the domain residing in different cores is achieved through MPI. This makes the code highly scalable and it is shown that the core can run on O(10^5) cores.

3.1.1.4 Performance and scalability:

Scalability analysis for Incompact3d are documented in these papers

1. Laizet S. & Li N., Incompact3d, a powerful tool to tackle turbulence problems with up to 0(10^5) computational cores, Int. J. of Numerical Methods in Fluids, Vol 67-11, pp 1735-1757, 2011.
2. Li N. & Laizet S., 2DECOMP&FFT - a highly scalable 2D decomposi on library and FFT interface, Cray User Group meeting: Simulation comes of age, Edinburgh, Scotland -- 24/05-27/05, 2010.

3.1.1.5 Publications:

1. Balakrishna, N., Mathew, J., & Samanta, A. On late stages of transition in round jets, 12th International Symposium on Turbulence and Shear Flow Phenomena (TSFP12), July 19–22, 2022; Osaka, Japan.
2. Balakrishna, N., Mathew, J., & Samanta, A. (2025). Reconnections of isolated and interacting hairpin vortices, J. Fluid Mech. (under review).

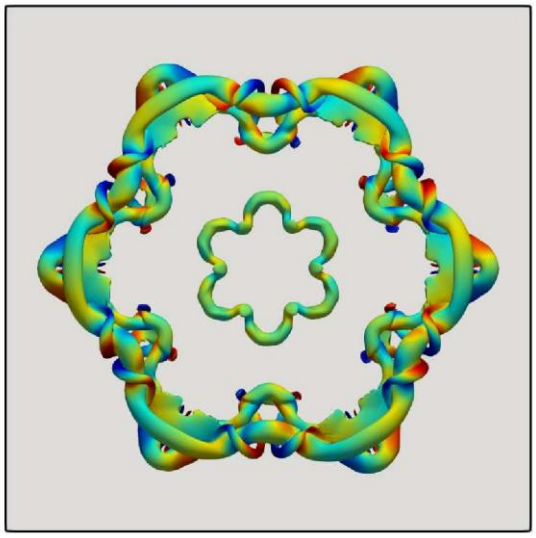

Figure1: *HairpinVortex1*

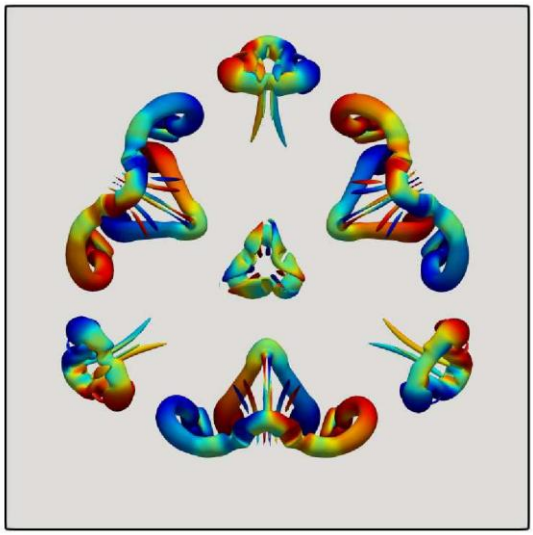

Figure2: *HairpinVortex1*

3.1.2 Prof. Kartik Venkatraman's Lab

3.1.2.1 Problem Areas:

Horizontal and vertical tail buffeting of a trapezoidal planform in a transonic flow

In modern high-performance combat aircraft, the sizing and placement of the vertical and horizontal tail is critical, especially in twin-tail configurations. The vertical tail is subjected to the effects of unsteady aerodynamic flow and gives rise to buffeting and flutter. At moderate angle of attack the strong energized vortex generated on the suction side surface breaks down into smaller eddies. These turbulent vortical structures then impinge upon the aft horizontal and vertical aerodynamic surfaces, such as the horizontal and vertical tail. Transonic flow over the vertical and horizontal tail, including the influence of the elastodynamics of the wing, nose, forward sweep intake, and fuselage, is investigated using an Unsteady Reynolds-Averaged Navier–Stokes (URANS) solver tightly coupled with a finite element solver for both steady and unsteady flows over over a flat plate model of a trapezoidal wing aircraft planform with vertical and horizontal tail at a moderate angle-of-attack. This study clearly shows that flexible aircraft structure elastodynamics to have significant effect on the unsteady flow over the aircraft when compared to that of a rigid aircraft.

All simulations were done on Param Pravega using approximately 500-700 cores.

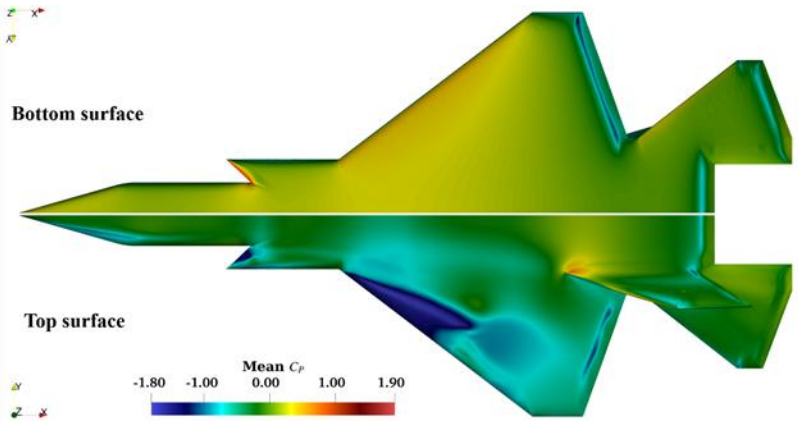

Fig. Full flexible aircraft mean C_P top and bottom surface

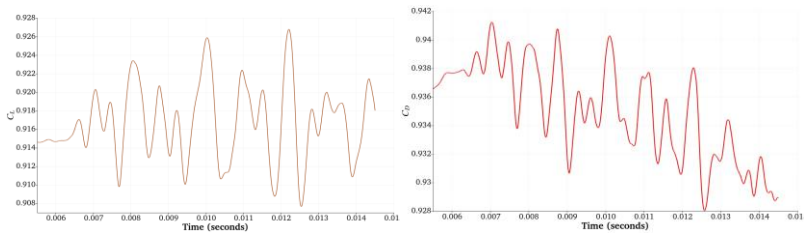

Fig. Temporal lift and drag variation on the flexible aircraft

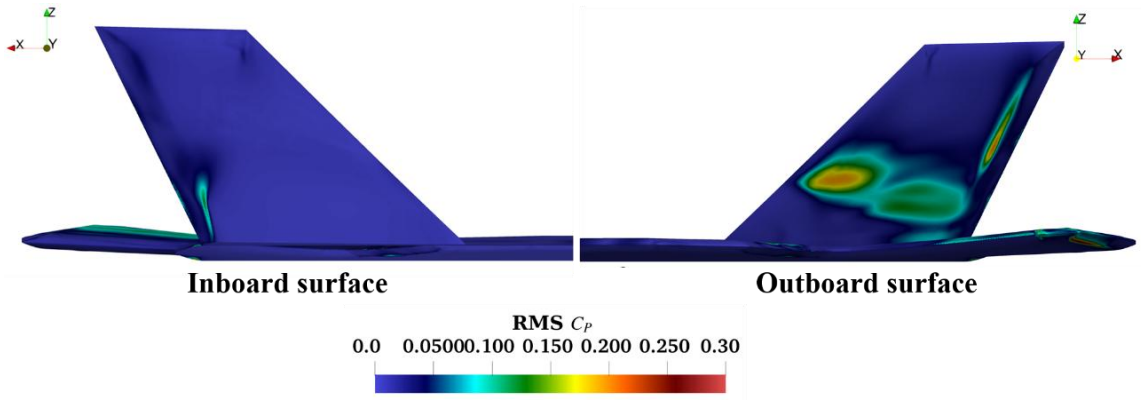

Fig. *RMS coefficient of pressure on the flexible vertical tail*

Transonic shock buffet in an axial flow fan

Transonic shock buffet, a self-sustained shock oscillation resulting from shock-boundary layer interaction, is observed across a range of operating points on the performance map of

a transonic axial flow fan. Shock oscillations impart time-varying air loads on fan blades with the potential of leading to fatigue-induced structural failure. Accurate estimations of shock buffet onset, shock displacement, and buffet frequency are critical to lifing assessment of turbomachinery blades. This study focuses on predicting transonic shock buffet in a transonic axial flow fan using high-fidelity numerical simulations, followed by investigation of its underlying mechanisms through wave propagation analysis and modal analysis of buffet flow. Steady flow solutions obtained using a RANS solver predict performance characteristics and capture key features of the fan's shock structure in conformation with experimental and numerical results from the literature. Unsteady flow simulations on a full-annulus model using URANS successfully capture shock buffet and its salient attributes at two operating points—near design mass flow and near stall. Wave propagation analysis and spectral proper orthogonal decomposition of buffet flow reveal a feedback loop of upstream and downstream propagating pressure perturbation waves driving shock buffet. A subtle modification to Lee's buffet model is proposed for accurately predicting buffet frequency in a turbomachinery context. Buffet flow is characterized by circumferential, radial, and stream-wise pressure perturbation waves, with circumferential flow periodicity breaking down during buffet. A global stability analysis framework is presented and its prognostic potential for predicting shock buffet in turbomachinery is evaluated. The global stability analysis framework enables accurate prediction of buffet frequencies and associated modes with drastically reduced computational cost compared to that required for unsteady simulations.

Simulations on Param Pravega. URANS typically on 250-500 cores and 16.5 days wall clock time. Global stability analysis on approximately 750 high memory cores and 3 hours of wall clock time.

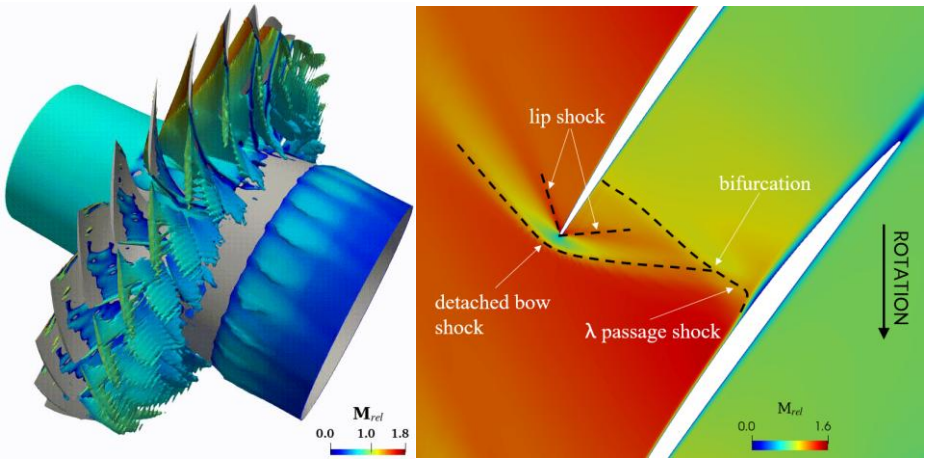

Fig. URANS simulation showing iso-surface of Q-criterion. Shock structure at 70% span across blade passage.

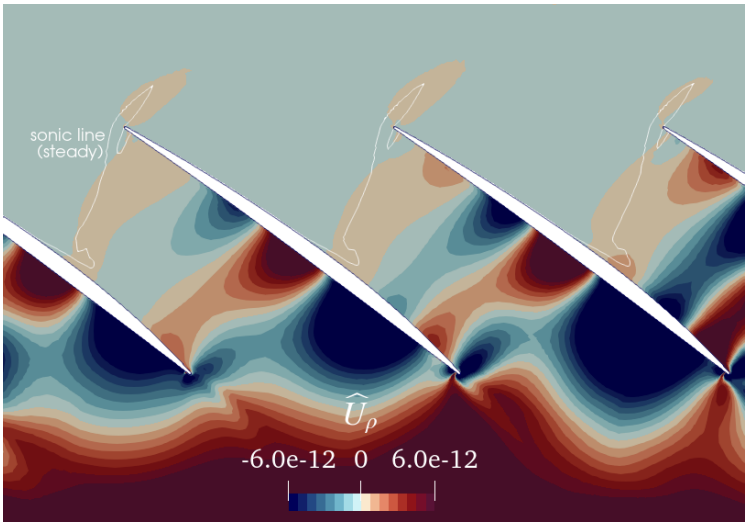

Fig. Unstable global mode at 70% span obtained from global stability analysis

3.1.2.2 SERC's Resources Used*:*

Param Pravega: URANS simulations on ~250–700 cores; global stability analysis on 750 high-memory cores.

3.1.2.3 Parallelization Strategies:

- Domain decomposition–based parallelization of URANS solvers.
- Coupling of CFD (URANS/RANS) with finite element solvers for elastodynamics.
- Global stability analysis frameworks implemented on high-memory nodes.

3.1.2.4 Performance & Scalability*:*

- URANS simulations ran up to **16.5 days wall clock time on 250–500 cores**.
- Global stability analysis achieved **3-hour turnaround on 750 cores**, offering drastic savings compared to full URANS runs.
- Demonstrated good scaling for aeroelastic and turbomachinery cases compared to experimental/numerical benchmarks.

3.1.2.5 Publications:

1. M I Vellaisamy Dinu, Adithya Udupa, Sudha U P V, and Kartik Venkatraman. 2025. Horizontal and vertical tail buffeting of a trapezoidal planform in a transonic flow. Aeronautical Society of India 26th Annual CFD Symposium 2025. August 11th -13th.
2. Jyoti Ranjan Majhi, Magan Singh, and Kartik Venkatraman (2024). Prediction of transonic buffet in a finite span wing using global stability analysis. In Second Buffet Workshop. JAXA Chofu Aerospace Center. August 30, 2024.
3. Jyoti Ranjan Majhi and Kartik Venkatraman (2024). Prediction of transonic buffet in an axial flow fan using global stability analysis. In International Forum on Aeroelasticity and Structural Dynamics 2024 (IFASD 2024). Den Haag, Netherlands. June 18-20, 2024.
4. Jyoti Ranjan Majhi and Kartik Venkatraman (2023). On the nature of transonic shock buffet in an axial flow fan. In: *AIAA Journal,* 2023.

5. Jyoti Ranjan Majhi and Kartik Venkatraman (2023). Numerical simulation of transonic buffet in an axial flow fan. In: *2023 AIAA Aviation Forum and Exposition*, San Diego, USA, June 12-16, 2023.
6. Jyoti Ranjan Majhi and Kartik Venkatraman (2023). Prediction and characterization of transonic buffet in an axial flow fan. In: *57th 3AF International Conference (AERO2023)*, Bordeaux, France, March 29-31, 2023.
7. Magan Singh and Kartik Venkatraman (2024). Transonic shock oscillations in an oscillating finite span wing. In International Forum on Aeroelasticity and Structural Dynamics 2024 (IFASD 2024). Den Haag, Netherlands. June 18-20, 2024.
8. Pawel Chwalowski, Garrett McHugh, Steven Massey, Lior Poplingher, Daniella E. Raveh, Adam Jirasek, Nicholas F. Giannelis, Kartik Venkatraman, Magan Singh, Behzad Ahrabi and Moeljo Hong (2023). Shock-Buffet Prediction Report in Support of the High Angle Working Group at the Third Aeroelastic Prediction Workshop. In: 2024 AIAA SciTech Forum, Orlando, FL, USA, January 8-12, 2024.
9. Magan Singh and Kartik Venkatraman (2023). The influence of angle of attack on the nature of transonic shock buffet in a finite span wing. In: 57th 3AF International Conference (AERO2023), Bordeaux, France, March 29-31, 2023.
10. Magan Singh and Kartik Venkatraman (2023). Transonic buffet in the Benchmark Supercritical Wing. In: 2023 AIAA SciTech Forum, National Harbor, MD, USA, January 23-27, 2023.
11. Arif Md, Magan Singh, Tumkur Pradeepa Karnick and Kartik Venkatraman (2023). Two-dimensional transonic buffet in a supercritical wing section. In: 2023 AIAA SciTech Forum, National Harbor, MD, USA, January 23-27, 2023.
12. Magan Singh, Tumkur Pradeepa Karnick and Kartik Venkatraman (2022). Transonic buffet in the finite span Benchmark Supercritical Wing (BSCW). In: 2022 AIAA Aviation Forum, Chicago, IL, June 27 - July 1, 2022.
13. Adithya Mayya, Magan Singh, and Kartik Venkatraman (2023). Transonic shock vortex shock boundary layer interactions over a delta wing. In: 57th 3AF International Conference (AERO2023), Bordeaux, France, March 29-31, 2023.
14. Adithya Mayya, Tumkur Pradeepa Karnick and Kartik Venkatraman (2022). Shock vortex interactions and transonic buffet over a flexible delta wing. In: 2022 AIAA Aviation Forum, Chicago, IL, June 27-July 1, 2022.

3.1.3 Prof. O. N. Ramesh' Lab

3.1.3.1 HPC-based Transonic Flow Research Group

3.1.3.1.1 Problem Areas:

This research focuses on the numerical investigation of transonic shock–boundary layer interaction over an axisymmetric hump geometry, which serves as a benchmark case for studying shock-induced separation. The work involved unsteady Reynolds-Averaged Navier–Stokes (URANS) and Detached Eddy Simulation (DES) based approaches to predict shock location, strength, and separation bubble characteristics. These computations helped in understanding the dynamics of unsteady shock motions and their effect on separation

bubble growth/shrinkage, which are critical for aerospace vehicle design at transonic Mach numbers.

3.1.3.1.2 SERC's Resources:

All computations were carried out on Parampravega (Large/Medium category) at SERC. A typical run utilized 340/170 nodes (Large/Med) for ~ 72 to 96 hours to resolve the unsteady flow features in DES/URANS simulations of the transonic hump.

3.1.3.1.3 Parallelization Strategies Employed:

The flow solver (HiFUN) was run in a hybrid MPI + OpenMP parallel environment. Domain decomposition was used to distribute the computational grid among MPI ranks, while OpenMP threading was employed within each node to maximize CPU utilization and reduce communication overhead.

3.1.3.1.4 Performance and Scalability:

The solver demonstrated near-linear scaling up to ~7000 cores for grids of O(50M) cells, with ~80% parallel efficiency. Compared to smaller in-house clusters, the SERC runs reduced turnaround time from weeks to days, making long-time unsteady simulations feasible.

3.1.3.1.5 Publications / Conference Participation:

1. Computational Predictions of Transonic Shock-Induced Flow Separation over Sandia Axisymmetric Hump, Symposium on Applied Aerodynamics and Design of Aerospace Vehicles (SAROD 2022), Dec 15–17, 2022, Hyderabad, India.
2. RANS Predictions of Transonic Shock-Induced Flow Separation over Sandia Axisymmetric Hump, 57th 3AF International Conference on Applied Aerodynamics, March 29–31, 2023, Bordeaux, France.
3. RANS and DES Predictions of Transonic Shock-Induced Flow Separation over Sandia Axisymmetric Hump, Asian Computational Fluid Dynamics Conference, Nov 2023, HAL Management Academy, Bengaluru, India.

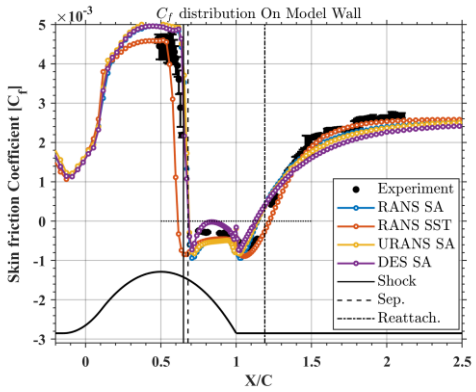

Fig- 1 Skin friction coeff't over the transonic hump.

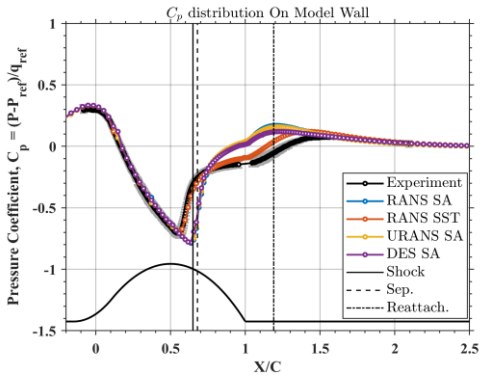

Fig- 2 Pressure coeff't over the transonic hump.

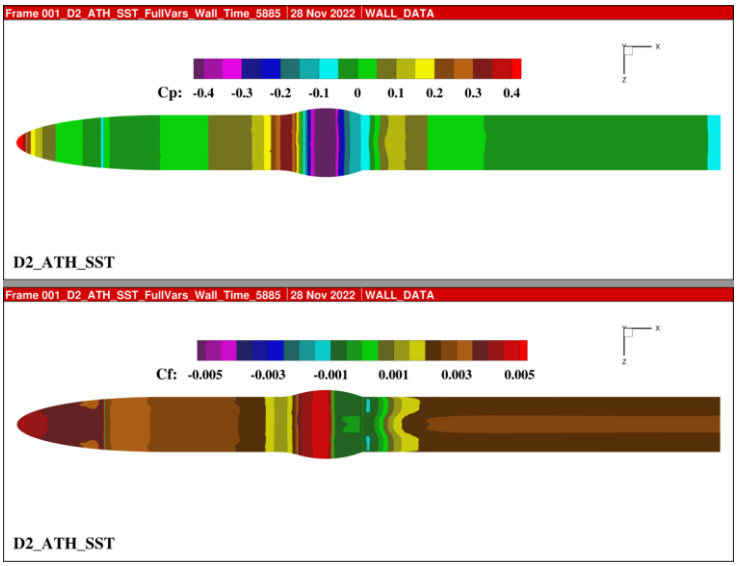

Figure 3 Geometry of the hump with skin friction and pressure coefficient.

3.1.3.2 HPC Research Report – Low Speed Aerodynamics Lab

3.1.3.2.1 Problem areas:

Wall-bounded Turbulence Research: This work is towards solving longstanding, unresolved problems in wall-bounded turbulent flows. Problems such as the scaling laws governing Very Large Scale Motions (VLSMs) and the "bursting" phenomenon—key components of turbulence production have been investigated. Understanding these is critical for applications like turbulence management and drag reduction. Direct Numerical Simulations (DNS) are performed for turbulent channel flow (TCF) using SERC's *Param Pravega* HPC facility to completely capture and resolve all scales of the flow, making such simulations computationally highly intensive. This is used to support the experimental data to establish the universality of the developed scalings.

3.1.3.2.2 SERC's resources:

This work uses SERC's Param Pravega supercomputers with jobs that involve up to small 72 cores at a frequency of 2 jobs/month. The frequency of usage is much higher when using smaller cores due to faster turn around times.

3.1.3.2.3 Parallelization strategies employed:

The open source code Incompact3d is employed in performing the DNS. A parallelisation strategy evolving from a 1D dual domain decomposition to a more advanced 2D "pencil" decomposition is employed. Both methods use MPI and global transpose operations to handle implicit high-order schemes.

3.1.3.2.4 Performance and scalability:

Excellent strong and weak scaling is achieved. The initial 1D decomposition scales well to 1024 cores, while the 2D "pencil" strategy scales acceptably up to $O(10^5)$ cores.

3.1.3.2.5 Publications:

1. Raghuram, S., & Ramesh, O. N. (2025). Bursting phenomenon in turbulent wall-bounded flows. *Physics of Fluids*, *37*(2).
2. "*Large Scale Motion in a Turbulent Channel Flow*" to be submitted to *Physical Review Letters* shortly.

Wall-bounded Turbulence Research:

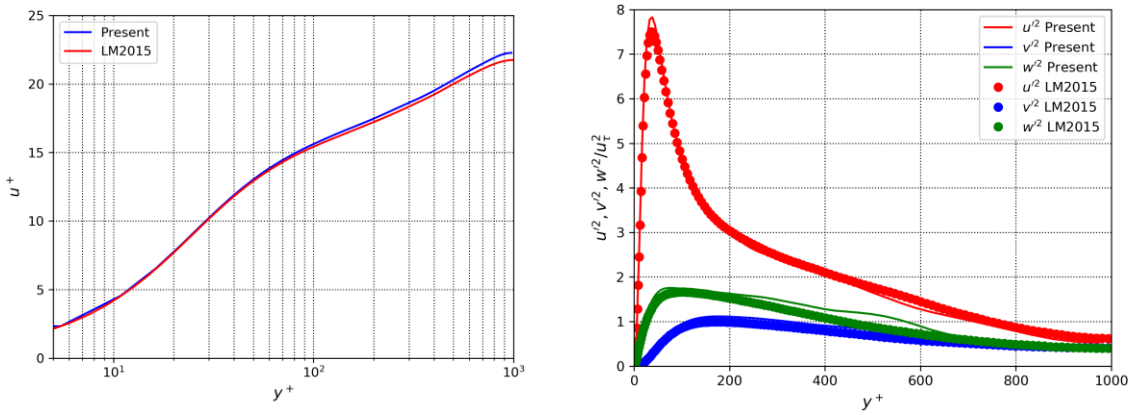

Fig. *Validation of mean velocity and turbulence intensities obtained from current DNS with renowned DNS data from literature.*

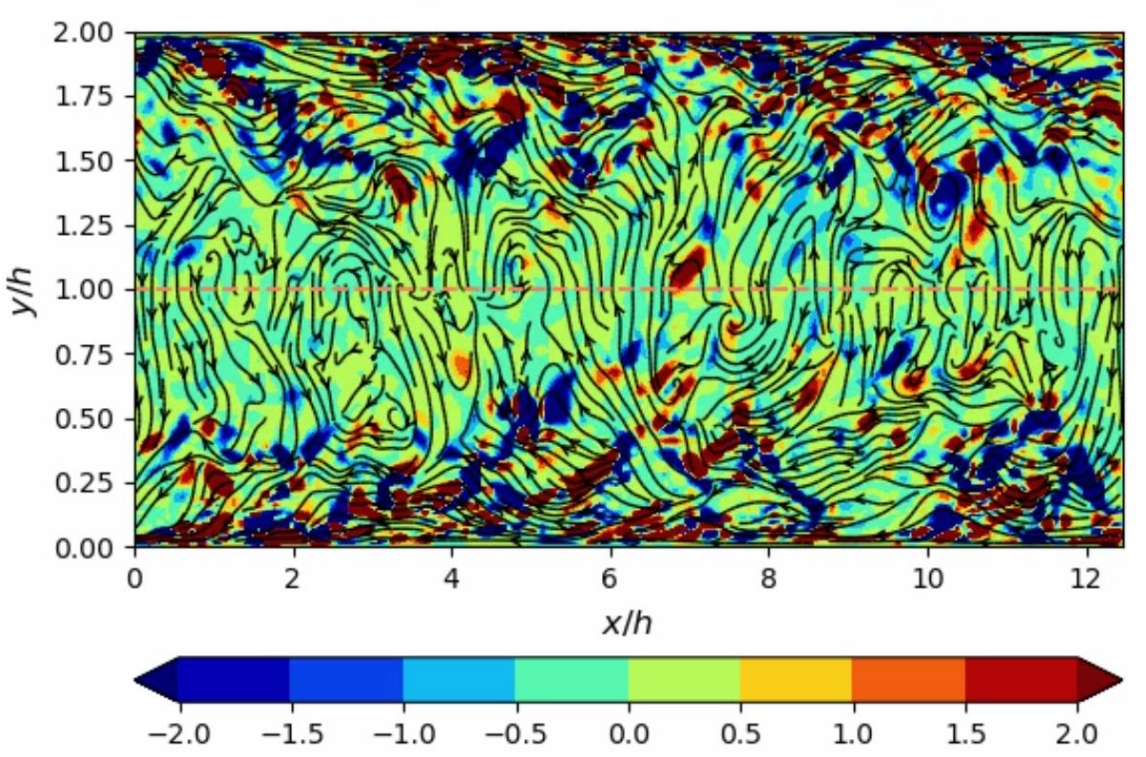

Fig. *Turbulence Production contours in a TCF along with streamlines (referenced with respect to the centerline), showing large scale correlated activity, computed using DNS.*

3.1.4 Prof. Rishita Das' Lab

3.1.4.1 Problem areas:

We have used Param Pravega supercomputer to run large-eddy simulations (LES) and direct numerical simulations (DNS) of different types of turbulent flows. Specifically, we are studying the following flow problems:

1. Supersonic turbulent boundary layer and interaction between an impinging oblique shock wave and the turbulent boundary layer.
2. Hypersonic flow through scramjet intake of ISRO.
3. Incompressible turbulent channel flow and near-wall drag-inducing coherent structures.
4. Incompressible isotropic turbulent flow and the quantification of turbulence intermittency.
5. Identifying source of jet noise in a supersonic jet.
6. Additionally, we have also used the GPUs on NVIDIA DGX-1 and NVIDIA DGX-H100 clusters to train AI/ML models for synthetic turbulent inflow generation, super-resolution and reconstruction of small scale dynamics of turbulence.

3.1.4.2 SERC's resources:

SERC resources were used for running these simulations as well as for postprocessing and data analysis with large DNS datasets. Typically, LES and DNS simulations are conducted using 40-50 nodes (1920-2400 cores) over long durations. Machine learning models for turbulence are trained using 1-2 H100 GPU cards at a time.

3.1.4.3 Parallelization strategies employed:

All our CPU codes are MPI-parallelized.

3.1.4.4 Publications:

1. Vempati, C., Thazhathattil, V., Das, R., & Hemchandra, S. (2024). Identifying noise source regions in a supersonic jet using information flux methods. In *30th AIAA/CEAS Aeroacoustics Conference (2024)* (p. 3259).

ISRO-IISc STC project on shock-wave turbulent boundary layer interaction and study of hypersonic flow through scramjet intake. Our simulations are helping understand the flow separation and unsteady characteristics of shock waves in a scramjet intake.

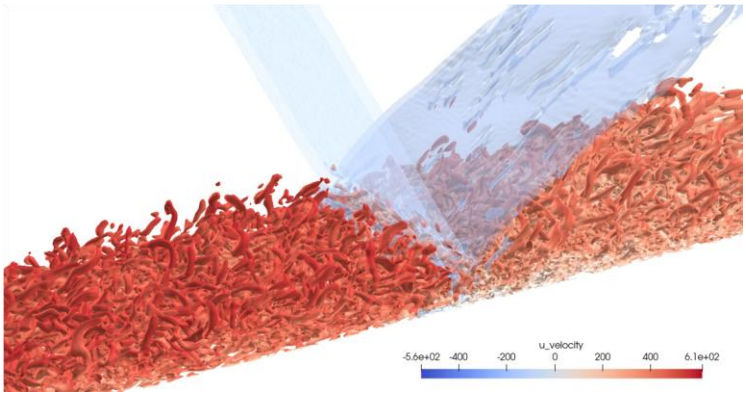

Fig1: *shock-wave turbulent boundary layer interaction*

3.1.5 Prof. Santosh Hemchandra's Lab

3.1.5.1 Problem Description:

Param Pravega was used for three main problems.

- Aeroacoustic noise radiation from a high Mach number (M=3.0) turbulent jet (Re ~ 7.5 million). This was a pilot study suggested by VSSC as being relevant for a computation they had in mind of relevance to the Gaganyaan program. We were successful in matching experimental noise measurements. New information theory based analysis was applied to understand where the source of the noise was. These results were presented at the AIAA Aeroacoustics conference, 2024 in Rome.
- A lifted turbulent slot jet H2 flame (Re ~ 8000). PARAM Pravega was used to test a new multi-regime combustion model for LES and understand autoignition propensity. Reference results were computed using DNS. Results were presented at the Asia-pacific symposium on combustion and a paper is under preparation for publication
- Critical regions in swirl nozzles. LES was used to understand the position and extent of critical regions driving precessing vortex core instability in a swirl nozzle flow (Re ~ 20,000) typically found in aeroengine combustors and gas turbines. Network analysis was performed and results were compared with linear stability showing good agreement. A similar study was performed on a related nozzle with different geometry at Re ~ 27,000. These studies have appeared in various conference and journal papers.

3.1.5.2 HPC resources used:

Param Pravega at SERC, IISc. Upto 2600-16000 cores CPU only.

3.1.5.3 Parallelization strategies:

Our LES flow solver uses MPI for parallelization on CPU only architectures. The inter node communication is performed largely in a non-blocking manner to achieve overlapping of communication and computation. Good linear scaling on problems of the size mentioned above has been observed. We are happy with the performance. However no other data is available for comparison.

3.1.5.4 Publications:

3.1.5.4.1 Conference papers:

1. Datta, A and Hemchandra, S, “A multi-regime combustion model for explicit filtering LES - Turbulent lifted hydrogen jet flame”, Asia-pacific symposium on combustion, 2025
2. Gupta, S., Datta, A., Hemchandra, S., & Boxx, I. (2023, June). Precessing vortex core suppression in a swirl stabilized combustor with hydrogen addition. In *Turbo Expo: Power for Land, Sea, and Air* (Vol. 86953, p. V03AT04A002). American Society of Mechanical Engineers.
3. Hemchandra, S., Datta, A., & Juniper, M. P. (2023, June). Learning RANS model parameters from LES using bayesian inference. In *Turbo Expo: Power for Land, Sea, and Air* (Vol. 86953, p. V03AT04A051). American Society of Mechanical Engineers.
4. Vempati, C., Thazhathattil, V., Das, R., & Hemchandra, S. (2024). Identifying noise source regions in a supersonic jet using information flux methods. In *30th AIAA/CEAS Aeroacoustics Conference (2024)* (p. 3259).

3.1.5.4.2 Journal papers:

1. Muthichur, N., Vempati, C., Hemchandra, S., & Samanta, A. (2023). Reduced-order models of aeroacoustic sources for sound radiated in twin subsonic jets. *Journal of Fluid Mechanics*, *972*, A33.
2. **Invited paper)** Muthichur, N., Vempati, S., Hemchandra, S. and Samanta, A, “An acoustically tuned spectral proper orthogonal decomposition”, *International journal of aeroacoustics,* (accepted)
3. Gupta, S., Shangbhogue, S., Ghoniem, A. and Hemchandra, S, “Self-excited flow instabilities in a swirl nozzle: passive control and intermittent dynamics”, *Journal of fluid mechanics*, (under revision).
4. Thazhathattil, V., Gupta, S. and Hemchandra, S., “Identification of wavemaker region in swirling flows using complex network analysis.”, *AIAA Journal*, https://doi.org/10.2514/1.J064066.
5. Datta, A., Mathew, J. and Hemchandra, S., “The explicit filtering method for large eddy simulations of a turbulent premixed flame”, *Combustion and flame,* 2022, vol. 237, https://doi.org/10.1016/j.combustflame.2021.111862.

Noise radiation from a Re ~ 7.5 million, M=3.0, perfectly expanded jet

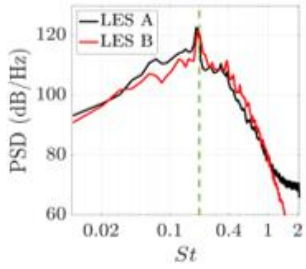

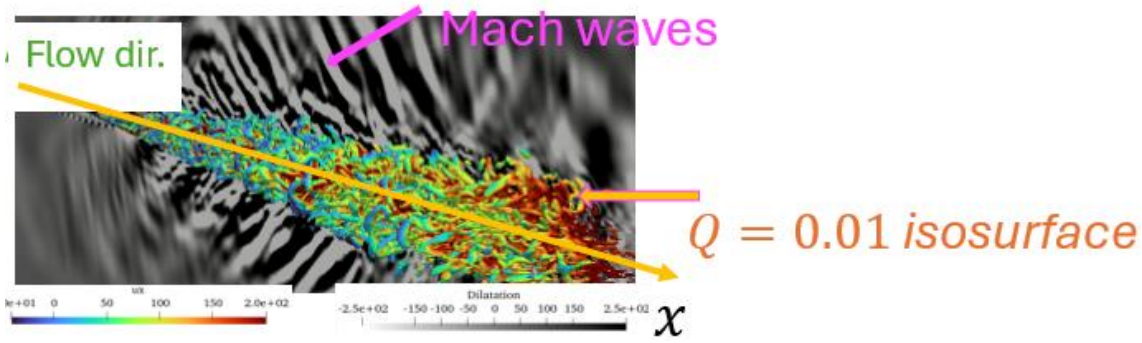

Lifted H2 slot jet flame (Re ~ 8000) DNS(left) and LES(right). Also shown are HO2 isosurface (green) and OH isosurface (orange). The turbulent structures are shown using isosurfaces of Q-criterion.

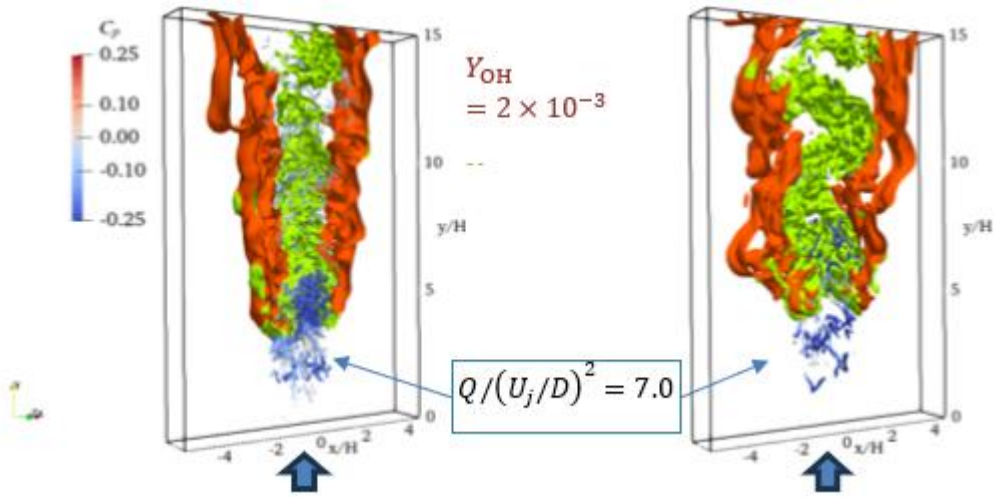

3.1.6 Prof Sourabh S. Diwan's Lab

3.1.6.1 Research area: DNS of Energy Cascade in Channel Flow

3.1.6.1.1 Problem areas:

Direct Numerical Simulation of a Turbulent Channel Flow at friction Reynolds numbers of $Re\tau$=530 and 1520 were performed using SERC HPC facilities. This data, along with open-source DNS data at $Re\tau$=550,950,2000 and 4000, is used to study the transfer of energy and enstrophy from the large scales of the flow to the smallest dissipative scales. The locality of scale interactions is validated in the physical space for a wall-bounded flow. The effect of shear, inhomogeneity and Reynolds number on the degree of locality is characterized. Further, the alignment behaviour of vorticity with the eigen strains of larger structures is also studied. The nature of stretching effects the morphology of structures, which is characterized using Minkowski function. Majority of the HPC usage is towards post-processing of the data.

3.1.6.1.2 SERC's Resources Used:

Param Pravega has been used. For large DNS simulation at $Re\tau$=1520, 2304 cores were used. Post-processing open-source data at $Re\tau$=4000 was the most resource-intensive and needed 528 cores on the high-memory queue. Fewer cores were used for smaller simulations and datasets.

3.1.6.1.3 Parallelization strategies:

The channel flow DNS was simulated using Incompact3D, which employs pencil decomposition and MPI for parallelization. The post-processing codes use slab decomposition and MPI for parallelization.

3.1.6.1.4 Performance and scalability:

Icompact3D is an established code and thus doing performance and scalability studies was not necessary. The postprocessing codes are developed in-house and the performance and scalability studies were not performed for these. The scalability is expected to be limited for these because of slab decomposition.

3.1.6.1.5 Publications:

1. Anand, A., Diwan, S. S., & Swaminathan, N. (2024). A comparative study of bandpass-filter-based multi-scale methods for turbulence energy cascade. Journal of Turbulence, 1–10
2. Anand, A., Diwan, S., & Swaminathan, N. (2023). Intermittent structures of intense inter-scale energy fluxes in turbulent channel flow, Bulletin of the 76th Annual Meeting of Division of Fluid Dynamics of American Physical Society.
3. Anand, A., Swaminathan, N., & Diwan, S. (2023). Dissipation structures in a turbulent channel flow. In 14th Asian Computational Fluid Dynamics Conference.

3.1.6.2 Research Area: DNS of human respiratory flows

3.1.6.2.1 Problem area:

Respiratory diseases like COVID-19 spread through droplets expelled during coughing, sneezing, breathing, and speaking. Speech flows generate turbulent jets carrying muco-salivary droplets, with the amount expelled strongly depending on speech loudness. Modelling realistic speech flows is challenging due to their complexity and variability. To address this, direct numerical simulations (DNS) of speech flows have been performed using the MEGHA-5 code at the IISc Supercomputing Facility. Two cases were studied: Case I with 10 speech cycles from person 1 and zero flow from person 2 (a silent listener), and Case II with 10 staggered speech cycles from both persons, simulating turn-taking conversation. These simulations accurately capture airflow and droplet transport during conversations. Simulations have also been carried out for two-phase cough flows by simulating thermodynamics of phase change.

3.1.6.2.2 SERC's resources:

Param Pravega was used for the simulations, utilizing a minimum of 256 cores and a maximum of 2048 cores, depending on whether it was a test run or the final high-resolution simulation. Some of the early simulations were performed on SahasraT (CRAY).

3.1.6.2.3 Parallelization strategies:

The MEGHA-5 code is used for this work, employing the pencil decomposition method to divide the computational domain among multiple processors along spatial directions. Processor communication is managed via the Message Passing Interface (MPI).

3.1.6.2.4 Publications:

1. Singhal R, Ravichandran S, Govindarajan R, Diwan SS. Virus transmission by aerosol transport during short conversations. Flow. 2022;2:E13. doi:10.1017/flo.2022.7
2. Rohit Singhal, S. Ravichandran & Sourabh S. Diwan (2021) Direct Numerical Simulation of a Moist Cough Flow using Eulerian Approximation for Liquid Droplets, International Journal of Computational Fluid Dynamics, 35:9, 778-797, DOI: 10.1080/10618562.2022.2057479

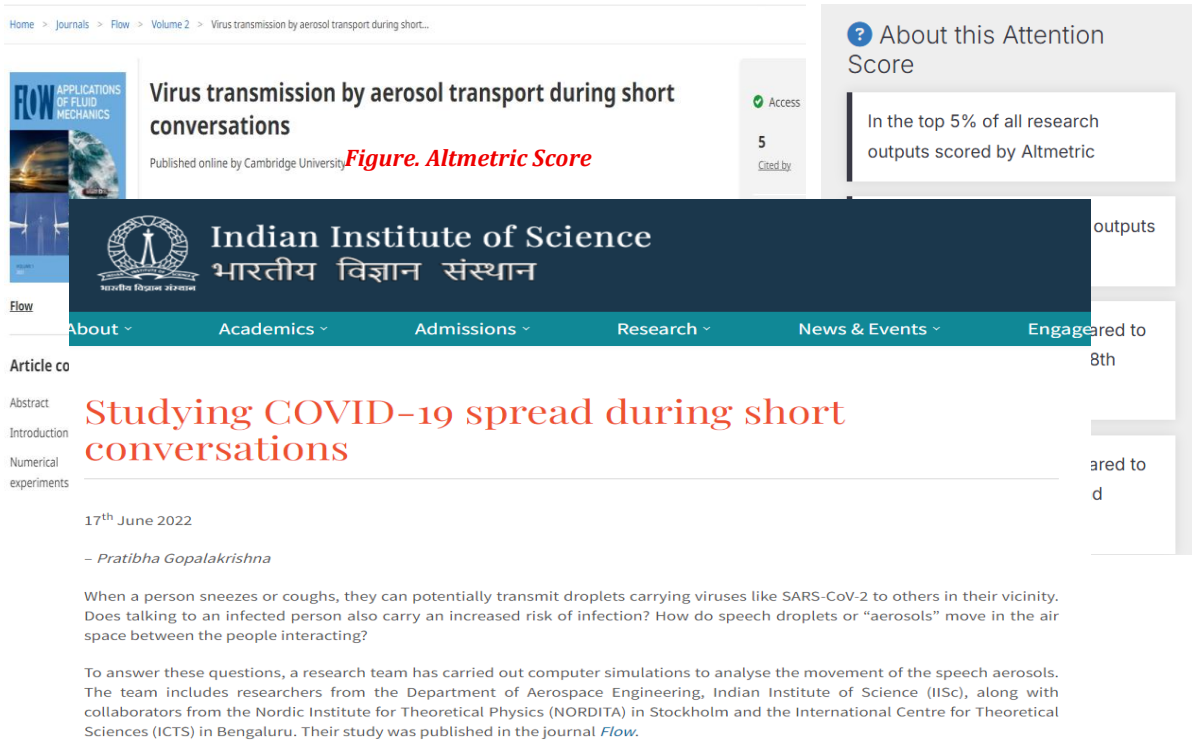

3.2 Centre for Atmospheric and Oceanic Sciences (CAOS)

3.2.1 Prof. Bishakhdatta Gayen's Lab

3.2.1.1 Problem Areas:

(a) **Indian Ocean Circulation and Bottom Water Pathways:** Our research focuses on understanding the circulation pathways of Antarctic Bottom Water (AABW) in the Indian Ocean, a key component of the global overturning circulation. These pathways regulate ocean heat and carbon storage, directly influencing global climate and sea level rise. Using high resolution turbulence-resolving simulations, we investigate how AABW upwells, mixes, and interacts with overlying water masses. The simulations also resolve mesoscale and submesoscale eddies that strongly modulate these pathways. Results from this work address long-standing uncertainties in Indian Ocean circulation, including deep water connectivity across major ridges and basins, the role of diapycnal mixing, and the sensitivity of abyssal flows to climate-driven buoyancy forcing. Applications of this work include improving climate model parameterizations and providing critical insight into long-term climate predictability.

(b) **Coupled Atmosphere–Ocean Boundary Layer and Evaporation:** We perform Large Eddy Simulations (LES) of the coupled air–sea boundary layer to study evaporation fluxes. These turbulence-resolving runs capture convective plumes, shear instabilities, and regime transitions between buoyancy-driven and wind-driven states. The results shed new light on evaporation processes under weak wind conditions, with implications for monsoon variability and improved air–sea flux parameterizations in climate and weather models. This research area is especially important because current climate models exhibit large biases in sea-surface properties due to their inadequate resolution of turbulent convection. By explicitly resolving convection and turbulence, our work provides a pathway to significantly reduce these biases and improve predictive skill in weather and climate projections.

3.2.1.2 SERC's Resources:

Both problem areas used the PARAM Pravega HPC system. Typical production runs employed ~2000 CPU cores concurrently, enabling high-resolution, long-duration integrations of Indian Ocean circulation as well as turbulence-resolving coupled LES studies.

Fig. IISc Press Release

3.2.1.3 Parallelization Strategies Employed:

We employed a hybrid MPI + OpenMP parallelization strategy with domain decomposition across spatial planes. Efficient parallel I/O, checkpoint–restart capability, and load balancing were used for long integrations. For the coupled boundary layer simulations, turbulence resolving LES solvers were optimized to maintain high throughput at ~2000 cores.

3.2.1.4 Publications (2022–24):

1. Eddy-freshwater interaction using regional ocean modeling system in the Bay of Bengal N Paul, J Sukhatme, Gayen, B., Sengupta, D. Journal of Geophysical Research: Oceans 128 (4), e2022JC019439, 2023
2. Tracing the Abyssal Water Pathways in the Indian Ocean. Mishara, B Gayen, K L Gunn, Vinayachandran, P N , Paul, N (under revision Geophysical Research Letter)

3.2.1.5 Contributions & Impact:

• Indian Ocean simulations (Kaushik Mishra) revealed new insights into abyssal pathways, relevant to India's national climate research programs.

• Coupled LES studies (Chetan Bankar) advanced understanding of evaporation under convective regimes, contributing to monsoon prediction and climate model improvements.

• Broader contribution to parameterization of mixing and fluxes in weather and climate prediction systems.

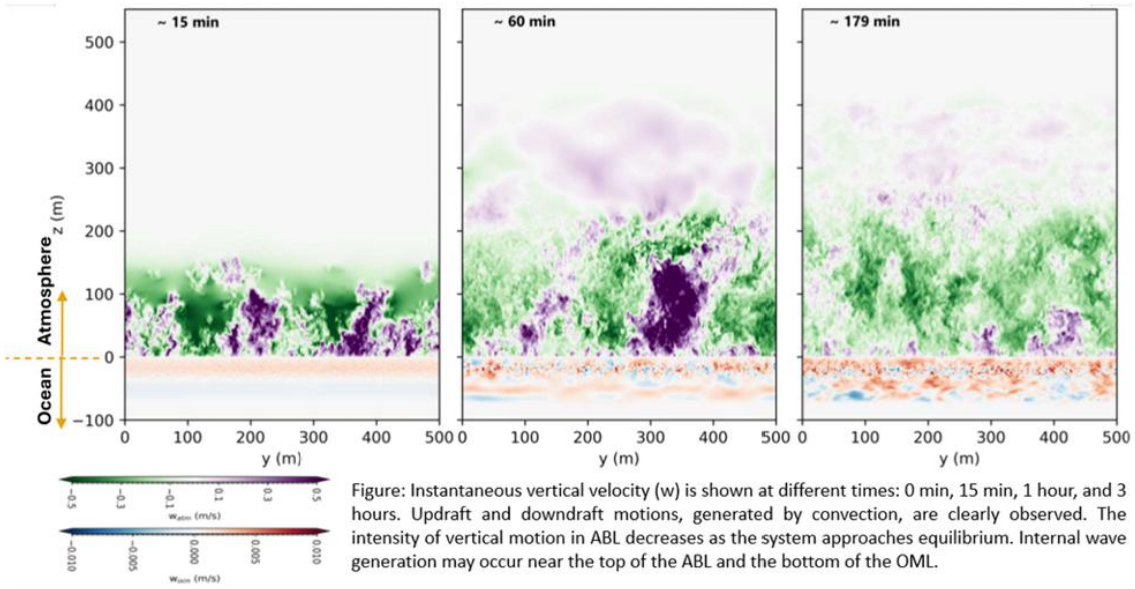

Figure: Instantaneous vertical velocity (w) is shown at different times: 0 min, 15 min, 1 hour, and 3 hours. Updraft and downdraft motions, generated by convection, are clearly observed. The intensity of vertical motion in ABL decreases as the system approaches equilibrium. Internal wave generation may occur near the top of the ABL and the bottom of the OML.

3.2.2 Prof. G. Bala's research Group:

3.2.2.1 Theme: Climate Change:

Sub themes: Climate system feedbacks, Solar geoengineering, Carbon cycle science

3.2.2.1.1 Problem Areas:

1. **Sensitivity of global warming to latitudinal distribution of radiative forcing**

- Conducted experiments by increasing solar insolation in different latitude bands using **NCAR CAM4**.
- Found that climate sensitivity is ~2× larger when forcing is imposed in **Northern Hemisphere high latitudes** and ~3× in **Southern Hemisphere high latitudes**, compared to low-latitude forcing.
- Differences mainly from **lapse rate, water vapor, and cloud feedbacks**, with contributions from albedo and Planck response.
- Study highlights strong dependence of climate sensitivity on **meridional structure of forcing**.

2. **Sensitivity of global mean warming to hemispheric differences in radiative forcing**
   - Compared uniform, NH-only, and SH-only radiative forcing.
   - Found larger warming for SH forcing, driven by shortwave cloud feedbacks.
   - ITCZ shifts toward hemisphere with larger forcing.
   - Provides insight into climate responses to volcanic aerosols, human emissions, and land cover changes.

3.2.2.1.2 SERC's resources:

Several century-long climate model simulations were run on Param Pravega. Each simulation used about 480 cores for 288 wall-clock hours.

3.2.2.1.3 Publication:

1. Harpreet Kaur, G. Bala & Ashwin Seshadri (2025). *Why is the temperature response larger for radiative forcing imposed in high latitudes than for forcing imposed in low latitudes?* Climate Dynamics. https://doi.org/10.1007/s00382-025-07659-y
2. Harpreet Kaur, G. Bala & Ashwin Seshadri (2024). *Climate response to interhemispheric differences in radiative forcing governed by shortwave cloud feedbacks*. Environmental Research: Climate. **https://iopscience.iop.org/article/10.1088/2752-5295/ad8df6**

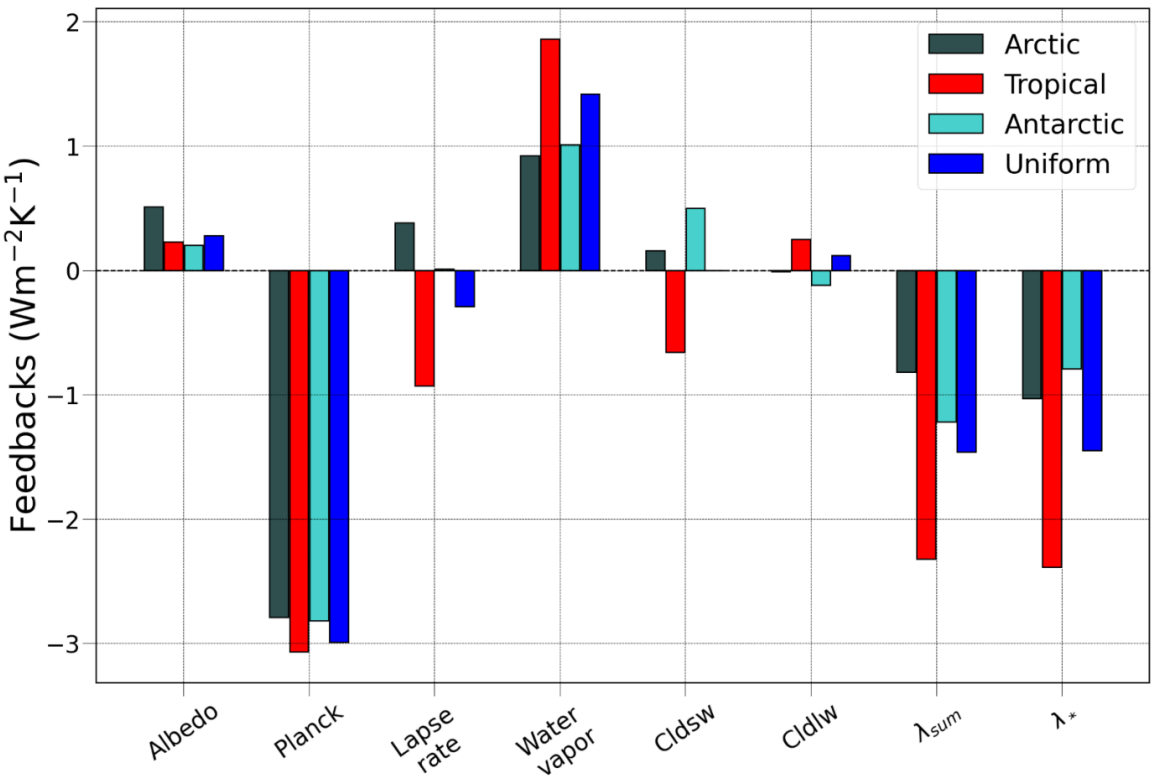

Figure caption: *The global-mean values of individual feedback parameters calculated using the radiative kernel technique for simulations with radiative forcing imposed globally in a uniform manner or only in the Arctic, Tropical, and Antarctic regions. Horizontal axis. identifies the individual feedbacks: albedo, Planck, lapse rate, water vapor (WV), shortwave cloud (Cldsw), longwave cloud (Cldlw) feedback, the sum of all feedback parameters (λ_{sum}), and the net feedback parameter (λ^*) estimated from model simulations for Arctic (grey), Tropical (red), Antarctic (turquoise) and Uniform (Blue) simulations.*

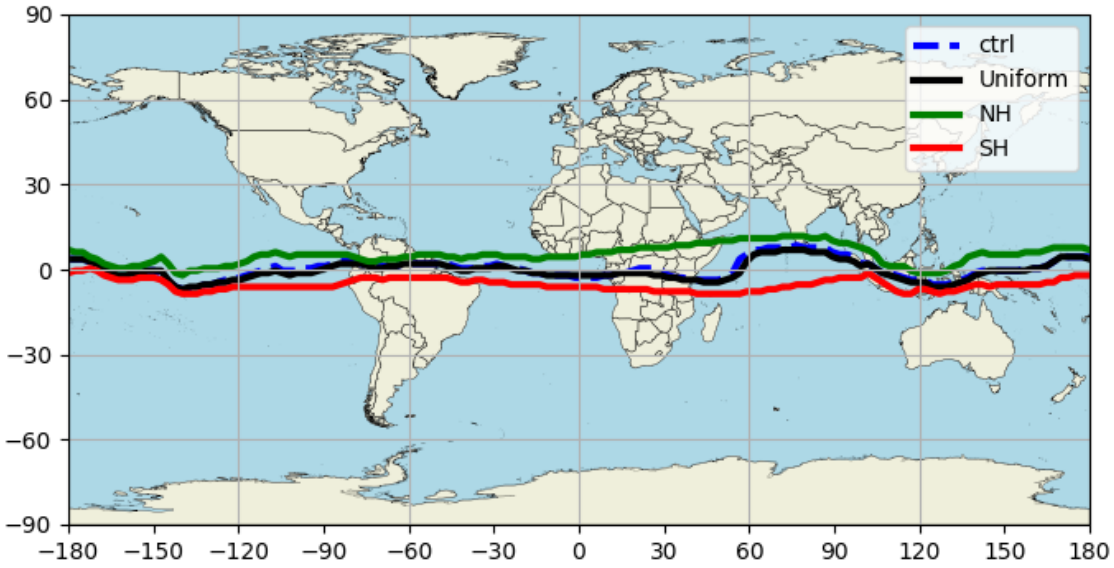

Figure caption: *Annual mean latitudinal position of Intertropical Convergence Zone (ITCZ) in the baseline simulation (dashed blue), simulation with uniform increase solar radiation (black), simulation with solar radiation increased only in the northern hemisphere (green) and simulation with solar radiation increased only in the*

southern hemisphere (red). ITCZ position is determined using the precipitation centroid metric, defined as the median latitude of zonal mean area-weighted precipitation between 20°S and 20°N (Donohoe et al. 2013). The results are estimated as the annual mean values over the last 50 years of the 100-yr Community Atmosphere Model version 4 (CAM4) slab ocean simulations

3.2.2.2 Solar Geoengineering

3.2.2.2.1 Problem areas:

1. **Sensitivity of tropical monsoon rainfall to the latitudinal distribution of stratospheric sulphate aerosols.**

Stratospheric aerosol geoengineering (SAG) is one of the several solar geoengineering options that have been proposed to counteract climate change. In the case of SAG, reflective aerosols injected into the stratosphere would reflect more sunlight and cool the planet. When assessing the potential efficacy and risks of SAG, the sensitivity of tropical monsoon precipitation changes should be also considered. Using a climate model, we performed several stylized simulations with different meridional distributions in the stratosphere. Because tropical monsoon precipitation responds to global mean and interhemispheric difference in radiative forcing or temperature, we quantified the sensitivity of tropical monsoon precipitation to SAG in terms of two parameters: global mean aerosol optical depth (GMAOD) and interhemispheric AOD difference (IHAODD). For instance, we find that the simulated northern hemisphere monsoon precipitation has a sensitivity of −1.33 ± 0.95% per 0.1 increase in GMAOD and −7.62 ± 0.27% per 0.1 increase in IHAODD. We also estimated precipitation changes in terms of the two sensitivity parameters for the global mean precipitation and for the indices of tropical, northern hemisphere, southern hemisphere and Indian summer monsoon precipitation changes. Similar sensitivity estimates are also made for unit changes in global mean and interhemispheric differences in effective radiative forcing and surface temperature. Our study which uses SERC resources for climate model simulations provides a simpler framework for understanding the tropical monsoon precipitation response to external forcing agents.

2. **Sensitivity of tropical monsoon rainfall to the height distribution of stratospheric sulphate aerosols.**

Previous modelling studies had shown that the efficacy of the cooling via stratospheric aerosol geoengineering SAG increases with altitude of the aerosol layer. It has been also shown that the stratospheric heating associated with SAG could stabilize the tropical atmosphere and weaken the tropical hydrological cycle. Using a global climate model, we performed a systematic study by prescribing volcanic sulphate aerosols at three different altitudes (22 km, 18 km and 16 km) and assessed the sensitivity of the global and tropical mean precipitation to the altitude. We found that even though the efficacy of cooling increases with altitude of the aerosol layer, the global and tropical mean precipitation changes are less sensitive to the height of the aerosol layer. This is because the magnitude of both the global and tropical mean precipitation reduction increases with aerosol altitude in response to increasing efficacy of aerosols, but this sensitivity related to the slow response (sea surface temperature change) is nearly offset by the sensitivity of fast precipitation adjustments to aerosol altitude. A perspective and analysis based on atmospheric energy budget was presented to explain the lack of sensitivity of the hydrological cycle to the altitude of the stratospheric sulphate aerosol layer. This work used SERC resources for several century-long climate model simulations.

3.2.2.2.2 Publications:

1. Anu Xavier, **G. Bala**, Shinto Roose and KH Usha; 2024: An investigation of the relationship between tropical monsoon precipitation changes and stratospheric sulfate aerosol optical depth, Oxford open climate change, https://academic.oup.com/oocc/article/4/1/kgae016/7737801)
2. Usha, KH, **G. Bala,** A. Xavier, 2024: Sensitivity of the global hydrological cycle to the altitude of stratospheric sulphate aerosol layer, Environmental Research Letters, https://doi.org/10.1088/1748-9326/ad5e9d)

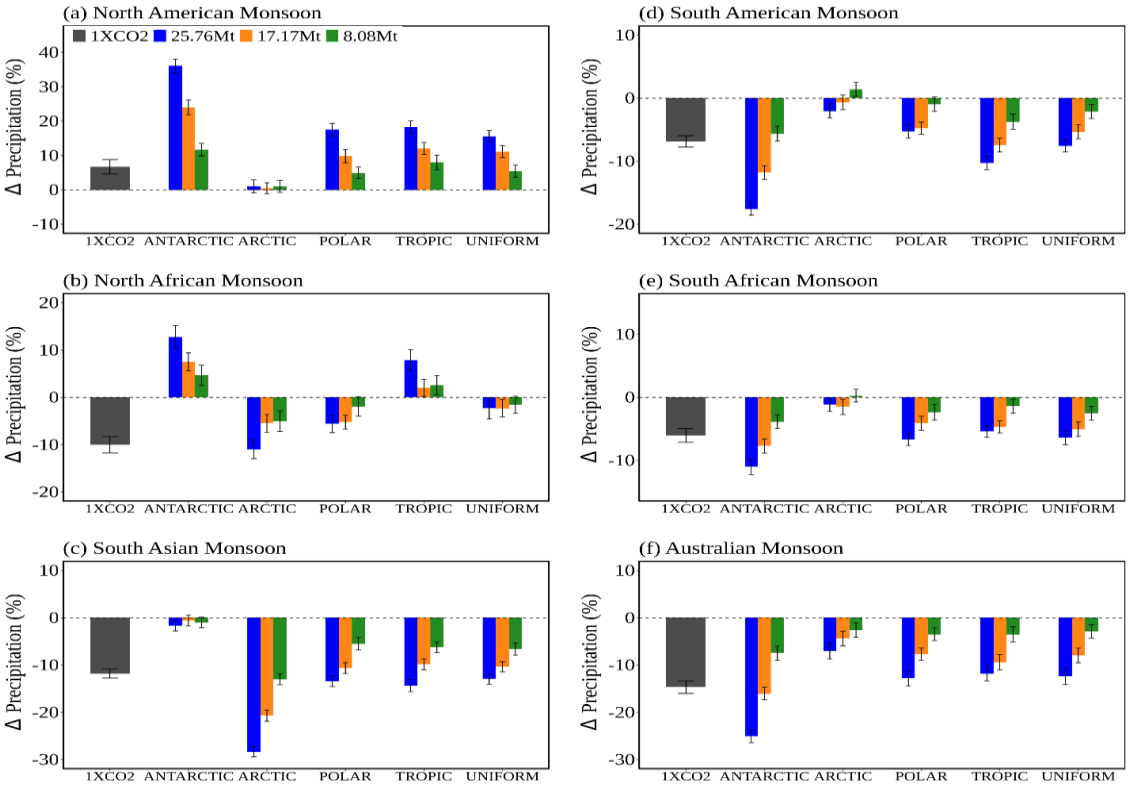

Figure caption: *Changes (%) in summer monsoon precipitation in the baseline (1×CO2) simulation and in the five stratospheric aerosol geoengineering (SAG) simulations for three amounts of prescribed aerosols (25.76, 17.17, 8.08 Mt) relative to the simulation where the CO_2 concentration is doubled relative to the baseline simulation for the northern hemisphere monsoon regions (a, b, c) and the southern hemisphere monsoon regions (d, e, f). The error bars show the standard error derived from the last 60 years of the 100-year slab-ocean simulations.*

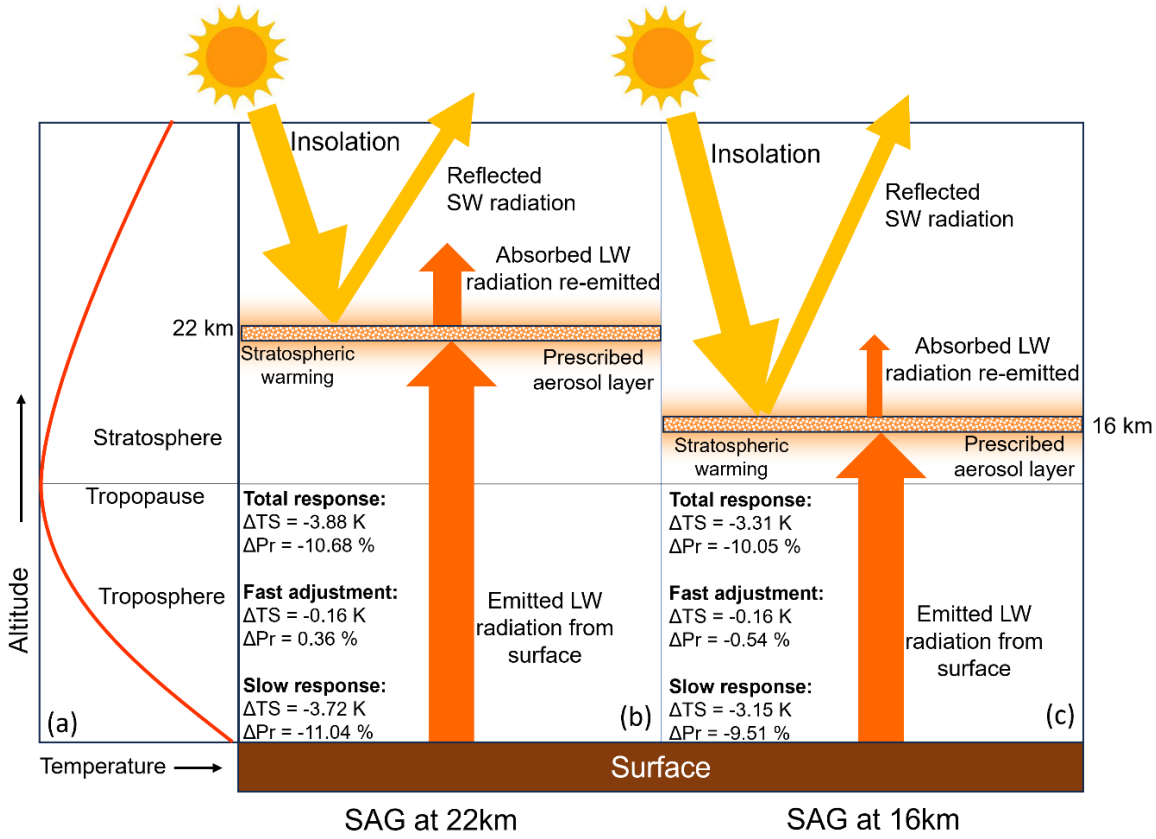

Figure caption: *A schematic illustration of the sensitivity of climate response to the altitude of the aerosol layer in stratospheric aerosol geoengineering (SAG). (a) A typical temperature profile of troposphere and stratosphere. (b) and (c) shows the implication of SAG at 22 km and lower 16 km respectively on temperature and precipitation for fast adjustment, slow response and total change. The values for fast adjustment and total response are from prescribed SST and slab ocean configuration respectively. The values for slow response are estimated as the difference between fast adjustment and total response. The yellow arrows show incoming (downward) and reflected (upward) shortwave radiation. The orange arrows show the emitted LW radiation from surface and re-emitted absorbed LW radiation from the aerosol layer. Thinner arrow for re-emitted absorbed LW radiation in the lower-altitude SAG case suggests more LW energy is trapped within the atmosphere (stronger greenhouse effect).*

3.2.2.3 Carbon Cycle Research

3.2.2.3.1 Problem Area:

Climate and Carbon Cycle Response in Net Zero Emission Pathways

In this Earth System modelling study, we examined the climate system response to a set of nine scenarios where emissions are followed by the removal of all carbon emitted into the atmosphere. The nine stylized simulations were driven by cumulative emissions of 1,000 GtC, 2,000 GtC, and 5,000 GtC over 150, 250, and 500 years, followed by the removal of all carbon over the same period. We found that the climate system returns to preindustrial state on millennial timescales independent of emission and removal pathways. However, larger changes in the climate system at the end of removals (on centennial timescales) were

simulated for a larger magnitude and longer duration of the emission and removal pulses. Since a delay in emission reduction implies a larger magnitude and longer duration for the emissions and consequently larger magnitude and longer duration for the removals to bring the climate state to preindustrial conditions, an earlier emission reduction would help to avoid large climate and carbon cycle impacts on centennial-timescales. This work used SERC resources for several 1000-year-long coupled climate-carbon model simulations.

3.2.2.3.2 Publication:

1. Jayakrishnan, KU, **G. Bala**, K Caldeira, 2024: Dependence of climate and carbon cycle response in net zero emission pathways on the magnitude and duration of positive and negative emission pulses, Earth's Future, https://doi.org/10.1029/2024EF004891

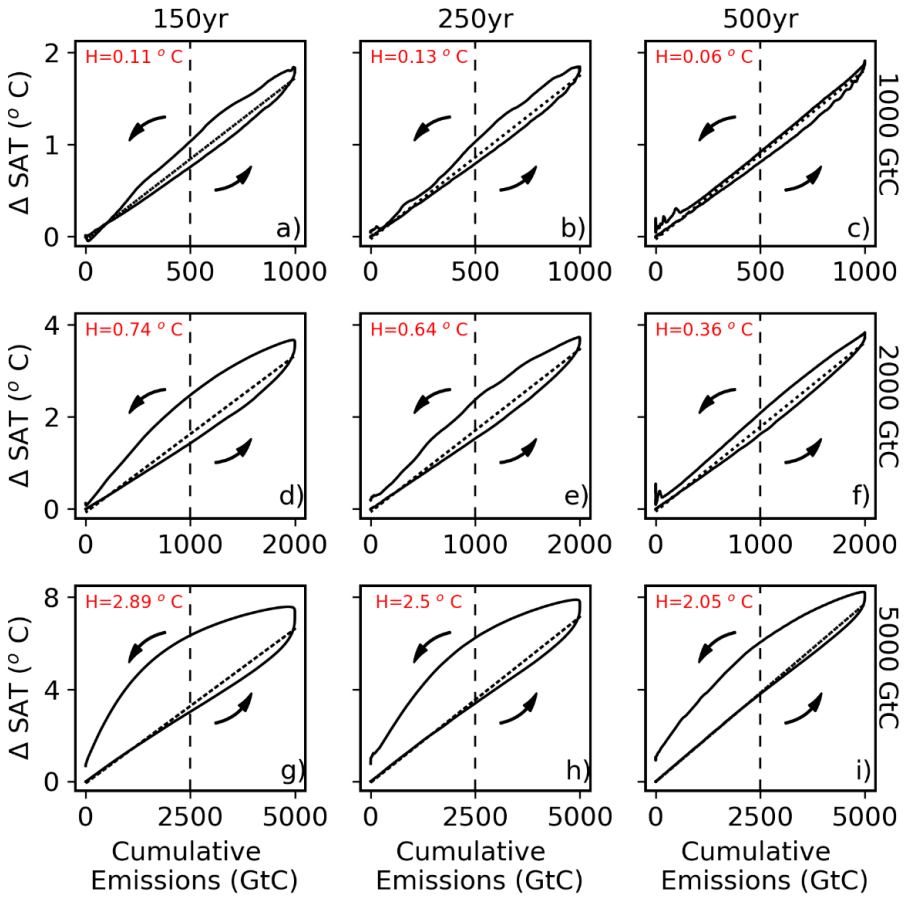

Figure 4 *The changes in global mean surface air temperature (SAT) relative to the preindustrial period as a function of changes in cumulative carbon emissions in nine "net-zero emissions" simulations. The top, middle, and bottom panels correspond to simulations with cumulative carbon emission magnitudes of 1000, 2000, and 5000 GtC in the positive and negative emission phases of the zero net emission cycle, respectively. The left, middle and right panels correspond to simulations with 150, 250, and 500 years for the duration of the positive and negative emission phases, respectively. The dashed vertical lines represent the timing of the peak emission or removal rates in the positive and negative emission phases. The dotted lines show the linear regression for positive emissions. The arrows show the*

direction of the hysteresis curves. 'H' denotes hysteresis magnitude at the point corresponding to 50% of the maximum cumulative emissions/removals. Note that the scales of the vertical axes are different.

3.2.3 Prof. Jai Sukhatme's Lab

3.2.3.1 Problem Area:

1.The effect of transient eddies on the tropical overturning circulation — The tropical overturning circulation, or the Hadley Cell, is one of the most important features of the atmosphere. Apart from thermal driving, momentum and heat fluxes associated with eddies or waves play a significant role in the strength of this cell. The quantitative assessment of this wave component requires intensive computation using some of the most sophisticated models of the Earth's atmosphere, namely General Circulation Models. To date, such efforts have largely focused on the contribution of midlatitude waves that impinge on the tropics. In this work, we devised a set of numerical experiments that involved adjustments to the underlying sea-surface temperature gradients, with the aim of elucidating the roles of both extratropical and tropical waves in driving the Hadley Cell. This helped advance our understanding of the tropical circulation, and these results are also relevant in a changing climate where the atmosphere is projected to interact with modified sea surface temperatures. The specific model used was the Community Earth System Model which was installed, tested, and run on the supercomputing facility in IISc. These simulations were carried out on the SahasraT and Param-Pravega supercomputers using a total of about 1.7 Lakh core hours of computation.

2. Eddy-freshwater Interaction in the Bay of Bengal — The Bay of Bengal (BoB) receives a large amount of freshwater from rivers during the summer monsoon season. This freshwater forms a very shallow layer on the surface of the Bay, and the shallow salinity-dominated stratification is important for regional air-sea interaction. However, the accurate simulation of the space-time evolution of upper ocean salinity remains a challenge for numerical models in the BoB. In this work, we elucidate one particular mechanism that involves the trapping of freshwater by a cyclonic eddy and its homogenization on a sub-monthly timescale along the western boundary of the north Bay through a high-resolution numerical simulation. The mesoscale dynamical processes involved in homogenization are identified and, for the first time, allow for an understanding of surface salinity evolution on a subseasonal scale in the Bay. The specific model used was the Regional Ocean Modeling System (ROMS) which was installed and tested on the supercomputing facility at IISc.

3.2.3.2 Publications:

1. A.B.S Thakur and J. Sukhatme, Changes in the tropical upper tropospheric zonal momentum balance due to global warming, Weather and Climate Dynamics, 10.5194/wcd-5-839-2024, 2024.
2. A.B.S Thakur, J. Sukhatme and N. Harnik, The role of Tropical and Extra-tropical Waves in the Hadley Circulation, Quarterly Journal of the Royal Meteorological Society, 10.1002/qj.4784, 2024.
3. P. Kushwaha, J. Sukhatme and R.S. Nanjundiah, Role of Bay of Bengal Low Pressure Systems in the Formation of Mid-Tropospheric Cyclones over the Arabian Sea and Western India, Quarterly Journal of the Royal Meteorological Society, 10.1002/qj.4726, 2024.

4. N. Paul, J. Sukhatme, B. Gayen and D. Sengupta, Eddy-Freshwater Interaction Using Regional Ocean Modeling System in the Bay of Bengal, Journal of Geophysical Research, 10.1029/2022JC019439, 2023.

3.2.4 Prof. P. N. Vinayachandran's Lab

3.2.4.1 Problem areas:

Motions in the ocean occurring at scales of O(1-10km) are known as submesoscale processes and are associated with fronts, eddies and filaments. These features are important as they determine the distribution of temperature, salinity, chlorophyll and other biogeochemical variables yet they are not represented in present-day Indian Ocean models. Recent observations have shown evidences for their presence as well as impact on upper ocean processes. We have developed a very resolution Regional Ocean Modelling System configured for the Bay of Bengal to simulate submesoscale processes ocean. These model runs carried out on the HPC system in the SERC produced a submesoscale resolving simulation for the Bay of Bengal. These models had a horizontal resolution of 1 km and 60 levels in the vertical. Two experiments were carried, one in which the river runoff into the model was switched off and the other with river runoff included. The goal was to understand the role played by river plumes in the Bay of Bengal in driving submesoscale processes.

3.2.4.2 SERC's resources:

The computations were performed on SERC's Param Pravega supercomputer. Up to 1,440 cores were utilized for running high-resolution model simulations. The simulations were carried out using the high-memory queue.

3.2.4.3 Parallelization strategies employed:

ROMS supports openMP parallel implementation.

3.2.4.4 Performance and scalability:

These simulations were not carried out on any other machines, so no performance comparison is available.

3.2.4.5 Publications:

1. Anup, N., Vinayachandran, P. N., & Subramani, D. N. (2025). High-resolution simulation of the Bay of Bengal rain plume. Journalof Geophysical Research: Oceans, 130, e2025JC02267.
2. Pargaonkar, S. M., Mallick, S. K., Kalita, B. K., & Vinayachandran, P. N. (2025). Submesoscale processes associated with the East India Coastal Current. Journal of Geophysical Research: Oceans, 130, e2023JC020451. https://doi.org/10.1029/2023JC020451.
3. Kalita, B. K., P.N. Vinayachandran, (2025), Bay of Bengal river plume response to a tropical cyclone in high-resolution numerical simulations, Ocean Modeling, https://doi.org/10.1016/j.ocemod.2025.102498.

4. Jain T., U. Singh, V. Singh, V. K. Boda, I. Hotz, S. S. Vadhiyar, P. N. Vinayachandran and V. Natarajan, (2025), A Scalable System for Visual Analysis of Ocean Data, (2025), Computer Graphics Forum, https://onlinelibrary.wiley.com/doi/epdf/10.1111/cgf.15279.
5. Singh U, P.N. Vinayachandran, V. Natarajan, (2024), Advection-Based Tracking and Analysis of SalinityMovement in the Ocean, Computers & Geosciences, https://doi.org/10.1016/j.cageo.2023.105493.

High-Resolution Simulation of the Bay of Bengal Rain Plume

N.Anup, P.N.Vinayachandran,and DeepakN.Subramani

JGR Oceans https://doi.org/10.1029/2025JC022676

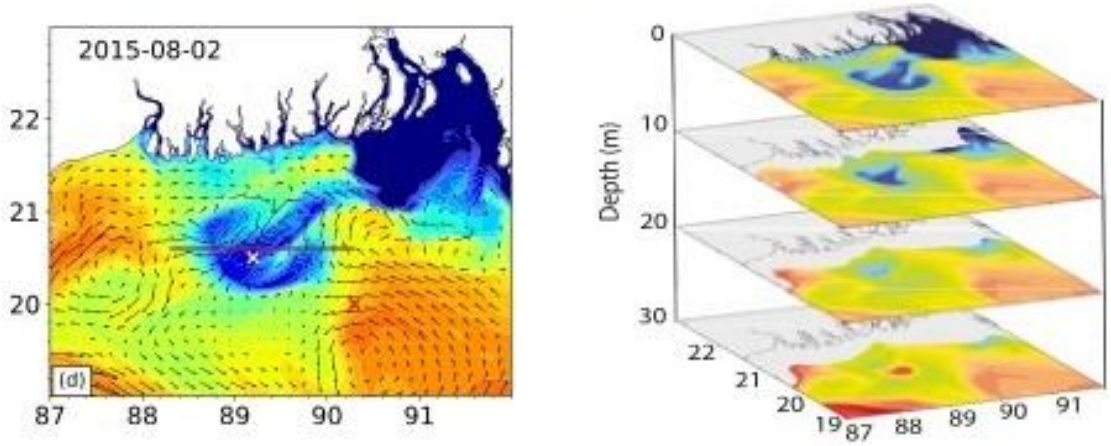

Structure of a Rain Plume simulated by 1km ROMS of Bay of Bengal

Centre for Atmospheric and Oceanic Sciences
Indian Institute of Science

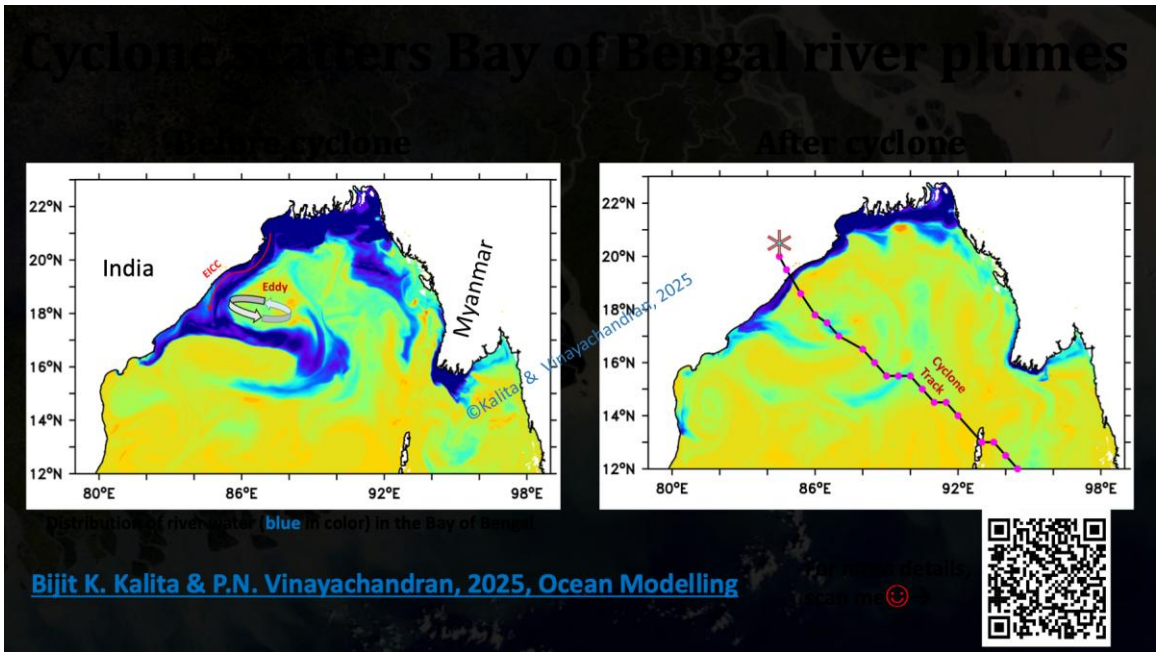

3.3 Computational and Data Science Department (CDS)

3.3.1 Prof. Danish Pruthi's Lab

3.3.1.1 Problem areas:

Our research focuses on enhancing the capabilities of language models. Recent efforts are investigating methods to enhance cross-lingual transfer and distilling understanding from proofs to improve theorem proving capabilities. Research questions around these efforts require us to often conduct experiments involving training of language models.

3.3.1.2 SERC's resources:

Following our requirements, we use the DGXH100 compute cluster, primarily for the H100 GPU devices. On average, our usage is of 1-2 GPUs per SLURM job, utilizing about 70-120 GB VRAM. Each job uses no more than 4 CPU cores per job.

3.3.1.3 Parallelization strategies employed:

We utilize optimized implementations of attention kernels provided as part of packages such as flash-attention (https://github.com/Dao-AILab/flash-attention
Dao-AILab/flash-attention – GitHub) to improve training and inference speeds on Hopper architectures (H100s). Apart from optimization provided by third-party packages, no further strategies are employed.

3.3.1.4 Performance and scalability obtained:

In comparison to a cluster with A6000 GPU cards, a speedup of about 2-4x was observed.

3.3.2 Prof. Konduri Aditya's Lab

3.3.2.1 Problem areas:

Our research comprises of three aspects: (1) developing scalable numerical methods for partial differential equations solvers for extreme scale, (2) machine learning to accelerate HPC simulations, and (3) massively parallel reacting flow simulations to capture key physics relevant to combustion processes in gas turbine and scramjet engines. Below are the details of these projects.

1. **Asynchronous computing:** Direct numerical simulations (DNS) of reacting flows—particularly those involving detailed combustion chemistry—require massive computational resources and extreme parallelism. While state-of-the-art solvers operate on hundreds of thousands of processing elements (PEs), scalability is increasingly limited by the cost of data movement and synchronization. To address this, we have developed an asynchronous computing framework using both finite-difference and discontinuous Galerkin (DG) schemes that relax communication synchronization at the mathematical level. In this approach, halo exchanges between PEs are no longer strictly synchronized, allowing computations to proceed independently of communication status. While standard schemes degrade in accuracy under relaxed synchronization, we developed asynchrony-tolerant (AT) schemes and fluxes that maintain numerical accuracy. We implemented and evaluated these AT schemes on GPU-accelerated platforms using a multi-GPU, multi-node solver for compressible Navier-Stokes equations, developed with an MPI + CUDA programming model. Our asynchronous DG (ADG) implementation in the deal.II framework achieved a 2.25× speedup on ~20,000 cores of the Param Pravega supercomputer. These developments showcase the potential of asynchronous algorithms to enhance both scalability and performance of PDE solvers, enabling accurate simulation of complex physical systems on next-generation supercomputers.

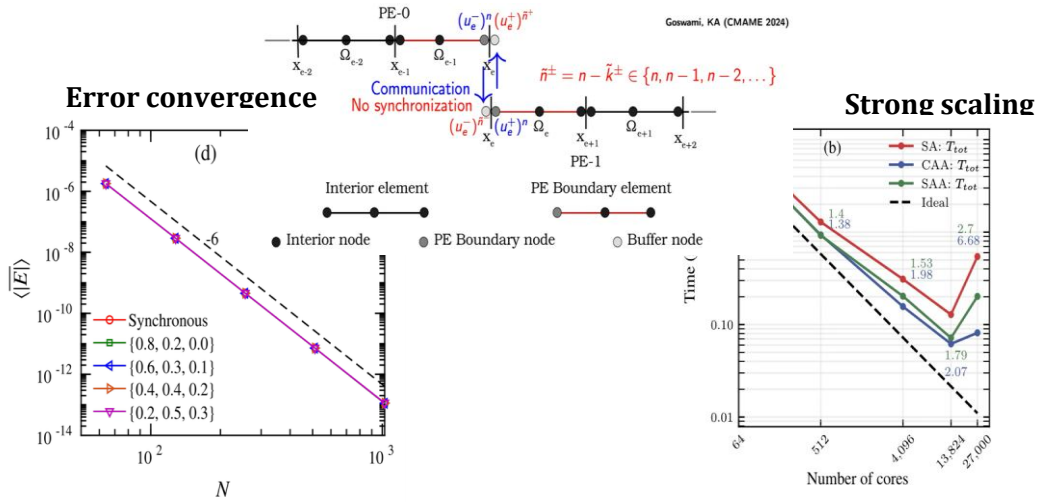

Figure: *Asynchronous computing*

2. **Low-dimensional manifolds for combustion chemistry:** High-fidelity simulations of turbulent reacting flows are indispensable for understanding and designing next-generation combustion systems, yet they remain prohibitively expensive due to the immense computational burden of resolving detailed chemical kinetics. Traditional dimensionality reduction methods, most notably principal component analysis (PCA), have helped mitigate computational challenges by projecting high-dimensional thermo-chemical data onto more compact low-dimensional manifolds. However, PCA's reliance on variance maximization often neglects the rare yet critical spatiotemporal events—such as ignition kernels and localized reaction zones—that govern combustion dynamics. To address this fundamental shortcoming, we have developed co-kurtosis principal component analysis (CoK- PCA), a framework that leverages fourth-order statistical moments to identify and retain the stiffest and most chemically significant directions in the state space. First, we established the theoretical foundation for CoK-PCA, demonstrating its superior ability to capture chemically stiff dynamics relative to PCA using a linear reconstruction framework. Furthermore, we expanded this work by pairing CoK-PCA with nonlinear neural network–based reconstruction, showing that this hybrid approach significantly improved the recovery of key thermo-chemical states and derived quantities such as species production and heat release rates, even under aggressive dimensionality truncation. Currently, we are extending the methodology to an a posteriori setting by integrating CoK-PCA manifolds with neural ODE solvers, enabling stable time evolution of reduced states while suppressing error propagation. Taken together, these contributions illustrate a coherent progression from conceptual development to applied methodology, establishing CoK-PCA as a powerful new paradigm for dimensionality reduction. By combining computational efficiency with strong physical fidelity, this body of work lays the foundation for its integration into massively parallel reacting flow.

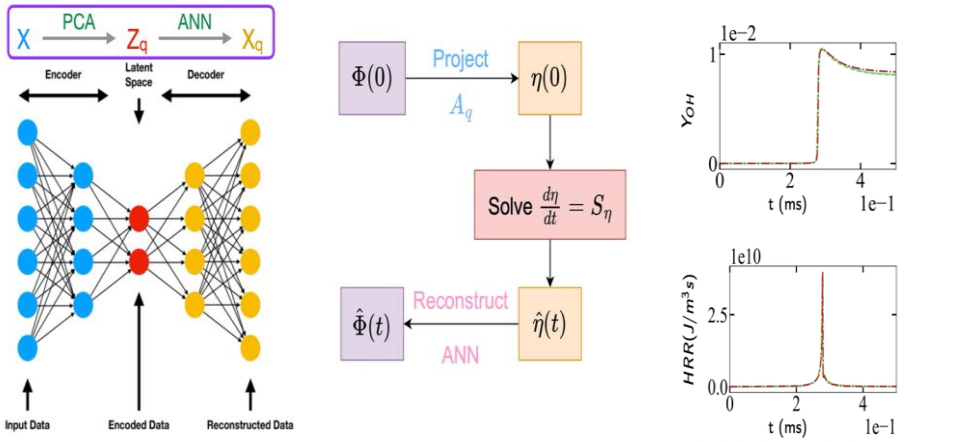

A priori analysis **A posteriori analysis** **Reconstructed profiles**

Fig. Low-dimensional manifolds for combustion chemistry

3. **Hydrogen combustion:** With the goal of achieving a net-zero energy supply, hydrogen, hydrogen-enriched natural gas, and biofuels, which reduce the carbon footprint, are being actively considered for firing stationary gas turbine engines. In this regard, longitudinally staged combustion concepts have been demonstrated to achieve low emissions and good fuel flexibility while operating under a wide range of load conditions. A particular implementation of such a concept is the constant-pressure sequential combustor in Ansaldo Energia's GT36 gas turbine, which comprises two fuel stages that implement lean premixed combustion with different characteristics. In the first stage, the flame is stabilized aerodynamically, and combustion occurs mainly through premixed flame propagation. The product gases from the first-stage combustion are then blended with additional air in a dedicated mixer before entering the second-stage combustor (also called the reheat burner), where additional fuel is added and combustion occurs under reheat conditions, that is, it is controlled by spontaneous ignition owing to the high temperature of the reactants. The reheat burner operation plays an important role in achieving the desired overall combustion characteristics. In this project, we performed high-fidelity two- and three-dimensional direct numerical simulations of a reheat flame to identify the modes of combustion and quantify their contributions to fuel consumption. We investigated the effect of operating pressure on the flame in a reheat combustor for pure hydrogen combustion. The results show that at higher pressures, the flame position is very sensitive to small perturbations in pressure/temperature and can easily transition to an unstable state of combustion. Furthermore, the flame structure and role of auto-ignition in achieving the desired output were investigated. To understand the performance compromises observed in the hydrogen-rich regime of hydrogen-natural gas blends, further simulations with methane-blended hydrogen were performed. The results illustrate a significant change in flame stability and structure. The findings from this project are being used to guide the engine design at Ansaldo Energia. Recently, we also started working on simulations of a compact trapped vortex combustor to understand its characteristics when fired with hydrogen. These simulations complement the experiments that are being conducted at Prof. Ravikrishna's laboratory at IISc.

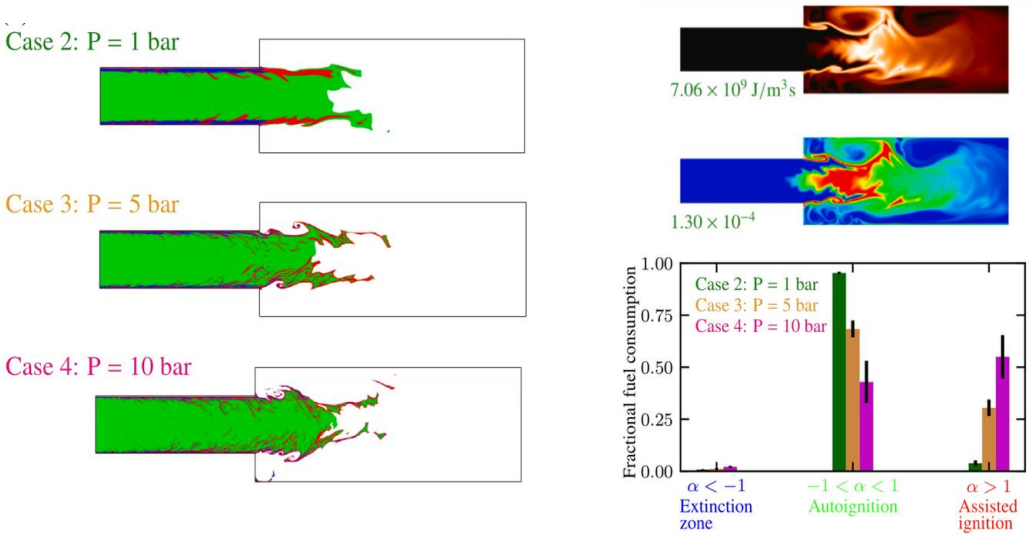

Fig. Hydrogen combustion

4. **Cavity-stabilized flames:** Recirculation ones are often used to stabilize flames in high-speed combustion, for example, in gas turbines and scramjet engines. In this recently started project, direct numerical simulations of lean ethylene-air turbulent premixed flames stabilized over the recirculation zone in a cavity configuration were performed to study the interactions between the flame and the shear layer vorticity. The results show that the recirculation zones transport the necessary hot radicals, such as OH, from the downstream region to the stabilization point. Vorticity, which is present mainly on the reactant side of the flame near the stabilization point, is advected into the products downstream. This leads to enhanced heat transfer from the flame to the wall and affects the CO and OH oxidation [C10]. The results from this study can guide the flame stabilization aspects relevant to DRDO scramjet engine design.

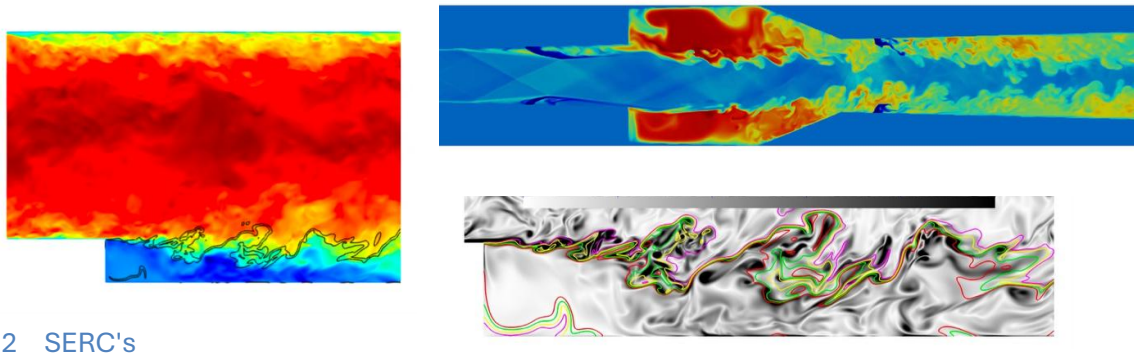

Figure: *Cavity-stabilized flames*

3.3.2.2 SERC's resources:

Param Pravega supercomputer was extensively used to perform benchmarks for methods development project and to perform production simulation for combustion application. Simulations were performed on core counts ranging from 2000 to 25000.

3.3.2.3 Parallelization strategies employed:

The code was parallelised based on domain-decomposition technique and communications were facilitated using MPI library. For GPUs, separate functions were developed using CUDA.

3.3.2.4 Publications:

1. Goswami, S.K., Aditya, K., 2024. An asynchronous discontinuous Galerkin method for massively parallel PDE solvers. Computer Methods in Applied Mechanics and Engineering.
2. Goswami, S.K., Matthew, V.J., Aditya, K., 2023. Implementation of low-storage Runge-Kutta time integration schemes in scalable asynchronous partial differential equation solvers. Journal of Computational Physics.
3. Nayak, D., Jonnalagadda, A., Balakrishnan, U., Kolla, H., Aditya, K., 2024. A co-kurtosis PCA based dimensionality reduction with nonlinear reconstruction using neural networks. Combustion and Flame.
4. Jonnalagadda, A., Kulkarni, S., Rodhiya, A., Kolla, H., Aditya, K., 2023. A co-kurtosis based dimensionality reduction method for combustion datasets. Combustion and Flame.
5. Rodhiya, A., Gruber, A., Bothien, M.R., Chen, J.H. and Aditya, K., 2024. Spontaneous ignition and flame propagation in hydrogen/methane wrinkled laminar flames at reheat conditions: Effect of pressure and hydrogen fraction. Combustion and Flame.

6. Gopalakrishnan, H.S., Maddipati, R., Gruber, A., Bothien, M.R. and Aditya, K., 2024. A Reactor-Network Framework to Model Performance and Emissions of a Longitudinally Staged Combustion System for Carbon-Free Fuels. Journal of Engineering for Gas Turbines and Power.
7. Dash, P., Mallik, T., Verma, N., Roy Choudhury, A., Ravikrishna, R.V. and Aditya, K., 2024, June. A Deep Learning Based Model for Identifying Recirculation Zones From Experimental Images of Trapped Vortex Combustors. In Turbo Expo: Power for Land, Sea, and Air. American Society of Mechanical Engineers.

3.3.3 Prof. Phani Motamarri's Lab

3.3.3.1 Problem areas:

a. An efficient and scalable computational methodology was designed for conducting large-scale chemical bonding analysis -via- projected population analysis from real-space finite-element (FE) based Kohn-Sham density functional theory calculations (DFT). This work provides an important direction towards extracting chemical bonding information from large-scale DFT calculations on materials systems involving thousands of atoms while accommodating generic boundary conditions on massively parallel architectures.
b. We explore scalable polynomial expansion approaches based on recursive Fermi-operator expansion using mixed-precision arithmetic as an alternative to the subspace diagonalization of the projected Hamiltonian matrix to reduce the computational cost. We perform a detailed comparison of these polynomial expansion approaches to the traditional approach of explicit diagonalization, utilizing state-of-the-art ELPA library on multi-node CPUs.
c. We propose efficient matrix-free algorithms for evaluating finite-element discretized matrix multivector products on both multi-node CPU architectures. To this end, we propose batched evaluation strategies, with the batch size tailored to underlying hardware architectures, leading to better data locality and enabling further parallelization. On CPUs, we utilize even-odd decomposition, SIMD vectorization, and overlapping computation and communication strategies.
d. We developed a computationally efficient methodology that utilizes a local real-space formulation of the projector-augmented wave (PAW) method discretized with a finite-element (FE) basis to enable accurate and large-scale electronic structure calculations on massively parallel CPU architectures.
e. We formulate an efficient and scalable real-space finite-element approach for large-scale pseudopotential density functional theory (DFT) calculations incorporating non-collinear magnetism and spin-orbit coupling.
f. Leveraging the ability of real-space density functional theory (DFT) codes to accommodate generic boundary conditions, we introduce two methods for applying an external potential bias that can be suitable for modeling surfaces and interfaces.

3.3.3.2 SERC's resources:

- We used around 1000 CPU cores on Param Pravega for conducting large-scale chemical bonding analysis using our proposed methodologies.

- Performance studies involving proposed scalable polynomial expansion approaches (item 1b) and the matrix-free algorithms (item 1c) used around 3000 CPU cores.
- We performed accuracy and performance benchmark studies of the proposed finite-element based methodologies for large-scale electronic structure calculations up to 6500 Pravega CPU cores involving calculations up to 15000 electrons.

3.3.3.3 Parallelization strategies employed:

a. Finite-element discretization of the given simulation domain is carried out by decomposing it into non-overlapping finite-element cells. Further for efficient distributed parallelism, the simulation domain is further partitioned into subdomains with each subdomain assigned to a corresponding MPI task t.
b. The finite-element discretised Hermitian sparse generalised eigenproblem arising in the above proposed methods benefit from fully iterative eigensolvers that rely on Chebyshev filtered subspace iteration strategy (ChFSI) in a distributed setting.
c. We rely on ChFSI strategy since it is naturally amenable to the efficient use of high-performance computing architectures, as the construction of the filtered subspace does not involve any coupling among the vectors, allowing for matrix-multivector multiplications to be performed blockwise or in parallel over few blocks, reducing the peak memory requirement.
d. The global finite-element discretized sparse matrix is not assembled but instead the action of the matrix on trial multi-vectors is carried out at the finite-element cell level leveraging low level threaded Blas Kernels or using matrix-free methods and then the cell-level matrix vector products are assembled in a local processor. Contributions from shared processor boundary nodes are then accounted by using MPI point-to-point communication routines.
e. To reduce time to solution, we optimize the data movement costs both intra and inter node, by leveraging algorithms that can exploit overlapping compute and communication. Furthermore, we reduce communication costs by leveraging lower precision domain decomposition communication without sacrificing robustness by employing ChFSI solver that are tolerant to inexact matrix-vector multiplications.

3.3.3.4 Performance and scalability obtained:

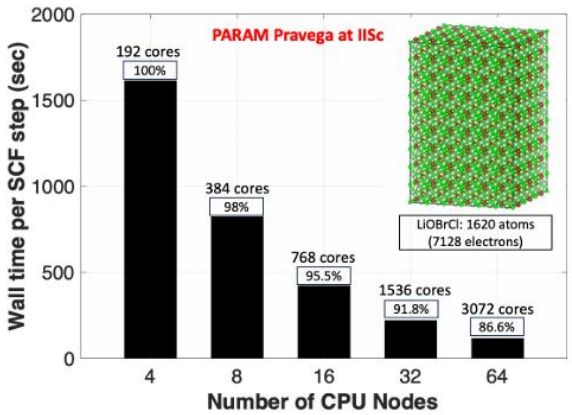

Fig1. *Scaling study of our in-house DFT-FE code on Param Pravega using norm-conserving pseudopotentials*

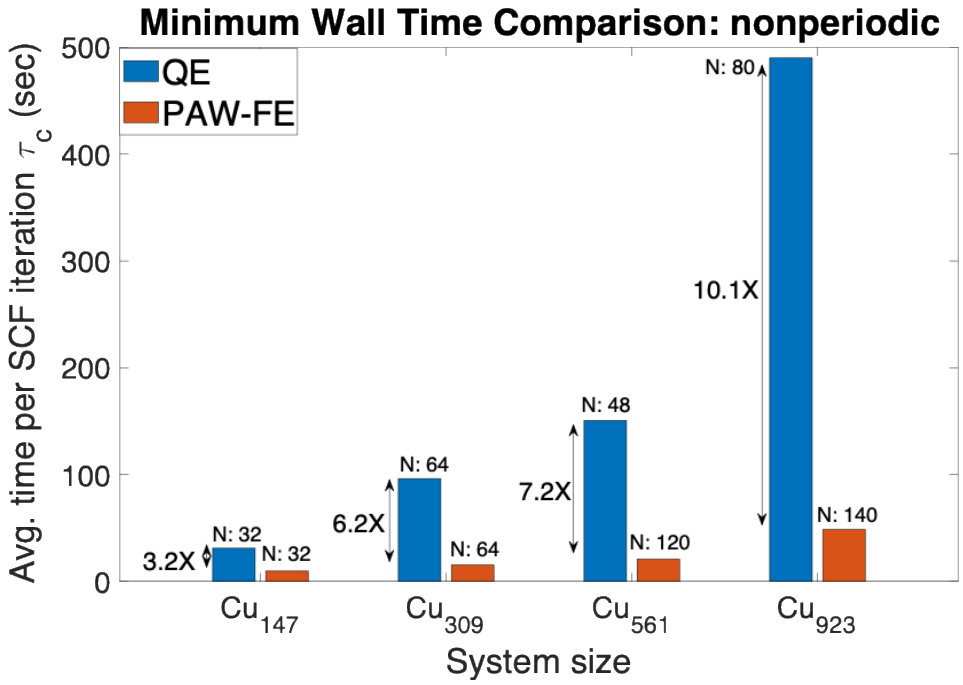

Fig2:

Minimum wall time comparison of our newly proposed PAW-DFT-FE formulation with state-of-the-art plane-wave basis code Quantum Espresso (QE). Case study: Cu nanoparticles of increasing size

3.3.3.5 Publications:

1. G. Panigrahi, N.Kodali, D. Panda, P. Motamarri. Fast hardware-aware matrix-free algorithms for higher-order finite- element discretized matrix multivector products on distributed systems. Journal of Parallel and Distributed Computing. Vol. 192, pp 104925, 2024.
2. S. Das, B. Kanungo, V. Subramanian, G. Panigrahi, P. Motamarri, D. M Rogers, P. Zimmerman, V. Gavini. Large-scale materials modeling at quantum accuracy: Ab initio simulations of quasicrystals and interacting extended defects in metallic alloys **(ACM Gordon Bell Prize).** Proceedings of SC23, The International Conference for High Performance Computing, Networking, Storage, and Analysis. 2023.
3. S. Khadatkar, P. Motamarri. Subspace recursive Fermi-operator expansion strategies for large-scale DFT eigenvalue problems on HPC architectures. Journal of Chemical Physics. Vol. 159, pp 031102, 2023.
4. K. Ramakrishnan, S. K. K. Nori, S. Lee, G. P Das, S. Bhattacharjee, P. Motamarri. Chemical Bonding in Large Systems Using Projected Population Analysis from Real- Space Density Functional Theory Calculations. Journal of Chemical Theory and Computation. Vol. 19, pp 4216, 2023.

3.3.3.6 Contributions:

Contributed to open-source code development -via- the development of novel real-space computational methodologies for material modelling using massively parallel density functional theory calculations. These were built under the umbrella of DFT-FE code, an open source code and is now currently being installed on NSM machines all over India to increase the user base thereby providing an efficient and a scalable alternative to existing

widely used plane-wave DFT codes like VASP or quantum espresso. These efforts are timely given that India is in the race to build exa-scale computer in the next 5 years.

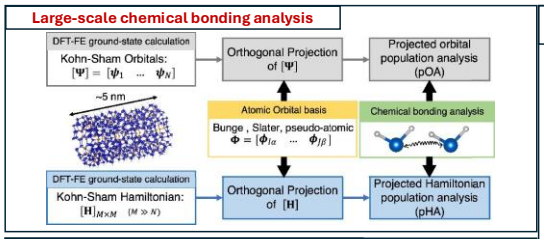

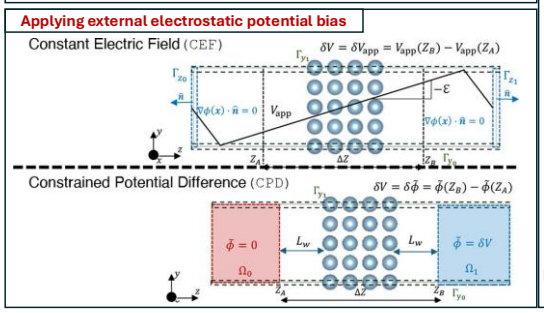

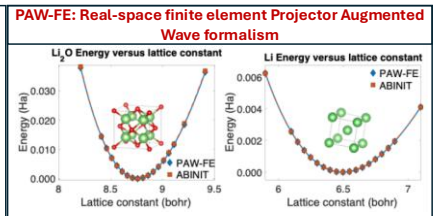

Equation of state comparison of PAW-FE with Abinit

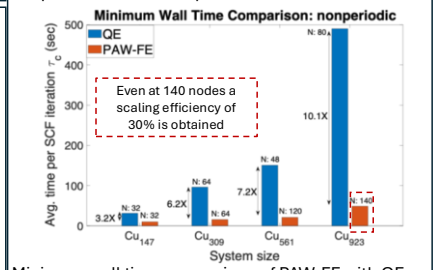

Minimum wall time comparison of PAW-FE with QE on Param Pravega.

Te atom adsorption on WS_2 surface with DFT calculations involving 2004 atoms

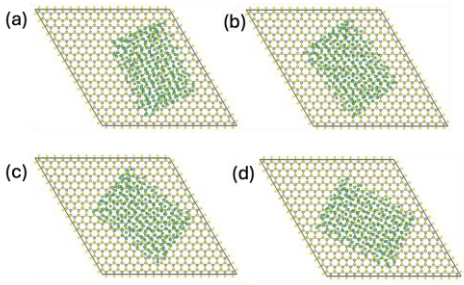

Figure: Top view of adsorption of Te on WS_2 surface for orientation angles (a) 0°, (b) 10°, (c) 20°, (d) 30°. Total number of S (Yellow) atoms = 1156, total number of W (Grey) atoms = 578, total number of Te(Green) atoms = 270.

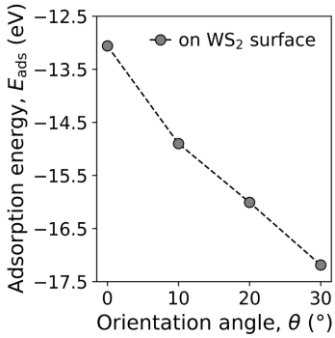

Figure: Total adsorption energy(eV) Vs. Orientation angle (°)

Finite-element methods for noncollinear magnetism and spin-orbit coupling in real-space pseudopotential DFT

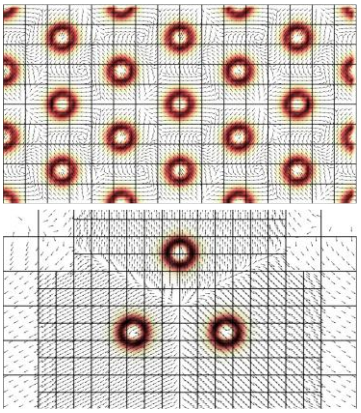

Spin-textures for Cr_3 cluster and Cr monolayer

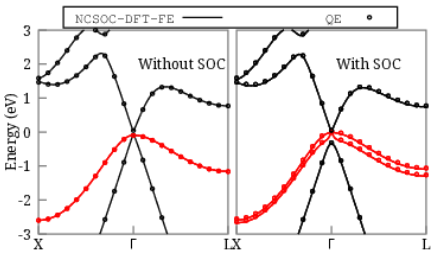

Bandstructure of GaAs with and without SOC, the bands shown in red serve as an example for band splitting

3.3.4 Prof. Sathish Vadhiyar's Lab

3.3.4.1 A Fault-tolerant Framework for MPI Applications based on Adaptive Partial Replication

3.3.4.1.1 Problem areas:

A Fault-tolerant Framework for MPI Applications based on Adaptive Partial Replication: We have implemented **FTHP-MPI** (Fault Tolerance and High Performance MPI), a novel fault-tolerant MPI library that augments checkpoint/restart with replication to provide resilience from failures. The novelty of our work is that it is designed to provide fault tolerance in a native MPI library that does not provide support for fault tolerance. This lets application developers achieve fault tolerance at high failure rates while also using efficient communication protocols in the native MPI libraries that are generally fine-tuned for specific HPC platforms. We have also implemented efficient parallel communication techniques that involve replicas. Our framework deals with the unique challenges of integrating support for checkpointing and partial replication.

3.3.4.1.2 SERC Resources Used:

We scaled our experiments up to 8192 processors.

3.3.4.1.3 Performance and scalability:

We have conducted experiments emulating the failure rates of exascale computing systems and showed that our replication-based library outperforms checkpointing-based approaches at a large scale.

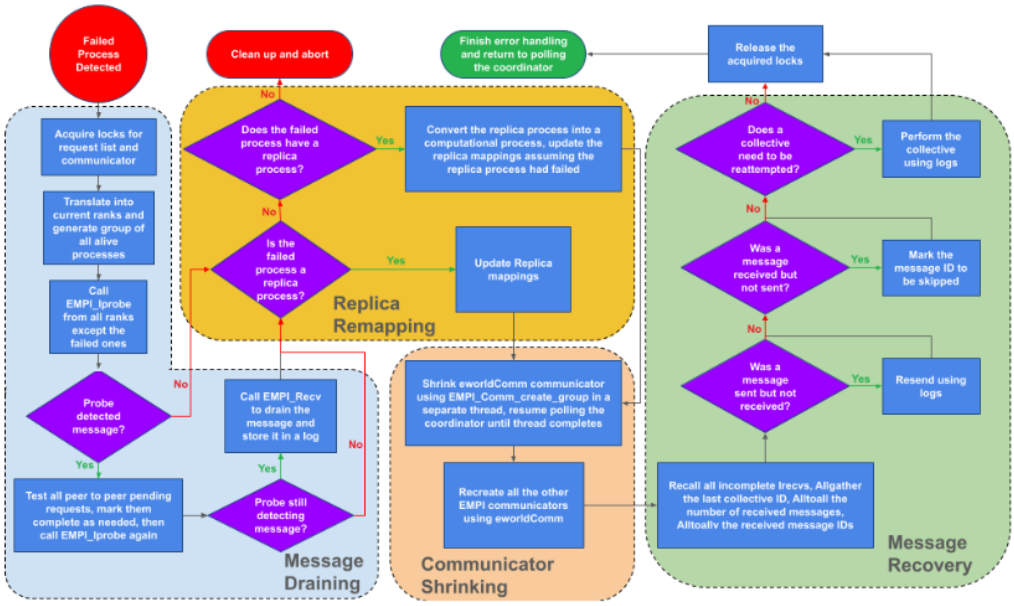

Workflow for Handling Failures

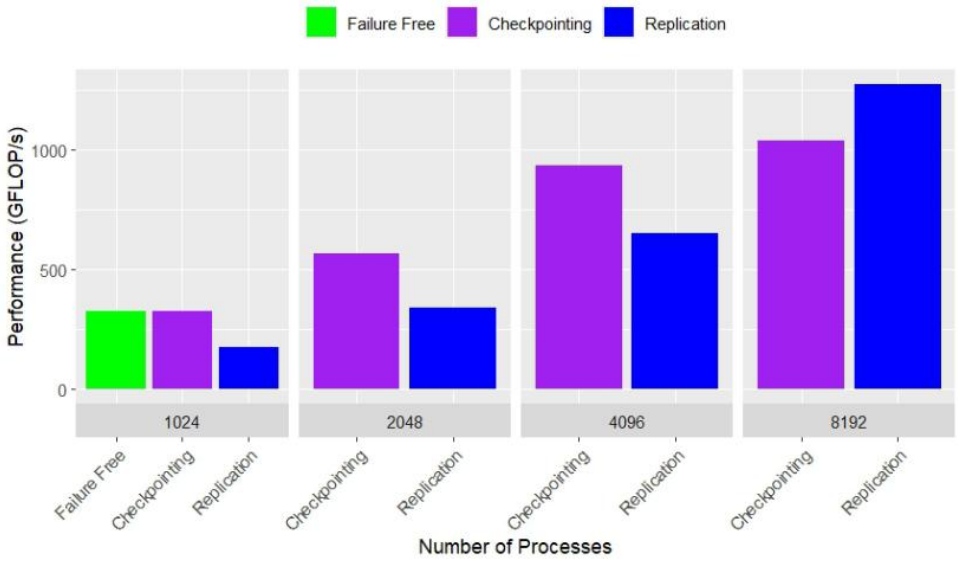

Fault Tolerance with HPCG Application

3.3.4.2 A Divide-and-conquer Model for Asynchronous Training of Large-Scale CNNs using Variational Dropouts

3.3.4.2.1 Problem areas:

We proposed a divide-and-conquer model for asynchronous training of large-scale Convolution Neural Networks (CNNs) for image classification tasks on multiple devices. Our work forms multiple small models from a given large model for asynchronous executions using the variational dropouts of the neurons. The sub-models retain only some of the

neurons and their corresponding edges from the original model. The sizes of the sub-models can be tuned to be accommodated in the GPU memory. Different sub-models are trained asynchronously on different GPUs, and the trained sub-models are merged to form the weights of the original large model. Unlike the existing parallelism models that require synchronization for every forward and back-propagation passes during the course of training, our framework, DiasDNN, performs synchronization only at the end of training after a certain number of epochs of the sub-models. Our framework effectively overcomes the memory-related limitations of data parallelism, communication and synchronization bottlenecks of tensor and hybrid parallelism, and device idleness of methods based on model parallelism.

3.3.4.2.2 SERC Resources Used:

The study was conducted using up to eight GPU nodes of Param Pravega.

3.3.4.2.3 Parallelization strategies:

The given *Large Model* is first trained for one epoch on the CPU. This limited training is used to calculate the *Dropout Information*. Using the *Large Model* and the *Dropout Information*, *Small Models* are generated for each process. Each small model is a sub-model containing a subset of the neurons and the edges from the large model. These small models are then distributed amongst the various processes and then asynchronously trained on the GPUs for a certain number of epochs, called a set of training. At the end of one set of asynchronous training, the small models are then merged in the master node to form a *Union Model*. The union model contains the union of the neurons and edges of the individual small models and is a sub-model of the original large model. The large model is then updated with the parameters of the union model. The updated large model is then used to generate the next set of small models for asynchronous computations on the nodes. The process is repeated until the accuracy of the union model converges.

3.3.4.2.4 Performance and scalability:

Our experiments with three models and two datasets on up to 16 GPUs show that overall, DiasDNN reduces the training times by 1-2 hours when compared to the default data parallel model and achieves 1.4x-2.4x speedup over PaSE, a state-of-art framework that employs hybrid parallelism model. DiasDNN also exhibits high scalability with increasing number of GPUs.

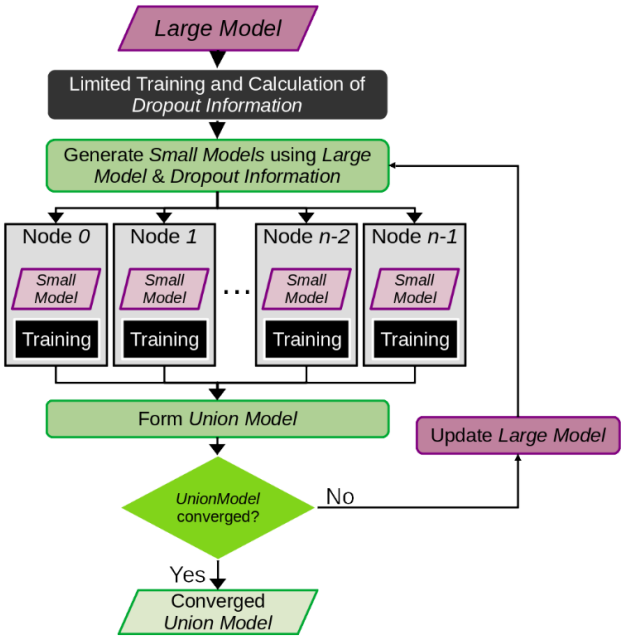

DiasDNN Architecture

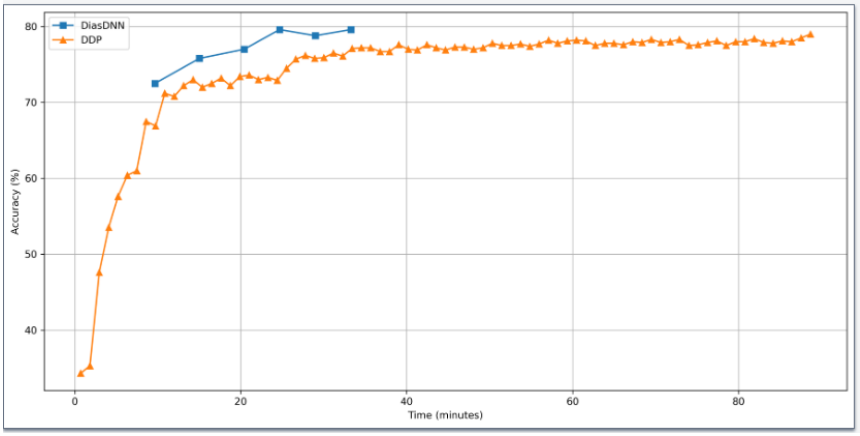

Superior Performance of DiasDNN over Distributed Data Parallelism (DDP)

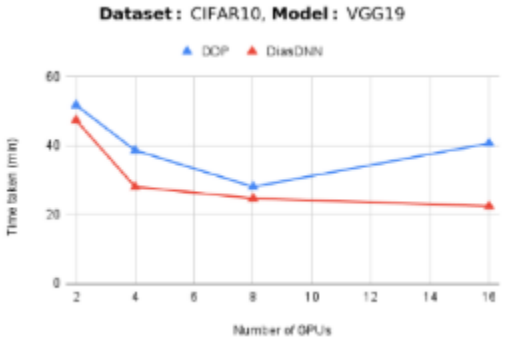

Scalability of DiasDNN

3.4 Chemical Engineering (CE)

3.4.1 Prof. Ananth Govind Rajan's Lab

3.4.1.1 Problem areas:

During 2022–24, SERC's HPC resources enabled large-scale simulations and machine learning studies spanning nanoporous 2D materials, catalysis, and energy applications. HPC runs were critical for generating chemical space datasets of nanopores, where molecular mechanics data-based ML models established structure–property relationships relevant to CO2 capture. High-throughput kinetic Monte Carlo simulations helped develop generalized models for 2D polymer growth and for predicting the topologies of nanopores in MoS2. Atomistic simulations uncovered nanoscale mechanisms of MoS_2 chemical vapor deposition, while first-principles studies explained the facet-dependent activity of NiFe oxyhydroxides in oxygen evolution. Intensive DFT and microkinetic analyses identified low-overpotential pathways for CO_2 reduction to CH_4 and screened single-atom catalysts for C1 hydrocarbon formation. Charge prediction models for long boron nitride nanotubes, enabled by HPC-driven quantum-mechanical data, advanced simulations of water transport in nanoconfinement. Simulations also clarified how grain boundaries, interfacial charges, and surface roughness affect wetting, slip, and desalination efficiency. Together, these studies highlight how SERC's HPC facility powered predictive modeling across scales, from electronic structure to molecular dynamics, solving fundamental problems in catalysis, separations, and nanomaterials design.

3.4.1.2 SERC's resources:

Our group utilized the Param Pravega supercomputer, the Roddam Narasimha cluster, as well as the DGX machine. We used both CPU and GPU resources, typically using anywhere between 96-240 CPU cores and several GPUs.

3.4.1.3 Parallelization strategies employed:

The parallelization strategies are based on the open-source LAMMPS (Large-scale Atomic/Molecular Massively Parallel Simulator) and cp2k packages, and the commercial VASP (Vienna Ab initio Simulation Package) code. In some cases, several runs of simulations were done in parallel to generate large datasets for training machine learning models.

3.4.1.4 Publications:

1. Sharma, P., Thomas, S., Nair, M., Govind Rajan, A.* Machine Learnable Language for the Chemical Space of Nanopores Enables Structure-Property Relationships in Nanoporous 2D Materials. J. Am. Chem. Soc. 2024, 146, 44, pp 30126–30138.
2. Paliwal, S., Li, W., Liu, P.*, Govind Rajan, A.* Generalized Model for Inhibitor-Modulated 2D Polymer Growth to Understand the Controlled Synthesis of Covalent Organic Frameworks. JACS Au 2024, 4, 8, pp 2862–2873
3. Govind Rajan, A.*, Martirez, J. M. P., Carter, E. A.* Strongly Facet-Dependent Activity of Iron-Doped β-Nickel Oxyhydroxide for the Oxygen Evolution Reaction. Phys. Chem. Chem. Phys. 2024, 26, pp 14721–14733. (Invited article for the special issue "25th PCCP Anniversary Issue".)

4. Kumar, S., Govind Rajan, A.* Predicting Quantum-Mechanical Partial Charges in Arbitrarily Long Boron Nitride Nanotubes to Accurately Simulate Nanoscale Water Transport. J. Chem. Theor. Comput. 2024, 20, 8, pp 3298–3307.
5. Ghorai, S., Govind Rajan, A.* From Molecular Precursors to MoS2 Monolayers: Nanoscale Mechanism of Organometallic Chemical Vapor Deposition. Chem. Mater. 2024, 36, 6, pp 2698–2710.
6. Lal, D., Konnur, T., Verma, A. M., Shaneeth, M., Govind Rajan, A.* Unraveling Low Overpotential Pathways for Electrochemical CO2 Reduction to CH4 on Pure and Doped MoS2 Edges. Ind. Eng. Chem. Res. 2023, 62, 49, pp 21191–21207. (Invited article for the special issue "2023 Class of Influential Researchers".)
7. Seal, A., Tiwari, U., Gupta, A., Govind Rajan, A.* Incorporating Ion-Specific van der Waals and Soft Repulsive Interactions in the Poisson-Boltzmann Theory of Electrical Double Layers. Phys. Chem. Chem. Phys. 2023, 25, pp 21708–21722.
8. John, A., Verma, A. M., Shaneeth, M., Govind Rajan, A.* Discovering a Single-Atom Catalyst for CO2 Electroreduction to C1 Hydrocarbons: Thermodynamics and Kinetics on Aluminum-Doped Copper. ChemCatChem 2023, 15 (14), e202300188.
9. Bhowmik, S., Warner, J. H., Govind Rajan, A.* Role of Chemical Etching in the Nucleation of Nanopores in 2D MoS2: Insights from First-Principles Calculations. J. Phys. Chem. C 2023, 127 (14), pp 6873–6883. (Invited article for the special issue "Early-Career and Emerging Researchers in Physical Chemistry Volume 2".)
10. Thomas, S., Silmore, K., Sharma, P., Govind Rajan, A.* Enumerating Stable Nanopores in Graphene and their Geometrical Properties Using the Combinatorics of Hexagonal Lattices. J. Chem. Inf. Model. 2023, 63 (3), pp 870–881.
11. Verma, A. K., Govind Rajan, A.* Surface Roughness Explains the Observed Water Contact Angle and Slip Length on 2D Hexagonal Boron Nitride. Langmuir 2022, 38 (30), pp 9210–9220. (This article was amongst the most-read ones in Langmuir a month after its publication.)
12. Sheshanarayana, R., Govind Rajan, A.* Tailoring Nanoporous Graphene Via Machine Learning: Predicting Probabilities and Formation Times of Arbitrary Nanopore Shapes. J. Chem. Phys. 2022, 156, 204703. (This article is a part of the "Emerging Investigators Special Collection" and was selected as an "Editor's Pick".)
13. Sharma, B. B., Govind Rajan, A.* How Grain Boundaries and Interfacial Electrostatic Interactions Modulate Water Desalination Via Nanoporous Hexagonal Boron Nitride. J. Phys. Chem. B 2022, 126 (6), pp 1284–1300.

3.4.1.5 Contributions:

The HPC-enabled studies advanced clean energy technologies by identifying catalysts for CO_2 conversion (for the Indian Space Research Organization) and water-splitting (with National Supercomputing Mission support), directly contributing to national goals on carbon neutrality and renewable energy. Insights into nanoscale water transport and nanoporous membranes support affordable desalination and clean water initiatives (research supported by Anusandhan National Research Foundation). Machine learning frameworks for nanoporous materials accelerate materials discovery relevant to gas separations (NSM-supported work). These contributions benefit industry by guiding catalyst design (collaborations with Shell and HPCL) and scalable synthesis of 2D materials (collaboration with Lam Research), while society gains through improved sustainability, clean water solutions, and reduced carbon emissions.

Designing nanopores for CO_2 capture via ML

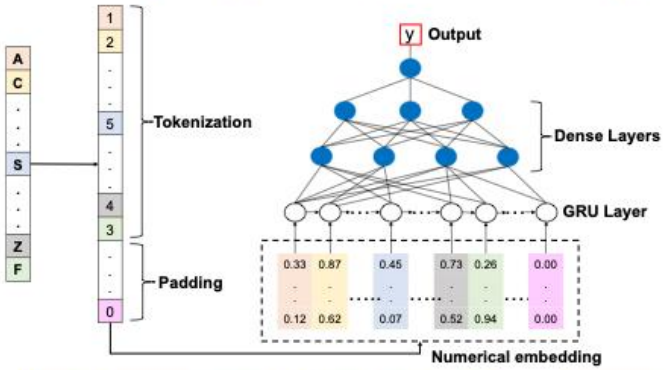

Metric	CO_2 barrier prediction	
	Training set (five folds)	Test set
R^2	0.98	0.95
MAE (kcal/mol)	0.95	1.52

Metric	N_2 barrier prediction	
	Training set (five folds)	Test set
R^2	0.99	0.96
MAE (kcal/mol)	0.65	1.18

Use of recurrent neural networks with a gated recurrent unit (GRU) enables prediction of nanopore properties directly from strings

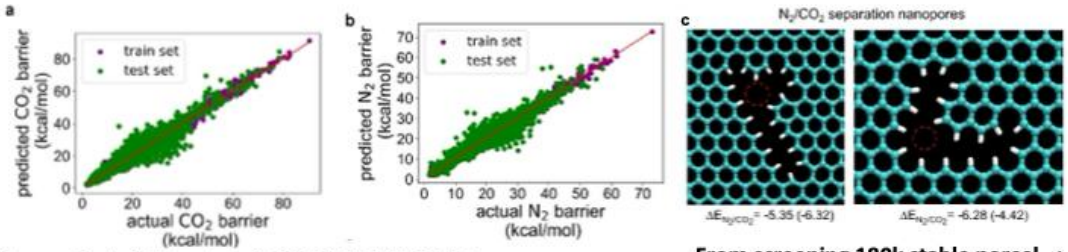

Sharma, **Govind Rajan**, et al. *JACS* **2024**, 146, 44, 30126

From screening 180k stable pores! 1

Can we predict 2D nanopore probabilities and formation times using ML?

Encoding nanopores into physical features

N = 12

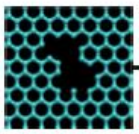

Shape factor (S):

$$A_{hex} = \frac{3\sqrt{3}}{2} {l_{CC}}^2$$

$$d_{circ} = \sqrt{\frac{4 n_{hex} A_{hex}}{\pi}}$$

$$S = \frac{d_{circ}}{d_{max}}$$

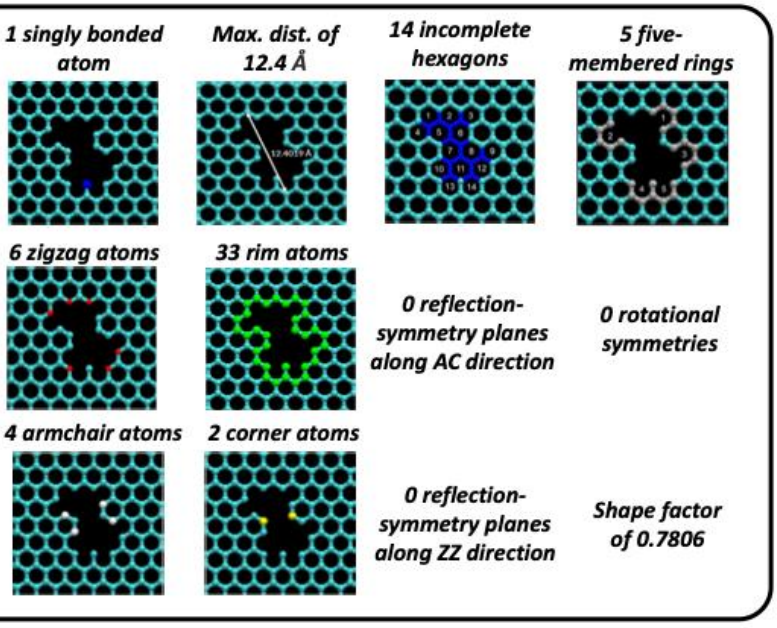

Sheshanarayana and **Govind Rajan**, *J. Chem. Phys.* **2022**, 156, 204703 2

Machine learnable language for nanopores in 2D materials

Edge atom type	Character
Fully bonded	F
Zigzag	Z
Armchair	A
Corner	C
Singly bonded	S

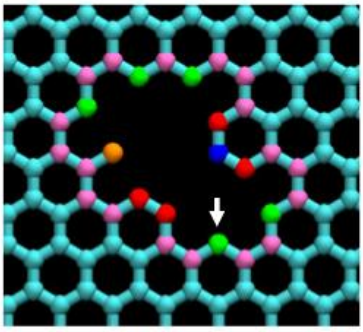

ZFFZFFFACAFFFZFZFFZFFFSFFAAFF

"STring Representation Of Nanopore Geometry (STRONG)" Enables…

Rapid comparison of nanopore topologies

Enumeration of unique functionalized configurations

Structure-property relationships via neural networks

Sharma, **Govind Rajan**, et al. *JACS* **2024**, 146, 44, 30126

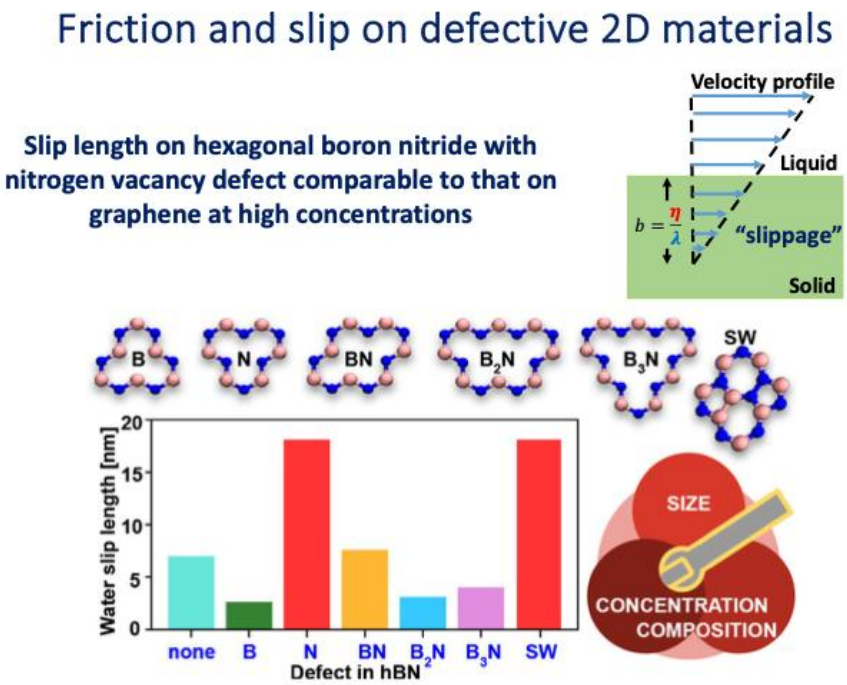

3.4.2 Prof. K Ganapathy Ayappa's Lab

3.4.2.1 Problem areas:

Membrane Biophysics: We have developed all-atom and coarse grained models to study the interaction of antimicrobial and surfactant molecules with bacterial membranes. A coarse-grained model for the outer membrane of Gram-positive bacteria has been developed for the first time enabling sampling dynamics up to 10-100's of microseconds. Path based free energy methods allowed us to decipher the role of membrane cholesterol in pore forming toxin membrane assisted folding pathways.

2D Nanoporous Materials: Graphene nanopores have been shown to enhance evaporation rates of water. These materials can potentially be used for low energy evaporative separations. A kinetic Monte Carlo method has been adapted to reliably estimate diffusion coefficients in gas mixtures to improved selectivity predictions.

3.4.2.2 SERC's Resource:

Param Pravega.

3.4.2.3 Publications:

1. Structure of the Bacterial Cell Envelope and Interactions with Antimicrobials: Insights from Molecular Dynamics Simulations, Pradyumn Sharma, Rakesh Vaiwala, Amar

Krishna Gopinath, Rajalakshmi Chockalingam, K. Ganapathy Ayappa, Langmuir, 40, 7791-7811 (2024). 10.1021/acs.langmuir.3c03474.

2. Martini-3 Coarse-Grained Models for the Bacterial Lipopolysaccharide Outer Membrane of Escherichia coli, Rakesh Vaiwala, K. Ganapathy Ayappa, Journal of Chemical Theory and Computation, 20, 1704-1716 (2024). https://doi.org/10.1021/acs.jctc.3c00471
3. Implementing Trajectory Extending Kinetic Monte Carlo Simulations to Evaluate Pure and Gas Mixture Diffusivities through Dense Polymeric Membrane, Subhadeep Dasgupta, K. S. Arun, K. Ganapathy Ayappa and Prabal K. Maiti, Journal of Physical Chemistry B, 127, 9841-9849 (2023). https://doi.org/10.1021/acs.jpcb.3c05661
4. Selective Photonic Gasification of Strained Oxygen Clusters on Graphene for Tuning Pore Size in Å-Regime, Bondaz, Luc; Ronghe, Anshaj; Li, Shaoxian; Cernevics, Kristians; Hao, Jian; Yazyev, Oleg; Ayappa, K. Ganapathy; Agrawal, Kumar Varoon, JACS Au 3, 10, 2844-2854 (2023). https://doi.org/10.1021/jacsau.3c00395
5. Cholesterol Catalyzes Unfolding in Membrane Inserted Motifs of the Pore Forming Protein Cytolysin A, Avijeet Kulshrestha, Rahul Roy, Sudeep Punnathanam, K. Ganapathy Ayappa, Biophysical Journal, 122, 4068-4081 (2023) https://doi.org/10.1016/j.bpj.2023.09.005
6. Graphene Nanopores Enhance Water Evaporation from Salt Solutions: Exploring the Effects of Ions and Concentration, Anshaj Ronghe and K. Ganapathy Ayappa, Langmuir, 39, 8787–8800 (2023). https://doi.org/10.1021/acs.langmuir.3c00797
7. Conformational Flexibility is a Key Determinant for the Lytic Activity of the Pore-Forming Protein, Cytolysin A: Kulshrestha, Avijeet; Maurya, Satyaghosh; Gupta, Twinkle; Roy, Rahul; Punnathanam, Sudeep; Ayappa, K. Ganapathy, Journal of Physical Chemistry B 127, 69-84 (2023). https://doi.org/10.1021/acs.jpcb.2c05785
8. Interactions of Surfactants with the Bacterial Cell Wall and Inner Membrane: Revealing the Link Between Aggregation and Antimicrobial Activity, Pradyumn Sharma, Rakesh Vaiwala, Srividhya Parthasarathi, Nivedita Patil, Anant Verma, Morris Waskar, Janhavi Raut, Jaydeep K. Basu and K. Ganapathy Ayappa, Langmuir, 38, 15714-15728 (2022). https://doi.org/10.1021/acs.langmuir.2c02520
9. Finite Temperature String Method with Umbrella Sampling using Path Collective Variables: Application to Secondary Structure Change in a Protein, Avijeet Kulshrestha, Sudeep N. Punnathanam and K. Ganapathy Ayappa, Soft Matter, 18, 7593-7603 (2022). https://doi.org/10.1039/D2SM00888B
10. Influence of Chain Length on Structural Properties of Carbon Molecular Sieving Membranes and their Effects on CO2, CH4 and N2 adsorption: A Molecular Simulation Study, Subhadeep Dasgupta, Rajasekaran M., Projesh K.Roy, Foram M.Thakkar, Amar Deep Pathak, K. Ganapathy Ayappa and Prabal K.Maiti, Journal of Membrane Science, 664, 121044 (2022). https://doi.org/10.1016/j.memsci.2022.121044
11. Differentiating Interactions of Antimicrobials with Gram-negative and Gram-positive Bacteria using Molecular Dynamics Simulations, Rakesh Vaiwala, Pradyumn Sharma and K. G. Ayappa, Biointerphases, 17, 061008 (2022).https://doi.org/10.1116/6.0002087
12. A Molecular Dynamics Study of Antimicrobial Peptide Translocation Across the Outer Membrane of Gram-negative Bacteria, Pradyumn Sharma, K. G. Ayappa, Journal of Membrane Biology, 255, 665–675 (2022). https://doi.org/10.1007/s00232-022-00258-6
13. Microtubule Dynamics and the Coupling to Mitochondrial Population Evolution in Fission Yeast Cells: A Kinetic Monte Carlo Study, Samlesh Choudhary, Vaishnavi Ananthanarayanan and Ganapathy Ayappa, Soft Matter, 18, 4483-4492 (2022). https://doi.org/10.1039/D2SM00155A

14. Enhanced Water Evaporation from Å-scale Graphene Nanopores, Wan-Chi Lee1, Anshaj Ronghe, Luis Francisco Villalobos, Shiqi Huang, Mostapha Dakhchoune, Mounir Mensi, Kuang-Jung Hsu, K. Ganapathy Ayappa and Kumar Varoon Agrawal, ACS Nano 16, 9, 15382–15396 (2022). https://doi.org/10.1021/acsnano.2c07193
15. Influence of the Extent of Hydrophobicity on Water Organization and Dynamics on 2D Graphene Oxide Surfaces,M. Rajasekaran and K. Ganapathy Ayappa, Physical Chemistry Chemical Physics (PCCP) 24, 14909-14923 (2022). https://doi.org/10.1039/D1CP03962H

3.4.2.4 Contributions:

Our work on bacterial membranes has been supported by Hindustan Unilever (HUL) Industries. Our coarse grained bacterial membrane models are currently being used by HUL to test and design novel antimicrobials for specific applications. Our work on assessing polymeric membranes for CO_2 separations was funded by Shell RandD Bangalore India. Our work has indicated the importance of accurately computing transport properties to reliably assess membrane performance.

International Collaborations: Our research on exploring low cost evaporative water separations using 2D graphene nanoporous materials was carried out in collaboration with the group of Kumar Varoon Agarwal at EPFL Switzerland where experiments were carried out

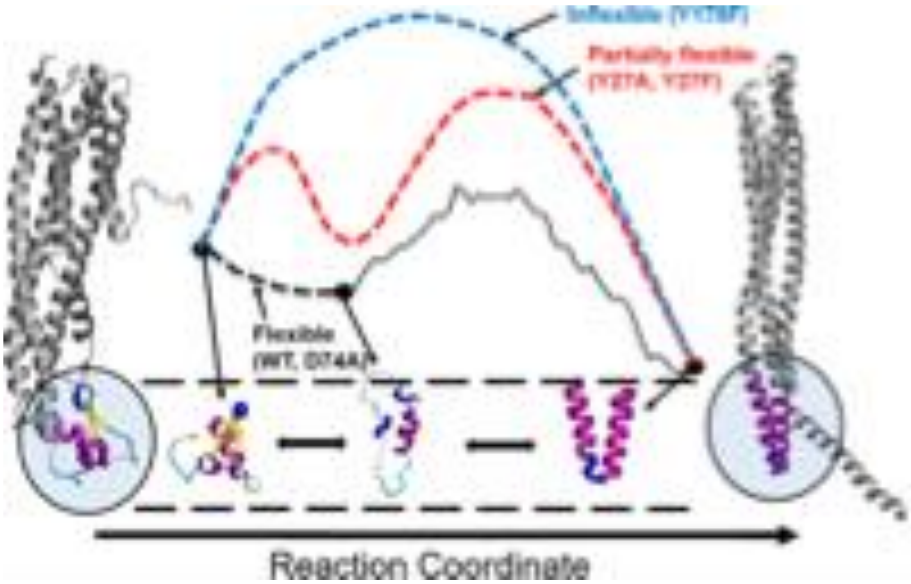

Path based free energy computations carried out on Param Pravega to illustrate the membrane assisted folding transition of the pore forming toxin cytolysin A, expressed by E. coli to mediate bacterial infections. Adapted from Kulshrestha et al. J. Phys. Chem B, 2023.

3.4.3 Prof. Sudeep N. Punnathanam's Lab

3.4.3.1 Problem Areas:

Studying the mechanism of NaCl crystal nucleation from aqueous solutions: We are trying to unravel the mechanism of crystal nucleation of sodium chloride using theoretical approach. In this approach we need the values of free energy changes for each step in the formation of a nuclei of sodium chloride to calculate the nucleation rate. However, such free energy calculations are required across a vast 3 dimensional phase space for the given system. In other words, there is a need to run many simulations corresponding to umbrella sampling method with different input parameters to obtain the free energy surfaces, which needs huge computational resources. Another factor that contributes to computational requirements is the nature of the system. The NaCl-water system is a simple looking system but has many complexities due to which it takes very long time to equilibrate the system. Hence, to study this system and obtain the free energy values, we need significant computational resources at our disposal.

3.4.3.2 SERC resources used:

Only Param-Pravega supercomputer was used.

- CPU queues – 15360 cores x 24 hours x 4 jobs (approximate)
- GPU queues – (1gpu + 16 cores) x 48 hours x 60 jobs (approximate)

3.4.3.3 Parallelization strategy:

The codes and software used in these simulations use MPI based parallelization.

3.4.3.4 Performance and Scalability:

The Param-Pravega supercomputer is very fast and offers comparable speed to the group-owned cluster machines, even when running jobs across multiple nodes, which is not the case elsewhere.

3.5 Earth Sciences

3.5.1 Prof. Attreyee Ghosh's Lab

3.5.1.1 Problem areas:

The Earth's mantle behaves as a fluid over very long time scales. Numerous studies have simulated the fluid dynamical behavior of the mantle in order to understand the various observed phenomena on the Earth's surface. We solve the governing equations for mantle convection, which are based on the conservation of mass, momentum, and energy, along with the constitutive equation, using a finite element open source code called CitcomS. Some of the problems that have been handled by my group during the period 2022-2024 are: stability of cratons (Paul et al., 2023), origin of the Indian Ocean geoid low (Ghosh & Pal, 2022; Pal & Ghosh, 2023), constraining the initial state of the mantle (Pal & Ghosh, 2024),

sudden acceleration of the Indian plate, understanding the complex anisotropy pattern in western United States (Aashruti et al., 2025). For the time-dependent convection models, we impose reconstructed plate motions as surface velocity boundary condition, which drive flow within the model mantle. Imposing these reconstructed velocities every 1 Myr starting from 140 Ma in forward models of mantle convection, we predict present day temperature anomalies throughout the mantle, as well as surface observations, such as the geoid and topography.

3.5.1.2 SERC's resources:

We used both the normal and high priority queues in Param Pravega as well as cores in RNC. The runs in Param Pravega mostly used 384 cores while those in RNC used 96 cores.

3.5.1.3 Publications:

1. Aashruti, A. Ghosh, E. Humphreys, Western US Anisotropy: Role of Slabs, Lateral Viscosity Varia tions and Small- Scale Heterogeneity, Journal of Geophysical Research, under Revision.
2. D. Pal, A. Ghosh, Present day mantle structure from global mantle convection models since the Cre taceous, Geophysical Journal International, 238, p. 1651-1675, 2024.
3. D.Pal, A. Ghosh, How the Indian Ocean Geoid Low Was Formed, Geophysical Research Letters, 50, e2022GL102694, doi:10.1029/2022GL102694, 2023.
4. J. Paul, C. P. Conrad, T. W. Becker, A. Ghosh, Convective Self-Compression of Cratons and the Stabi lization of Old Lithosphere, Geophysical Research Letters, 50, e2022GL101842, doi:10.1029/2022GL101842, 2023.
5. A. Ghosh, D. Pal, Do lower mantle slabs contribute in generating the Indian Ocean Geoid Low? Tectonophysics, 822, doi:10.1016/j.tecto.2022.229176, 2022.

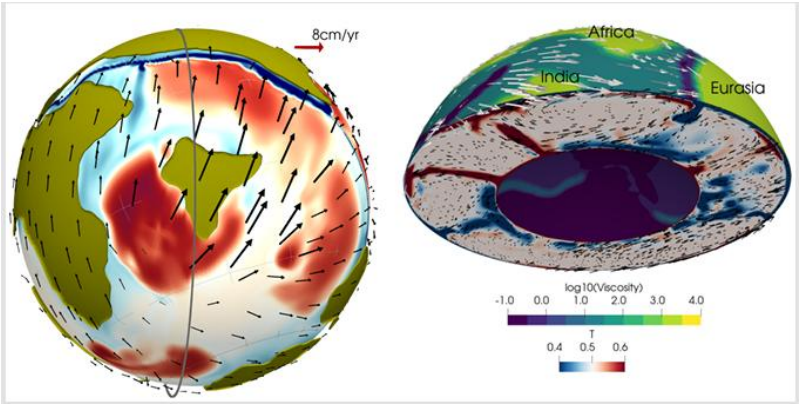

Figure: Mantle structure plate velocity

3.5.2 Prof. Binod Sreenivasan' Lab

3.5.2.1 Problem area:

This study shows that the suppression of the hybrid slow magnetic–Archimedean–Coriolis (MAC) waves serves as a powerful criterion for the dipole–multipole transition of the magnetic field in rapidly rotating dynamos. Similarly, the generation of slow MAC waves is found to be essential for the formation of a dipole from a chaotic multipolar state. Figure (a) shows the variation of the modified Rayleigh number Ra with the peak Elsasser number Λ (square of the peak magnetic field) at both excitation and suppression of slow MAC waves. The hollow symbols represent the states where slow waves are first excited as the dynamos evolve from a small seed field; the filled symbols represent the states where slow waves are suppressed in the polarity-reversing dynamos. When Ra is scaled by the buoyant perturbation length scale, a self-similar relation with Λ results (Figure b), confirming that the two regimes—(i) dipole–multipole transition through the suppression of slow MAC waves and (ii) dipole formation through the excitation of slow MAC waves—are dynamically similar

processes. Figures (c) and (d) show contour plots of the radial magnetic field at the outer boundary, illustrating the transition from a chaotic multipolar state to a dipolar magnetic field in the dynamo simulation marked '1' in Figure (b).

3.5.2.2 SERC Resources:

- SERC's HPC systems have been used to solve the planetary dynamo problem, where the processes that generate and sustain the magnetic fields in Earth and other planets in our Solar system are investigated. The problems of particular interest are the preference for the axial dipole field in planets and mantle control of planetary core convection.
- Most of our problems are solved using 1440 CPUs on Param Pravega.
- The problems are solved in a spherical shell geometry, with 2D MPI parallelism employed in the radial and latitudinal directions.
- The planetary dynamo code scales approximately linearly up to 3000 CPUs.

3.5.2.3 Publications:

1. D. Majumder, B. Sreenivasan and G. Maurya, Self-similarity of the dipole–multipole transition in rapidly rotating dynamos, J. Fluid Mech., 980, A30, 2024.
2. D. Majumder and B. Sreenivasan, The role of magnetic waves in tangent cylinder convection, Phys. Earth Planet. Inter., 344, 107105, 2023.
3. Varma and B. Sreenivasan, The role of slow magnetostrophic waves in the formation of the axial dipole in planetary dynamos, Phys. Earth Planet. Inter., 106944, 2022.

3.5.2.4 National programmes:

The work done by the Deep Earth research group in IISc led to a discussion meeting on 'Vitalizing Indian Earth Science with Necessary Cross-displinary Contents' held at the Indian Academy of Sciences on 25 & 26 October, 2024. Subsequently, a White Paper on this topic has been formulated by Binod Sreenivasan through the Academy.

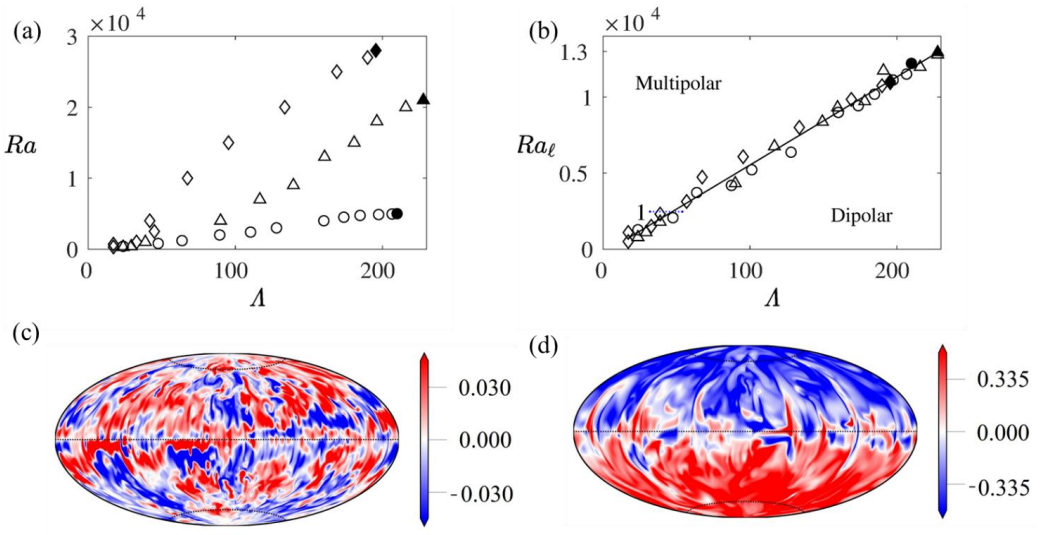

Figure: *Suppression of the hybrid slow magnetic–Archimedean–Coriolis (MAC) waves serves as a powerful criterion for the dipole–multipole transition of the magnetic field in rapidly rotating dynamos.*

3.5.3 Prof. D. Nagesh Kumar's Lab

3.5.3.1 Problem statement(s):

The following objectives of the work were carried out in PARAM Pravega.

1. To systematically identify the sensitive parameters within various hydrologic model structures and employ them to discern the dominant hydrological processes of the catchment.
2. To investigate the impact of various modeling decisions like model structure, spatial discretization, spatial representation of forcing and performance metrics on flood simulation.
3. To simulate unprecedented rainfall events using Stochastic Rainfall Generator (SRG) across India to evaluate hydrologic risk.

3.5.3.2 SERC's resources employed:

Objectives 1–2 : All simulations and analyses required to meet the study objectives were computationally intensive. The modelling framework used in the sudy i.e., SUMMA (Structure for Unifying Multiple Modelling Alternatives), involves hundreds of parameters, making sensitivity analysis computationally demanding as it required nearly four thousand model runs. To address this challenge, we parallelised the simulations across multiple cores of the Param Pravega supercomputer.

Ex: If run serially, the time taken to execute one model run for sensitivity analysis would be:

= 4950 runs * 47 min/run = 2,32,650 min ~ 162 days ~ 5. 4 months

The same task when run parallelly in multiple cores in Param Pravega with the following resources took,

No of nodes requested = 10

No of cores = 10 *48 cores/node = 480

Model runs per core =10 runs

Additional runs = 150 runs

Time taken = 10 runs per core * 47min/run + time taken for additional runs in each core (47 min) = 470 + 47 = 517 min ~ 8.6 hours (wall time)

Similarly, the calibration strategy for evaluating different model configurations required each configuration to be executed about a thousand times, which was infeasible when run in serial. Therefore, all computationally demanding tasks were executed in parallel using MPI-based parallelism across multiple nodes of Param Pravega.

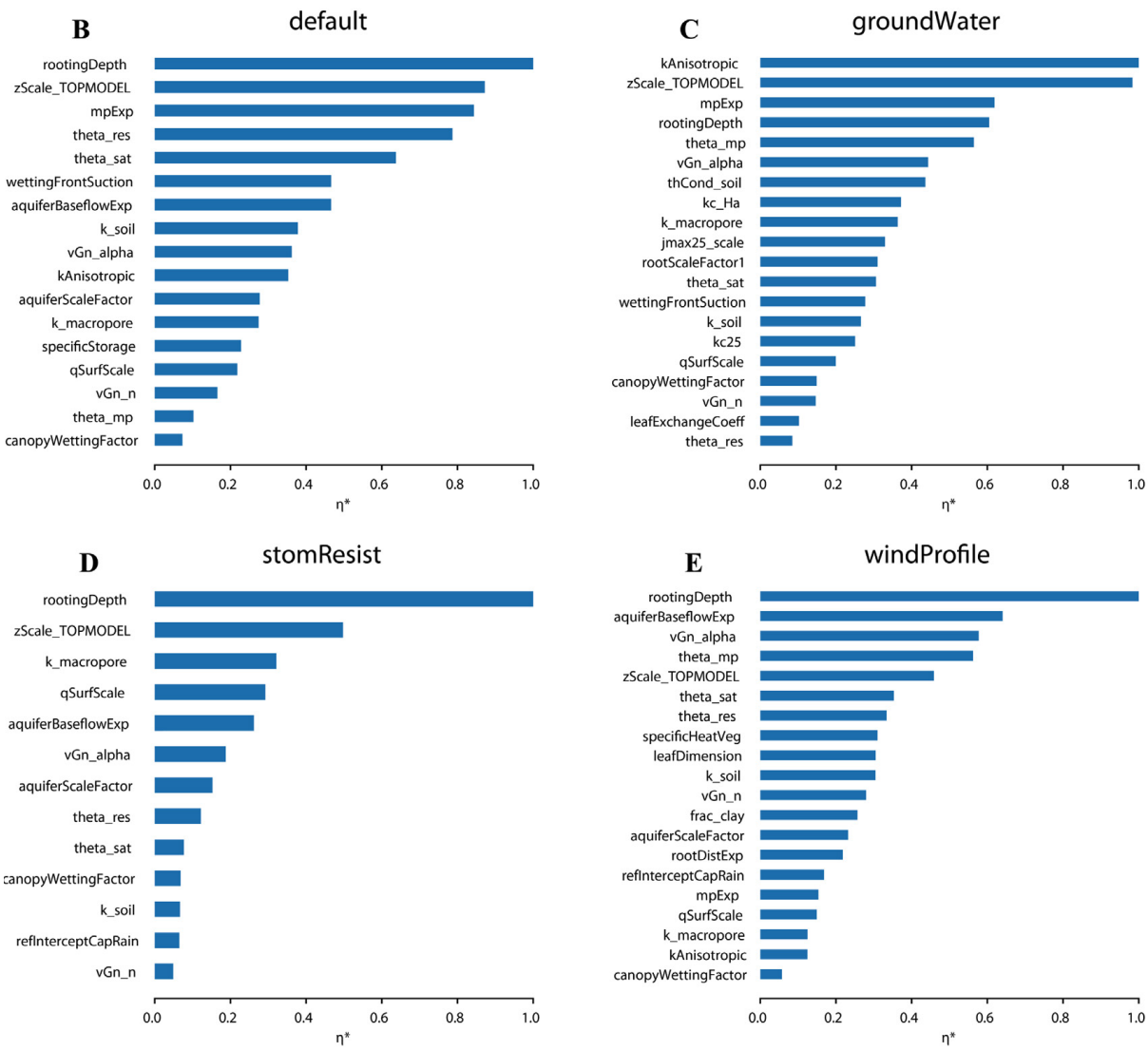

Fig.1: *Sensitive parameters of SUMMA for various model structures for the Netravathi basin of India.*

Objective 3: To investigate the impact of unprecedented rainfall events across India due to climate change, we carried out simulations on 285 grid points across India spaced at one-degree latitude–longitude resolution, using a Stochastic Rainfall Generator (SRG). Historical rainfall data from the India Meteorological Department (1901–2004) were employed at each grid point. Simulating rainfall series for a single grid point on a standard lab desktop took approximately five hours. Consequently, running the SRG model serially across all 285 grid points for one scenario would take approximately 2.5 months (285 grid points * 5 h ≈ 1425 h ≈ 60 d). Likewise, we had to simulate thirty-six scenarios for the study. To expedite the process, we parallelized the simulations on the Param Pravega supercomputer. By parallelizing the process, we reduced the computational time to just one day per scenario by utilizing 96 cores (2 nodes) of Param Pravega.

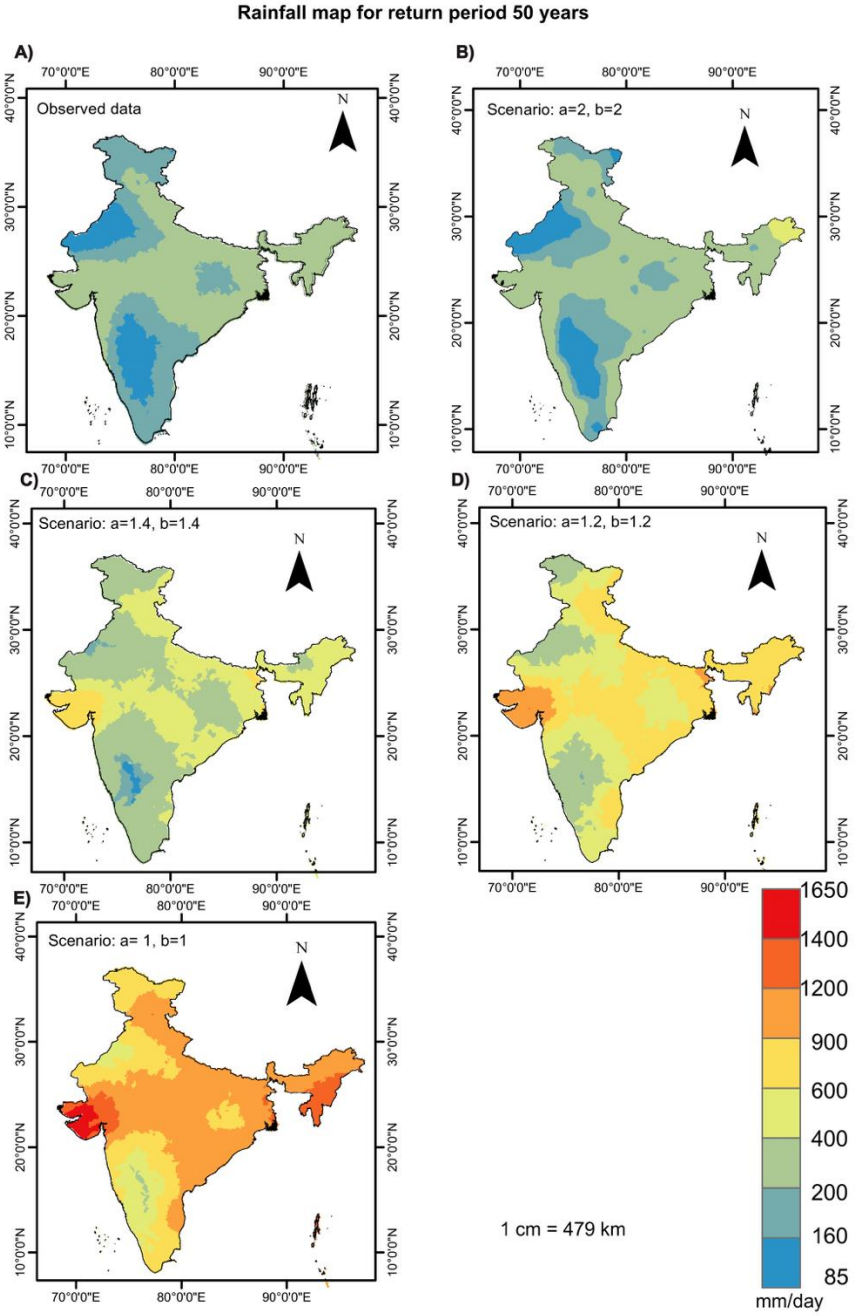

Fig. 2: *Rainfall depths (mm) for 50-year return period across India using daily observed and simulated rainfall series from SRG for four extreme scenarios*.

3.5.3.3 Publications:

1. Alexander, D. N. Kumar, W. J. Knoben, and M. Clark, “Evaluating the parameter sensitivity and impact of hydrologic modeling decisions on flood simulations,” Advances in Water Resources, p. 104 560, 2023, issn: 03091708. doi: https://doi.org/10.1016/j.advwatres.2023.104560.
2. Alexander, T. Rasool, C. Kumar, S. Sahoo, R. D. Bhowmik, and D. N. Kumar, “Unprecedented rainfall events increase the magnitude of design storms,” Environmental Research Letters, p. 064011, 2025. doi: https://doi.org/10.1088/1748-9326/add175 .

3.6 Department Of Inorganic and Physical Chemistry (IPC)

3.6.1 Sai G. Ramesh’ Lab

3.6.1.1 Problem areas:

SERC's resources were used along with that available in the group in order to address a few interesting and compute intensive problems in theoretical chemistry. One was the study of nuclear quantum effects in small molecular systems through the use of simulations based on path integral methods. Another involves dynamics of excited state proton transfer via mixed quantum-classical simulations. In both, the approaches used were CPU intensive and benefited from the availability of high core count for intra-node parallelism in SERC's resources (RNC).

3.6.1.2 SERC's resources:

The Roddam Narasimha Cluster (RNC) was used, along with the group's compute resources.

3.6.1.3 Parallelization strategies employed:

In certain cases, OpenMP parallelism was used with code developed by the student, with simulations using either several or all available cores in a node. In other use cases, the intra-node parallelism as provided by the used package, such as Gaussian 16, was employed, with about 12-16 cores per Gaussian job.

3.6.1.4 Performance and scalability:

Students who used RNC did find it to be faster than the group's own resources.

3.6.1.5 Publications:

1. M. Arandhara and S. G. Ramesh, "Nuclear quantum effects in gas-phase ethylene glycol", Phys. Chem. Chem. Phys. 26, 19529 (2024).
2. M. Arandhara and S. G. Ramesh, "Nuclear quantum effects in hydroxide hydrate along the H-bond bifurcation pathway", J. Phys. Chem. A 128, 1600 (2024).
3. M. Arandhara and S. G. Ramesh, "Nuclear quantum effects in gas-phase 2-fluoroethanol", Phys. Chem. Chem. Phys. 26, 6885 (2024).

3.7 Molecular Biophysics Unit

3.7.1 Prof. Anand Srivastava's Lab

3.7.1.1 Problem areas:

NSM resource allowed us to work on several large-scale molecular simulations and mesoscopic simulations of biological systems that would not have been possible otherwise. For example, we worked on a 2 million all-atom biological membrane systems and show the presence of soft dynamic channels in outer ordered membrane, which can have huge influence in the way molecules encounter each other on plasma membrane (Journal of Chemical Physics, 2025[see image below]).

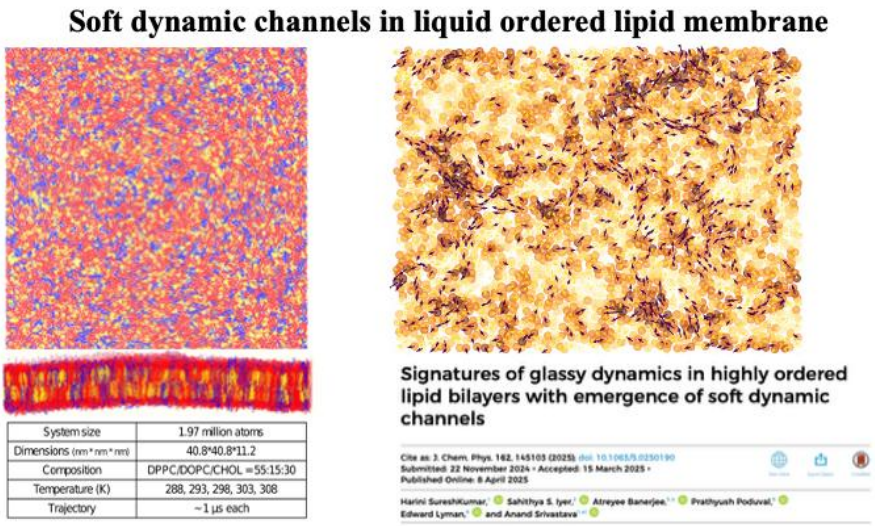

Similarly, we have carried out large scale simulations that have shed critical insights into processes such as (i) membrane vesicular trafficking, (ii) molecular grammar and mechanistic origins of neurological diseases such as Parkinson's and Alzheimer's diseases, (iii) ageing and molecular mechanism behind telomere maintenance and (iv) effect of mutations in Glioblastoma brain tumor patients. All of the above projects are described with images and movie files in the companion PPTX file (also see the collage below).

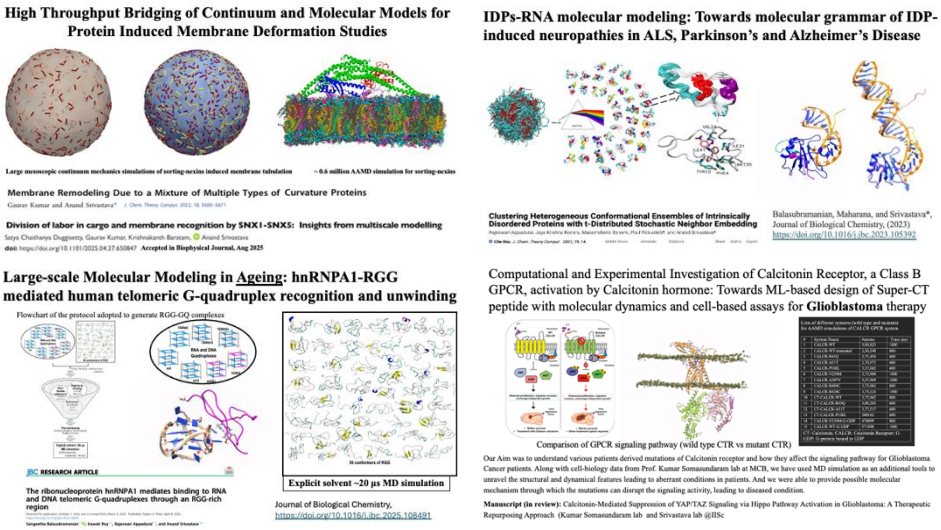

3.7.1.2 SERC's resources:

We have used SERC resources to simulate system size as big as 2 million atom simulations, where we have used as many as 4800 cores. Other systems have been of the order of 0.2 million to 1.0 million atoms, and we have employed anywhere between 480-4800 cores for these runs.

3.7.1.3 Parallelization strategies employed:

We use the available strategy in the software, which is mostly domain decomposition and multithreading. We do not code our own parallelization software.

3.7.1.4 Performance and scalability obtained:

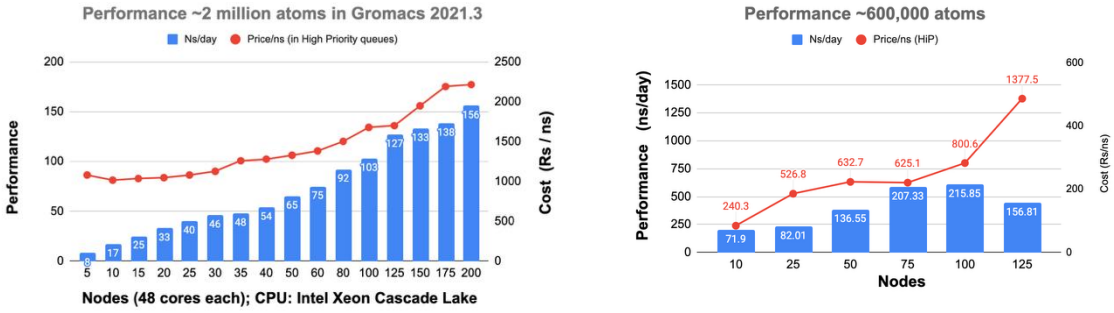

- EHD system (No. of atoms = 543817)

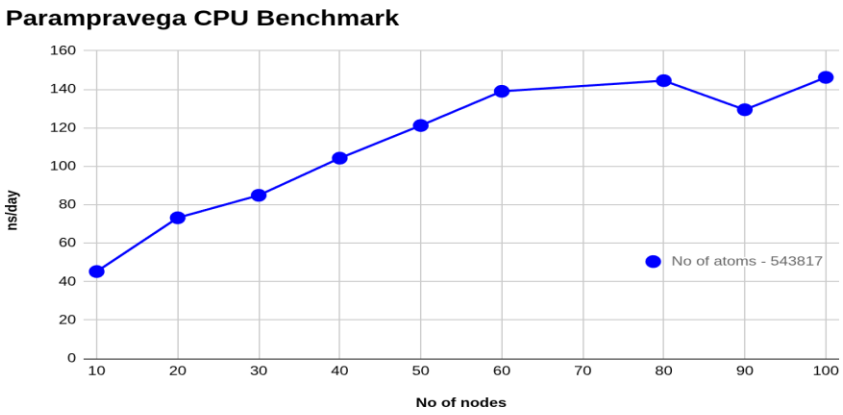

- Pure membrane system (No. of atoms = ~ 2 million)

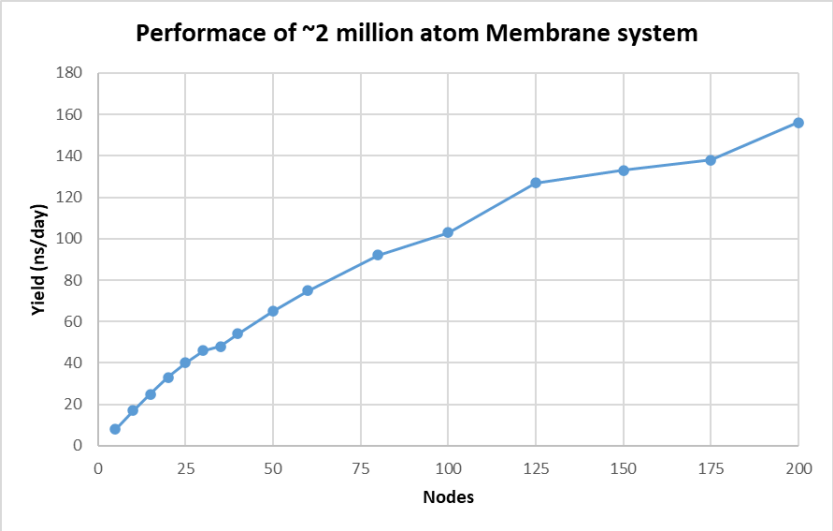

- Peripheral membrane protein & membrane system (No. of atoms = ~376,000 atoms)
  Alpha-synuclein with HMMM membrane

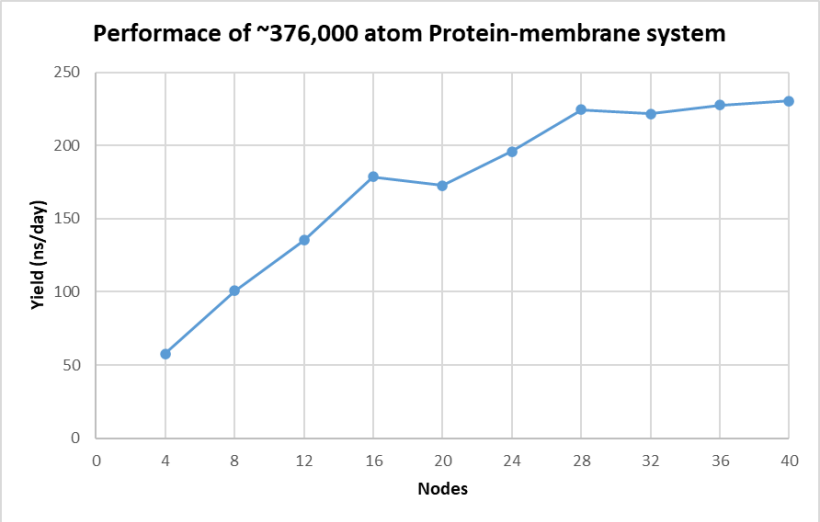

- Peripheral membrane protein & membrane system (No. of atoms = ~652,000 atoms)
  Alpha-synuclein with membrane

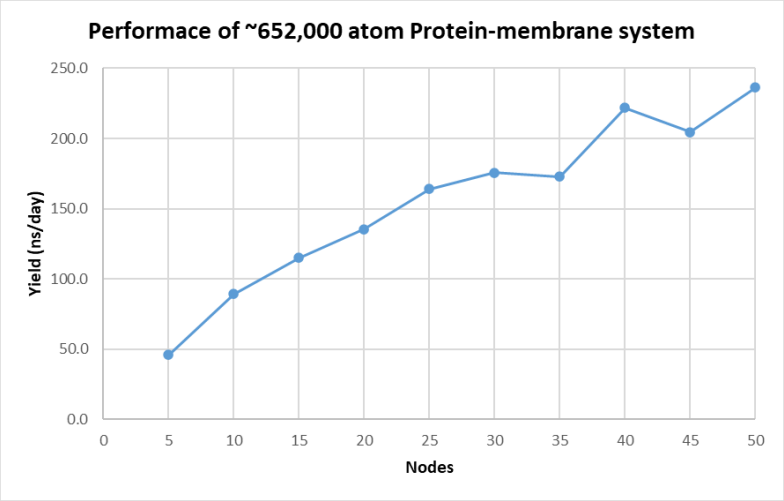

- Transmembrane protein & membrane system (No. of atoms = ~600,000 atoms)
  GPCR with membrane

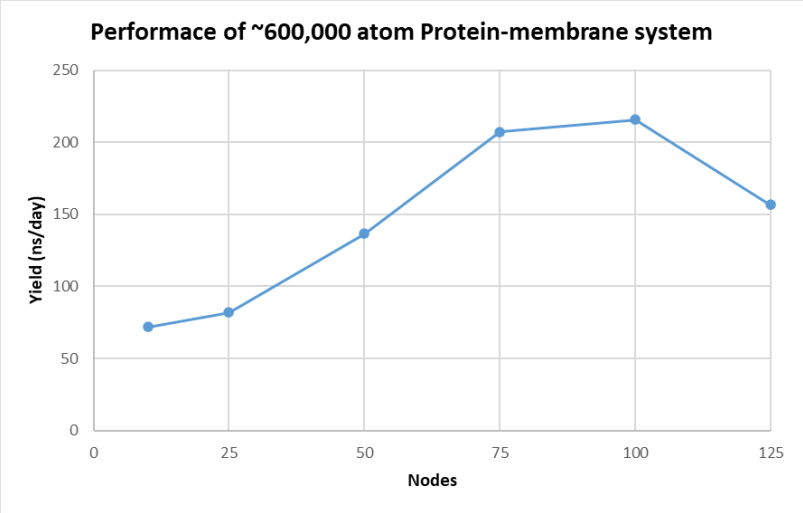

3.7.1.5 Published (2022-2024)

1. (2024) Krishnakanth Baratam and Anand Srivastava*, "SOP-MULTI: A self-organized polymer based coarse-grained model for multi-domain and intrinsically disordered proteins with conformation ensemble consistent with experimental scattering data (Accepted, JCTC)", https://doi.org/10.1021/acs.jctc.4c00579
2. (2024) Chandramouli Natarajan and Anand Srivastava*, " Efficiently determining membrane-bound conformations of peripheral membrane proteins using replica exchange with hybrid tempering, submitted", The European Physical Journal Special Topics, https://doi.org/10.1140/epjs/s11734-024-01386-x
3. (2024) Oishika Jash, Anand Srivastava, and Sundaram Balasubramanian*, "HP35 Protein in the Mesopore of MIL-101(Cr) MOF: A Model to Study Cotranslocational Unfolding" ACS Omega (https://doi.org/10.1021/acsomega.4c05452)
4. (2024) Sahithya Iyer and Anand Srivastava*, "Membrane lateral organization from potential energy disconnectivity graph", Review article, Biophysical Chemistry, Special Issue on Biomolecular Energy Landscapes (https://doi.org/10.1016/j.bpc.2024.107284)
5. (2024) Madhusmita Tripathy* and Anand Srivastava*, "Non-affine deformation analysis and 3D packing defects: A new way to probe membrane heterogeneity in molecular simulations", Invited contribution to Methods in Enzymology book series (Biophysical Approaches for the Study of Membrane Structure), Editors: Tobais Baumgart and Markus Deserno) (https://linkinghub.elsevier.com/retrieve/pii/S0076687924000958)
6. (2024) Poonam Pandey and Anand Srivastava*, "sAMP-VGG16: Drude polarizable force-field assisted image-based deep neural network prediction model for short antimicrobial peptides", PROTEINS: Structure, Function, and Bioinformatics, https://onlinelibrary.wiley.com/doi/10.1002/prot.26681
7. (2024) Rajlaxmi Saha, Prathyush Poduval, Krishnakanth Baratam, Jayashree Nagesh, Anand Srivastava*, “Membrane catalysed formation of nucleotide clusters and its role in the origins of life”, JPCB, https://pubs.acs.org/doi/10.1021/acs.jpcb.3c08061
8. (2023) Harini SureshKumar, Rajeswari Appadurai and Anand Srivastava*, "Glycans modulate lipid binding in Lili-Mip lipocalin protein", Glycobiology Journal, https://doi.org/10.1093/glycob/cwad094
9. (2023) Sangeetha Balasubramanian, Shovamayee Maharana, and Anand Srivastava*, “Boundary residues” between the folded RNA recognition motif and disordered RGG

domains are critical for FUS–RNA binding" , Journal of Biological Chemistry, https://doi.org/10.1016/j.jbc.2023.105392 (In Press,)

10. (2023) Rajeswari Appadurai, Jaya Krishna, Massimiliano Bonomi, Paul Robustelli* and Anand Srivastava*, "Clustering Heterogeneous Conformational Ensembles of Intrinsically Disordered Proteins with t-Distributed Stochastic Neighbor Embedding" Journal of Chemical Theory And Computation, https://doi.org/10.1021/acs.jctc.3c00224
11. (2023) Madhusmita Tripathy* and Anand Srivastava*, "Lipid packing in biological membranes governs protein localization and membrane permeability", Biophysical Journal, https://doi.org/10.1016/j.bpj.2023.05.028
12. (2023) Himani Khurana, Krishnakanth Baratam, Soumya Bhattacharyya, Anand Srivastava, Thomas J Pucadyil*, "Mechanistic analysis of a novel membrane-interacting variable loop in the pleckstrin-homology domain critical for dynamin function." PNAS, https://doi.org/10.1073/pnas.2215250120
13. (2022) Tripathy, M., Srivastava, A., Sastry, and Madan Rao*, "Protein as evolvable functionally constrained amorphous matter". Journal of Biosciences . https://doi.org/10.1007/s12038-022-00313-3
14. (2022) Kumar, G., Duggisetty, S.C. & Srivastava, A. A Review of Mechanics-Based Mesoscopic Membrane Remodeling Methods: Capturing Both the Physics and the Chemical Diversity. J Membrane Biol (2022). https://doi.org/10.1007/s00232-022-00268-4
15. (2022) Gaurav Kumar and Anand Srivastava,"Membrane Remodeling Due to a Mixture of Multiple Types of Curvature Proteins",J. Chem. Theory Comput. 2022, 18, 9, 5659–5671(2022) https://doi.org/10.1021/acs.jctc.2c00126
16. (2022) Akshara Sharma, Aniruddha Seal, Sahithya S. Iyer, and Anand Srivastava,"Enthalpic and entropic contributions to interleaflet coupling drive domain registration and antiregistration in biological membrane",Phys. Rev. E 105, 044408 (2022) https://doi.org/10.1103/PhysRevE.105.044408
17. (2022) Prakash Kulkarni, Vitor B. P. Leite, Susmita Roy, Supriyo Bhattacharyya, Atish Mohanty, Srisairam Achuthan, Divyoj Singh, Rajeswari Appadurai, Govindan Rangarajan, Keith Weninger, John Orban, Anand Srivastava, Mohit Kumar Jolly, Jose N. Onuchic, Vladimir N. Uversky, and Ravi Salgia , "Intrinsically disordered proteins: Ensembles at the limits of Anfinsen's dogma", Biophysics Rev. 3, 011306 (2022) https://doi.org/10.1063/5.0080512.

3.7.1.6 Contributions:

Patent for kidney cancer treatment. Sinha Roy R., Srivastava A., Mallick A. M., Chatterjee A., Gurung A. B., Uttarasili P., Tripathi A., Hembram M. Indian Institute of Science Education and Research Kolkata. Pharmaceutical Composition for Treatment of Kidney Cancer. Indian patent application no. 202533004009 (patent of addition to granted Indian patent number – 444719). 2025 Jan 17.

3.8 Mechanical engineering

3.8.1 Prof. Ratnesh K Shukla's Lab

3.8.1.1 Problem areas:

Our research focuses on development and implementation of novel predictive simulation capabilities that make use of advanced discretization techniques on modern high performance computing platforms to resolve spatiotemporally complex flows with and without shocks to an unprecedented detail. The high fidelity computational tools developed in our group are being utilized to establish the operability limits of high-speed propulsion systems, to investigate cavitating flows (cavitation bubble dynamics, high-speed liquid jets, submerged supersonic gas jets, prediction of sound produced from collapsing bubbles) and for understanding thrust generation mechanics of undulatory propulsion.

3.8.1.2 SERC's resources:

Our typical runs utilize 1000 to 14400 CPU cores of parampravega.

3.8.1.3 Parallelization strategies employed:

The parallelization utilizes MPI, OpenMP and their combination.

3.8.1.4 Performance and scalability:

Our codes have been found to scale well from 100 to 10000 cores (typical parallel efficiency we achieve is about 95% for billion cell calculations using 14400 cores).

3.8.1.5 Publications:

1. S. Dasika, D. Vaghani, & R. K. Shukla, "Constrained least-squares based adaptive-order finite-volume WENO scheme for the simulation of viscous compressible flows on unstructured grids," Journal of Computational Physics, 470, 111534, 2022.
2. Das, R. K. Shukla & R. N. Govardhan, "Universal scaling laws for propulsive performance of thrust producing foils undergoing continuous or intermittent pitching, Fluids, 7(4), 142, 2022.
3. P. Giri & R. K. Shukla, "Optimal transport of surface-actuated microswimmers," Physics of fluids, 34, 043604, 2022.
4. Das, R. K. Shukla & R. N. Govardhan, "Contrasting thrust generation mechanics and energetics of flapping foil locomotory states characterized by a unified St-Re scaling," Journal of Fluid Mechanics, 930, A27, 2022.
5. S. Dasika & R. K. Shukla, "Simulations of shock induced bubble collapse in a Newtonian fluid,"10th International and 50th National Conference on Fluid Mechanics and Fluid Power, Indian Institute of Technology, Jodhpur, India, December 20 – 22, 2023.
6. R. K. Shukla, P. Das & J. B. Freund, "A least-squares constrained sharp-interface method for bubble dynamics," Cavitation & Bubble Dynamics Mini symposium, 19th US National Congress on Theoretical and Applied Mechanics, Austin, Texas, US, June 19 – 24, 2022.
7. R. K. Shukla, M. Sawardekar, P. Das & J. B. Freund, "Adaptive high-resolution interface capturing simulations of bubble growth and collapse dynamics in generalized Newtonian fluids," Cavitation meets Data Science: Advances, applications, and challenges at the interfaces of nonlinear physics, data processing, and machine learning, Göttingen, Germany, June 10 –11, 2022.

8. M. Sawardekar & R.K. Shukla, “A Sharp Interface Immersed Boundary Method for Three-Dimensional Flow Past Moving Boundaries”, Proceedings of the 10th International and 50th National Conference on Fluid Mechanics and Fluid Power (FMFP) December 20-22, 2023.
9. M. Sawardekar & R.K. Shukla, ”An Adaptive Sharp Interface Immersed Boundary Technique for coupled Fluid-Rigid body dynamics”, Proceedings of the 9th International and 49th National Conference on Fluid Mechanics and Fluid Power (FMFP) December 14-16, 2022, IIT Roorkee.

3.8.1.6 Contributions:

Computational prediction of acoustic emissions from collapsing bubbles using interface capturing multiphase flow simulations. Naval Research Board Project
High-resolution unstructured mesh simulations of shock-boundary layer interaction and flow separation for accurate prediction of start/unstart characteristics of hypersonic intakes, Project under the hypersonic vertical of DIA-COE IIT Bombay
Hydrodynamic tuning and vibration control of the wet end of a twin towed array system. Contract for Acquisition of Research Services, NPOL Kochi.

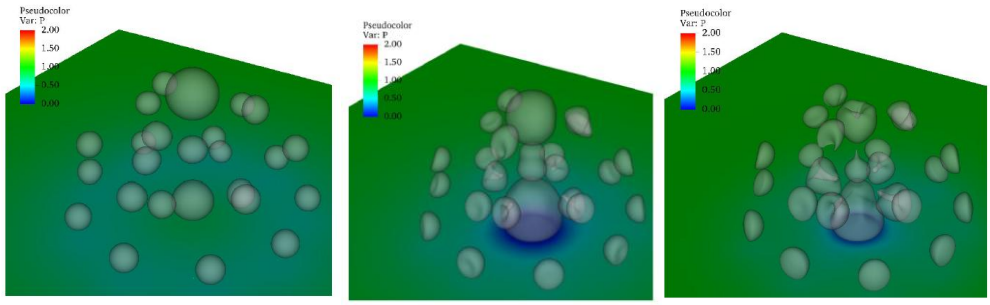

Figs. caption. *Growth and jetting collapse of a bubble cluster near a wall (bubbles are shown as grey/white isosurfaces). Coloured contour indicates the pressure exerted on the wall*

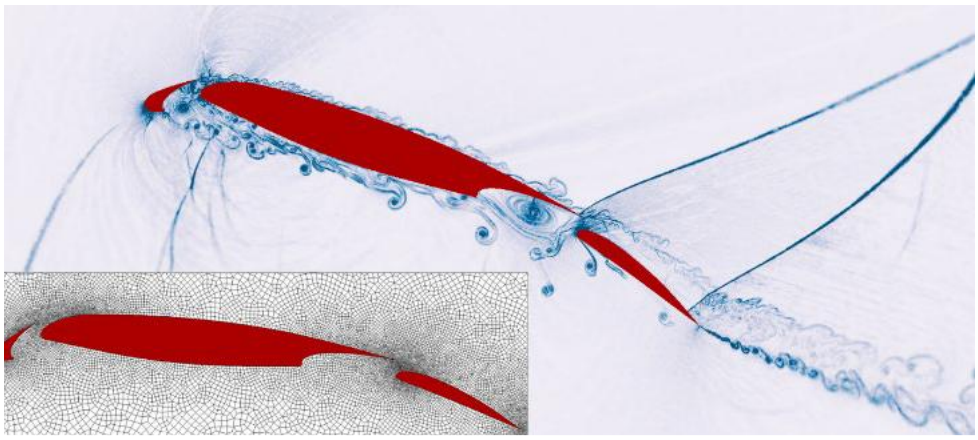

Fig. caption. Simulation of Mach 0.8 past a three-element airfoil consisting of a slat, a main element and a flap using high-resolution unstructured mesh methods. Blue coloured contours depict normalized density gradient. Inset depicts the unstructured mesh used for discretization.

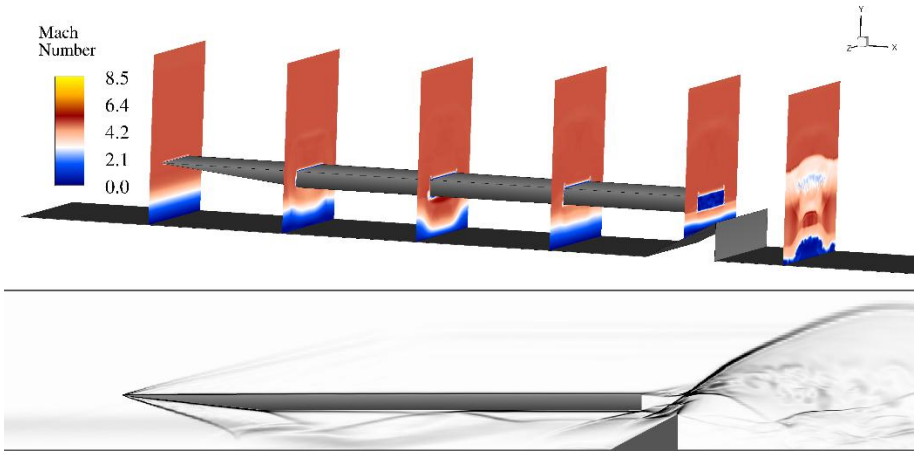

Fig. caption: *Shock boundary layer interactions in a hypersonic intake. Gray coloured regions depict the solid boundaries. The top frame illustrates Mach number contours along slices taken at select locations along the intake. The bottom frame depicts exponentially spaced normalized density gradients.*

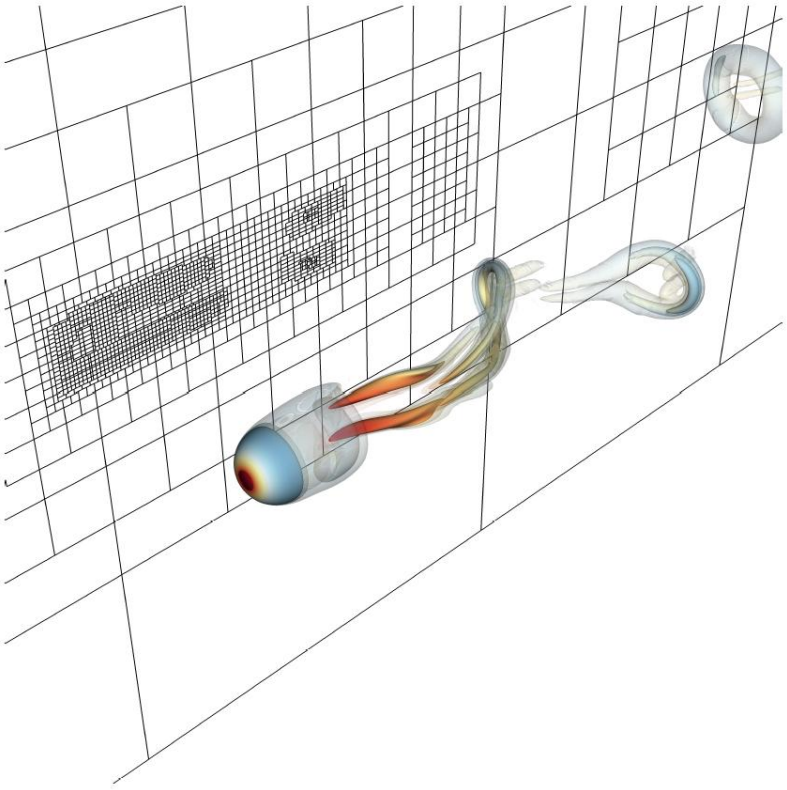

Fig. caption: *Vortical structures (coloured isosurfaces) in the wake of a translating sphere computed using a high-order immersed boundary method implemented in AMReX.*

3.9 Material Research Centre

3.9.1 Prof. Abhishek Singh's Lab

3.9.1.1 Problem areas:

Our research leverages large-scale density functional theory (DFT) and molecular dynamics simulations on HPC platforms to address diverse problems in materials science. In **catalysis**, we explored CO_2 reduction, CO oxidation, and hydrogen evolution by mapping adsorption energetics and C–C coupling pathways, extending beyond conventional descriptors using high-entropy alloys and bimetallic nanostructures. For **structural materials**, ab initio and machine learning methods were combined to study phase stability and high-temperature strength in Ni-based superalloys and Ti alloys, enabling alloy optimization. Investigations of **defects in semiconductors** revealed how intrinsic and extrinsic dopants in TMDs and oxides tune optoelectronic and catalytic properties. Studies on **topological materials** captured nontrivial band structures and their robustness under strain and doping. In **thermoelectrics**, high-throughput calculations unravelled anharmonic phonon scattering and band convergence effects in low-thermal-conductivity materials.

Finally, for **2D materials**, we modeled twisted bilayers and heterostructures, uncovering charge transfer and strain-tunable functionalities.

3.9.1.2 SERC's HPC Resources Used:

The work extensively used **Param Pravega** and **Narashima (RNC)** clusters. Over the period 2022–24, our group utilized approximately **600,000 CPU cores**. The simulations relied on **VASP** for DFT calculations and ab-initio molecular dynamics, supported by high-performance storage and interconnects.

3.9.1.3 Parallelization Strategies:

VASP simulations were parallelized using:

- **k-point parallelization** (distribution of k-points),
- **band parallelization** (distribution of electronic states).

3.9.1.4 Performance and Scalability:

Medium-sized catalytic systems (~200 atoms) scaled efficiently up to **512 cores**, while larger models (>400 atoms) maintained good parallel efficiency up to **1024 cores**. Compared to smaller departmental clusters, HPC wall-times were reduced by **3–4 times**, enabling high-throughput screening and large descriptor datasets.

3.9.1.5 Publications (2022–2024):

1. Valley-Polarized Topological Phases with In-Plane Magnetization, Nano Lett., 24, 42, 13213–13218 (2024) R. K. Barik, S. Mishra, M. Khazaei, S. Wang, Y. Liang, Y. Sun, A. Ranjbar, T. L. Tan, J. Wang, S. Yunoki, K. Ohno, Y. Kawazoe, and A. K. Singh
2. Symmetry-assisted anomalous Hall conductivity in a CrS2−CrBr3 heterostructure, Phys. Rev. B, 110, 125406 (2024), S. Mishra, N. Maity, and A. K. Singh
3. Moisture-Sensitive Fe2O3 Nanoparticle-Based Magnetic Soft Actuators, ACS Appl. Nano Mater, 7, 17, 21200-21208, 2024, S. Narendhiran, S. Meher, S. Midya, S. Mishra, S. P. Prusti, M. Balachandran, A. K. Singh, and P. Kumbhakar
4. Utilization of High Entropy Alloy (Co–Cu–Fe–Mn–Ni) and Support (CeO2) Interaction for CO2 Conversion into Syngas, Adv. Sustain. Syst. , 8, 11, 2400219 (2024), B. P. Gangwar, R. Mitra, A. Parui, P. Gakhad, P. K. Yadav, A. K. Singh, C. S. Tiwary, K. Biswas, S. Sharma
5. Low-temperature dry reforming using high entropy alloy (Co-Fe-Ga-Ni-Zn)-cerium oxide (CeO_2) hybrid nanostructure, Chem. Eng. J., 495, 153291, (2024), B. P. Gangwar, P. Tripathi, R. Das, S. Sarkar, A. K. Singh, C. S. Tiwary, and S. Sharma
6. Chemistry and Local Environment Adaptive Representation Graphs as Material Descriptors, Acta Mater., 276, 120122 (2024), S. Swetlana and A. K. Singh
7. Green Synthesis of Magnesium Single Atom Catalyst from Spinacia oleracea-Chlorophyll Extracts for Sustainable Electrocatalytic Nitrate Reduction to Ammonia, Green Chem., Just Accepted, (2024), K. Kumar , P. Tripathi , G. Raj , D. Kalyan , D. B. Gorle , N. G. Mohan , S. K. Makineni , K. Ramanujam , A. K. Singh and K. K. Nanda
8. Strain-Induced Tribocatalytic Activity of 2D ZnO Quantum Dots, J. Phys. Chem. C, Just Accepted (2024), P. Kumbhakar, S. Mishra, P. Kumbhakar, R. K. Barik, C. S. Tiwary, and A. K. Singh
9. Combined approach to capture the evolution of oxidation of Nickel based superalloys using data driven approaches, Phys. Rev. Materials, 8, 053601 (2024), N. Khatavkar, and A. K. Singh

10. Combinatorial modulation to augment all-round HER activity of Ru-CrN catalyst, J. Mater. Chem. A, 12, 8291-8301 (2024), B. Sarkar , B. K. Barman , A. Parui , A. K. Singh and K. K. Nanda
11. Probing Interlayer Interactions and Commensurate–Incommensurate Transition in Twisted Bilayer Graphene through Raman Spectroscopy, ACS Nano, 18, 4756–4764 (2024), V. Pandey, S. Mishra, N. Maity, S. Paul, Abhijith M. B, A. K. Roy, N. R. Glavin, K. Watanabe, T. Taniguchi, A. K. Singh, and V. Kochat
12. Nickle Telluride Quantum Dots as a Counter Electrode for an Efficient Dye-Sensitized Solar Cell, ACS Appl. Electron. Mater., 6, 487–495 (2024), S. Narendhiran, S. Midya, P. L. Mahapatra, M. Balachandran, C. S. Tiwary, A. K. Singh, and P. Kumbhakar
13. Shape Change of Cu Thin Films on Nonreacting Metal Substrates and the Effects of Oxidation during Vacuum Annealing, J. Phys. Chem. C., 127, 49, 23862-23869 (2023), Y. Yamada, S. Swetlana, A. K. Singh, Y. Kawazoe, M. Yahagi, and J. Koike
14. Acetylene Semi-hydrogenation at Room Temperature over Pd-Zn Nanocatalyst, Chem. Eur. J., 29, e202301932 (2023), G. Tiwari, G. Sharma, R. Verma, P. Gakhad, A. K. Singh, V. Polshettiwar and B. R. Jagirdar.
15. Utilization of structural high entropy alloy for CO oxidation to CO_2, Mater. Today Energy, 37, 101386 (2023), S. Dhakar, A. Sharma, N. K. Katiyar, A. Parui, R. Das, A. K. Singh, C. S. Tiwary, S. Sharma, K. Biswas
16. Broad photoluminescence from large Frank-Condon relaxation dynamics of hole polarons in $LiGaO_2$, Phys. Rev. B 108, L041201 (2023) M. Dey and A. K. Singh
17. Intrinsic Charge Polarization in $Bi_{19}S_{27}Cl_3$ Nano Roads Promotes Selective C-C Coupling Reaction During Photoreduction of CO_2 to Ethanol, Adv. Mater., 35, 2205994 (2022), K. Das, R. Das, M. Riyaz, A. Parui, D. Bagchi, A. K. Singh, A. K. Singh, C. P. Vinod, S. C. Peter
18. Machine Learning Assisted Interpretation of Creep and Fatigue Life in Titanium Alloys, APL Machine Learning, 1, 016102 (2023), S. Swetlana, A. Rout, A. K. Singh
19. Highly interpretable machine learning framework for prediction of mechanical properties of nickel based superalloys, Phys. Rev. Materials, 6, 123603 (2022), N. Khatavkar, and A. K. Singh
20. Selective Reduction of CO_2 on $Ti_2C(OH)_2$ MXene through Spontaneous Crossing of Transition States, ACS Appl. Mater. Interfaces, 14, 40913-40920 (2022), A.Parui, P. Srivastava, and A. K. Singh
21. Growth of Highly Crystalline Ultrathin Two-dimensional Selenene, 2D Mater., 9, 045004 (2022), P. V. Sarma, R. Nadarajan, R. Kumar, R. M. Patinharayil, N. Biju, S. Narayanan, G. Gao, C. S. Tiwary, M. Thalakulam, R. Kini, A. K. Singh, P. M Ajayan and M. Shaijumon
22. Quantum Confinement Effect on Defect Level of Hydrogen Doped Rutile VO_2 Nanowires, J. Appl. Phys., 131, 235702 (2022), M. Dey, S. Chowdhury, S. Kumar, and A. K. Singh
23. Origin of layer-dependent electrical conductivity of transition metal dichalcogenides, Phys. Rev. B, 105, 165430 (2022), Singh, M. Dey, and A. K. Singh
24. Electroreduction of CO_2 with Tunable Selectivity on Au-Pd Bimetallic Catalyst: A First Principle Study, ACS Appl. Mater. Interfaces, 14, 11313-11321 (2022), S. Agarwal, A. K. Singh
25. Interfacial electron transfer strategy to improve the hydrogen evolution catalysis of CrP heterostructure, Small, 18, 2106139 (2022), B. Sarkar, A. Parui, D. Das, A. K. Singh and K. K. Nanda
26. Enhanced Covalency and Nanostructured Phonon Scattering Lead to High Thermoelectric Performance in n-type PbS, Mater. Today Energy, 24, 100953 (2022), E.

Rathore, R. Juneja, D. Sarkar, S. Roychowdhury, M. Kofu, K. Nakajima, A. K. Singh, and K. Biswas

27. Diffusion-enhanced preferential growth of m-oriented GaN micro-domains on directly grown graphene with a large domain size on Ti/SiO_2/Si(001), H. Lee, J.-H. Park, N. Maity, D. Kim, D. Jang, C. Kim, Y.-G. Yoon, A. K. Singh, Y. Han, and S.-G. Yoon
28. Noble Metal Free Heterojunction Photocatalyst for Selective CO_2 Reduction to Methane upon Induced Strain Relaxation, ACS Catal., 12, 687-697 (2021), R. Das, S. Sarkar, R. Kumar, S. D. Ramarao, A. Cherevotan, M. Jasil, C. Vinod, A. K. Singh, and S. Peter
29. Chemical Hardness-driven Interpretable Machine Learning Approach for Rapid Search of Photocatalysts, npj Comput. Mater., 7, 197 (2021), R. Kumar, and A. K. Singh
30. Electrooxidation of Hydrazine Utilizing High-Entropy Alloys: Assisting the Oxygen Evolution Reaction at the Thermodynamic Voltage, ACS Catal., 11, 14000–14007 (2021), N. K. Katiyar, S. Dhakar, A. Parui, P. Gakhad, A. K. Singh, K. Biswas, C. S. Tiwary, and S. Sharma.
31. Feature Blending: An Approach Towards Generalized Machine Learning Models for Property Prediction, ACS Phys. Chem Au, 2, 16-22 (2022), S. Satsangi, A. Mishra, and A. K. Singh.

3.9.1.6 Contributions to National / Societal Goals:

Our work contributed to national research initiatives through a **SERB project** on Ag-based bimetallic nanoparticles for efficient CO_2 reduction and a **DRDO project** providing theoretical insights into the growth and optical properties of GaN quantum dot emitters on AlN, supporting clean energy and defence technologies.

3.10 Department of Physics

3.10.1 Prof. Animesh Kuley's Lab

3.10.1.1 Problem areas:

Plasma Physics and Fusion Energy:

Nuclear fusion — the same process that powers the Sun and stars — holds immense promise as a clean, safe, and virtually limitless source of energy. However, achieving controlled fusion on Earth presents formidable scientific and engineering challenges. At the core of these challenges lies the need for predictive modelling of plasma behaviour in fusion devices such as tokamaks and stellarators, where plasma is magnetically confined within complex 3D geometries.

A major physics challenge in present-day fusion reactors is understanding and controlling turbulence and transport in the plasma. Turbulence is particularly detrimental because it drives energy losses from the superheated plasma, cooling the core and, in severe cases, triggering premature termination of the discharge in an event known as a disruption. Effectively managing and predicting plasma turbulence is therefore critical to sustaining the high-temperature, stable conditions required for fusion energy.

To address this, the Plasma Theory Group (PTG) at IISc Bangalore has developed a global gyrokinetic toroidal code, G2C3, to simulate plasma behavior in fusion devices and gain deeper insights into turbulence. G2C3 and GTC codes have been used to validate experimental observations and to help optimize the design of next-generation machines. In this effort, we have explored a range of geometries, including tokamaks such as DIII-D and ADITYA-U, as well as stellarators such as LHD and W7-X.

3.10.1.2 SERC's resources:

To model fusion devices such as tokamaks and stellarators, we utilize extensive computational resources on PARAM-PRAVEGA. Our code demonstrates excellent scalability across different PARAM systems. However, due to constraints related to node availability and queue times, the PTG group typically runs simulations on over 2,000 CPUs, with multiple restarts required to achieve the time scales necessary for the specific problems under investigation.

3.10.1.3 Parallelization strategies employed:

Currently, G2C3 employs three levels of parallelism: (i) inter-node distributed memory domain decomposition using MPI, (ii) inter-node distributed memory particle decomposition using MPI, and (iii) intra-node shared memory work partitioning implemented with OpenMP. The G2C3 team is presently collaborating with application scientists to design and optimise software components tailored to system architecture, ensuring maximum scalability. G2C3 has already been ported to NSM's high-performance computing infrastructure, including PARAM-PRAVEGA, PARAM-RUDRA, and the DAE supercomputer ANTYA.

3.10.1.4 Performance and scalability:

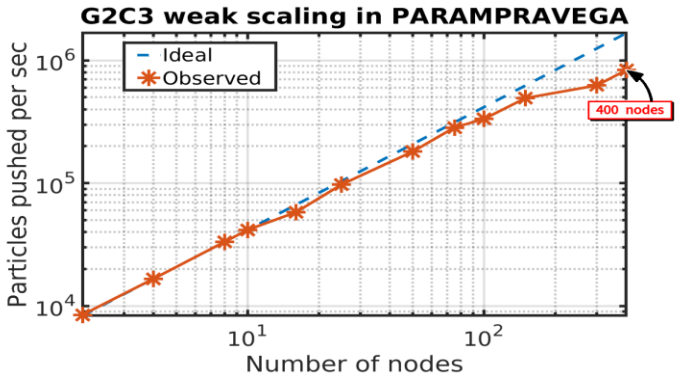

Fig1. *Scaling of G2C3 on PARAM-PRAVEGA (IISc), with the number of nodes ranging from 2 to 400.*

3.10.1.5 Publications:

1. Gyrokinetic simulations of electrostatic microturbulence in ADITYA-U tokamak with argon impurity, Tajinder Singh, Kajal Shah, Deepti Sharma, Joydeep Ghosh, Kumarpalsinh A. Jadeja, Rakesh L. Tanna, M. B. Chowdhuri, Zhihong Lin, Abhijit Sen, Sarveshwar Sharma, Animesh Kuley, Nuclear Fusion 64, 086038 (2024).
2. Global gyrokinetic simulations of electrostatic microturbulent transport in LHD stellarator with boron impurity, Tajinder Singh, Javier H Nicolau, Federico Nespoli, Gen Motojima, Zhihong Lin, Abhijit Sen, Sarveshwar Sharma, Animesh Kuley, Nuclear Fusion 64, 016007 (2024).

3. Gyrokinetic simulation of electrostatic microturbulence in ADITYA-U tokamak, Tajinder Singh, Deepti Sharma, Tanmay Macwan, Sarveshwar Sharma, Joydeep Ghosh, Abhijit Sen, Zhihong Lin, and Animesh Kuley, Nuclear Fusion 63, 056008 (2023).
4. Global gyrokinetic simulations of electrostatic microturbulent transport using kinetic electrons in LHD stellarator, Tajinder Singh, Javier H Nicolau, Zhihong Lin, Sarveshwar Sharma, Abhijit Sen, and Animesh Kuley, Nuclear Fusion 62, 126006 (2022).

3.10.1.6 Contributions:

Supporting the domestic fusion program in close collaboration with our nodal agency, the Institute for Plasma Research (IPR), Gandhinagar, along with additional contributions from C-DAC Pune through DAE-BRNS, NSM 1.0, and SERB projects. The primary objective of this effort is to develop clean energy solutions that strengthen national energy security and promote the country's sustainable socio-economic growth.

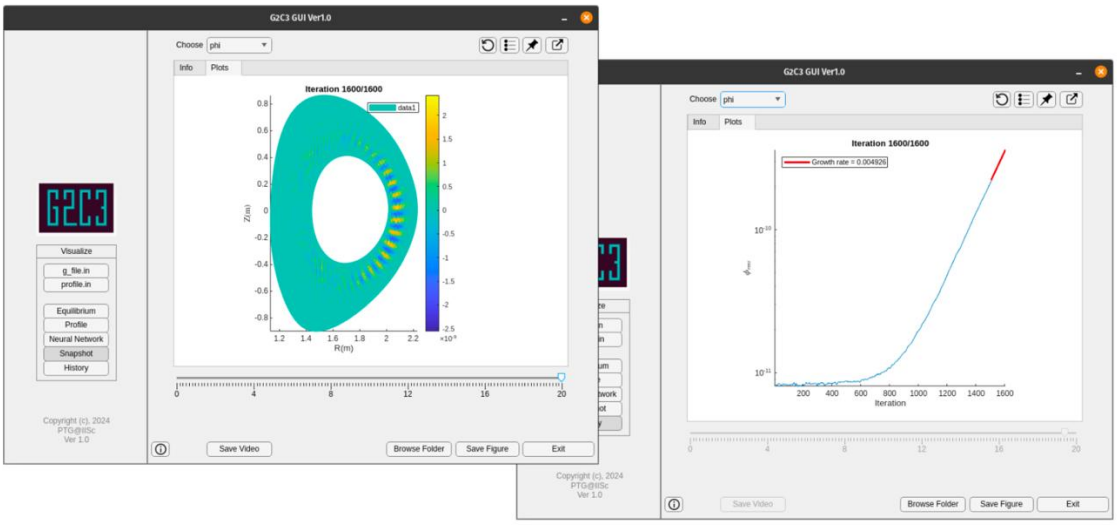

Fig2. *G2C3 GUI visualizations: (left) ITG mode structure; (right) exponential growth of the mode amplitude.*

3.10.2 Prof. Manish Jain's Lab

3.10.2.1 Problem areas:

Our runs on SERC HPC were in context of computational condensed matter physics/computational materials science. A large number of problems that were run used off-the-shelf software---Quantum Espresso and BerkeleyGW--- for calculating ground and excited states properties of materials, respectively. In addition, we also used in-house-developed-codes, PARPHOM and ElPhanSo, for calculating moiré phonons and moiré electron-phonon coupling, respectively. All these codes are MPI and openMP parallelized and scale well with the number of processors.

3.10.2.2 SERC's resources:

We used Param Pravega for our runs. The small runs were run on the small queue with 5 nodes while the larger runs used much more resources and were run in the medium queue (~100 nodes). High-memory nodes were used very often as the per core memory requirements of the jobs is high.

3.10.2.3 Parallelization strategies employed:

All the codes used were MPI parallelized. To get best performance, we used openMP (these are all Fortran codes) for intranode communication and MPI for internode communication. Some of the OpenMP usage was done to fit the codes in memory.

3.10.2.4 Performance and scalability*:*

We don't have access to other supercomputers – so this is not possible for us to do. Having said that, some of these codes, Quantum Espresso and BerkeleyGW are routinely run on some of largest supercomputers in the world.

3.10.2.5 Publications:

1. Shinjan Mandal, Indrajit Maity, H. R. Krishnamurthy, and Manish Jain, Phonon linewidths in twisted bilayer graphene near the magic angle, Physical Review B 110, 125421 (2024).
2. Krishna Prasad Bera, Darshit Solanki, Shinjan Mandal, Rabindra Biswas, Takashi Taniguchi, Kenji Watanabe, Varun Raghunathan, Manish Jain, A. K. Sood, and Anindya Das, Twist Angle-Dependent Phonon Hybridization in WSe2/WSe2 Homobilayer, ACS Nano 18, 24379 (2024).
3. Shaili Sett, Rahul Debnath, Arup Singha, Shinjan Mandal, K. M. Jyothsna, Monika Bhakar, Kenji Watanabe, Takashi Taniguchi, Varun Raghunathan, Goutam Sheet, Manish Jain, and Arindam Ghosh, Emergent Inhomogeneity and Nonlocality in a Graphene Field-Effect Transistor on a Near-Parallel Moiré Superlattice of Transition Metal Dichalcogenides, Nano Letters 24, 9245 (2024).
4. Robin Bajaj, Seung-Cheol Lee, H. R. Krishnamurthy, Satadeep Bhattacharjee, and Manish Jain, Calculation of Gilbert damping and magnetic moment of inertia using the torque-torque correlation model within an ab initio Wannier framework, Physical Review B 109, 214432 (2024)
5. Shashank Kumar Ojha, Sankalpa Hazra, Surajit Bera, Sanat Kumar Gogoi, Prithwijit Mandal, Jyotirmay Maity, Andrei Gloskovskii, Christoph Schlueter, Smarajit Karmakar, Manish Jain, Sumilan Banerjee, Venkatraman Gopalan, and Srimanta Middey, Quantum fluctuations lead to glassy electron dynamics in the good metal regime of electron doped KTaO3, Nature Communications 15, 3830 (2024).
6. Mohit Kumar Jat, Priya Tiwari, Robin Bajaj, Ishita Shitut, Shinjan Mandal, Kenji Watanabe, Takashi Taniguchi, H. R. Krishnamurthy, Manish Jain, and Aveek Bid, Higher order gaps in the renormalized band structure of doubly aligned hBN/bilayer graphene moiré superlattice, Nature Communications 15, 2335 (2024).
7. Prasanna, K. M. Usha, Manish Jain, and M. S. Hegde, Lattice oxygen and feed oxygen exchange for the high rate of H2+O2 recombination on Ti1−xPdxO2−x catalyst at room temperature, Catalysis Letters 154, 868 (2024).
8. Mohit Kumar Jat, Shubhankar Mishra, Harsimran Kaur Mann, Robin Bajaj, Kenji Watanabe, Takashi Taniguchi, H. R. Krishnamurthy, Manish Jain, and Aveek Bid, Controlling Umklapp Scattering in a Bilayer Graphene Moiré Superlattice, Nano Letters 24, 2203 (2024).

9. Bhaskar Ghawri, Phanibhusan S Mahapatra, Manjari Garg, Shinjan Mandal, Aditya Jayaraman, Kenji Watanabe, Takashi Taniguchi, Manish Jain, U Chandni, and Arindam Ghosh, Non-Boltzmann thermoelectric transport in minimally twisted bilayer graphene, Physical Review B 109, 045436 (2024).
10. Sudipta Kundu, Tomer Amit, HR Krishnamurthy, Manish Jain, and Sivan Refaely-Abramson, Exciton fine structure in twisted transition metal dichalcogenide heterostructures, npj Computational Materials 9, 186 (2023).
11. [97] Mitta Divya, Nikhil Cherukupally, Sanat Kumar Gogoi, Jyoti Ranjan Pradhan, Sandeep Kumar Mondal, Manish Jain, Anatoliy Senyshyn, and Subho Dasgupta, Super Flexible and High Mobility Inorganic/Organic Composite Semiconductors for Printed Electronics on Polymer Substrates, Advanced Materials Technologies 8, 2300256 (2023).
12. Rahul Debnath, Shaili Sett, Sudipta Kundu, Rabindra Biswas, Varun Raghunathan, Manish Jain, Arindam Ghosh, and Akshay Singh, Tuning exciton complexes in twisted bilayer WSe2 at intermediate misorientation, Physical Review B 106, 125409 (2022).
13. Anjali Lalithambika, V Kranthi Kumar, Manish Jain, and Srinivasan Raghavan, Molybdenum and Tungsten Di-sulfides: First Principles Investigation of Adatom Attachment and Diffusion on c-plane Alpha Sapphire and Correlation with Growth, Crystal Growth & Design 22, 4708 (2022).
14. Bhaskar Ghawri, Phanibhusan S Mahapatra, Manjari Garg, Shinjan Mandal, Saisab Bhowmik, Aditya Jayaraman, Radhika Soni, Kenji Watanabe, Takashi Taniguchi, H R Krishnamurthy, Manish Jain, Sumilan Banerjee, U Chandni, and Arindam Ghosh, Breakdown of semiclassical description of thermoelectricity in near-magic angle twisted bilayer graphene, Nature Communications 13, 1 (2022).
15. Saismit Naik, Mit H. Naik, Indrajit Maity, and Manish Jain, Twister: Construction and structural relaxation of commensurate moiré superlattices, Computer Physics Communications 271, 108184 (2022).
16. Sudipta Kundu, Mit H. Naik, H. R. Krishnamurthy, and Manish Jain, Moiré induced topology and flat bands in twisted bilayer WSe2: A first-principles study, Physical Review B 105, L081108 (2022).

3.10.3 Prof. Prateek Sharma's Lab

3.10.3.1 Problem Areas:

We study **multiphase astrophysical flows** in galaxies and clusters, focusing on **radiative boundary layers** and their role in mass, momentum, and energy exchange between hot and cold phases. These problems are inherently turbulent and multiphase, requiring large 3D simulations.

With SERC HPC resources, we have:

- Quantified **radiative cooling-driven turbulence** and cloud survival.
- Investigated **AGN jet–ISM interactions**, **ram-pressure stripping in clusters**, and **multiphase condensation in halos**.
- Compared simulations with **X-ray and H I observations**.

3.10.3.2 SERC's Resources:

We primarily used **Param Pravega**, both the CPU-only and GPU nodes, typically with 480-2880 cores pur run and up to 10 GPU nodes, and cumulative usage exceeding 2 million hours.

3.10.3.3 Parallelization & Performance:

Our codes Athena++ and PLUTO use **MPI parallelization,** and AthenaK uses Kokkos library for GPU cluster. All these codes are well tested scaling well on PetaFlop clusters. AthenaK is Exascale-ready. SERC reduced run times from weeks (local clusters) to days, enabling parameter sweeps and ensemble statistics.

3.10.3.4 Publications (selected, 2022–24):

1. Dutta et al., *Dissipation of AGN jets in a clumpy ISM*, ApJ 973, 148 (2024).
2. Ghosh, Dutta & Sharma, *Ram pressure stripping in clusters*, MNRAS 531, 3445 (2024).
3. Mohapatra, Sharma et al., *Multiphase condensation in cluster haloes*, MNRAS 525, 3831 (2023).
4. Sarkar, Mondal, Sharma & Piran, *Misaligned jets from Sgr A* and Fermi/eROSITA bubbles*, ApJ 951, 36 (2023).
5. Mohapatra, Federrath & Sharma, *Multiphase turbulence in galactic haloes*, MNRAS 514, 3139 (2022).

(*Total: ~20 journal papers in 2022–24 making heavy use of SERC HPC resources.*)

3.10.3.5 Contributions

- Advanced **HPC algorithm performance benchmarks** in India.
- Strengthened **observational–theory connections** for Indian astronomy (e.g., X-ray and 21 cm comparisons).

3.10.3.6 Remark,

SERC HPC resources have been **central to advancing computational astrophysics in India**, enabling high-resolution simulations of multiphase flows, dozens of publications in leading journals, training of students.

4. Awards and Recognitions based on Research with SERC HPC Resources

- Dr Aditya Konduri
    - Dr. APJ Abdul Kalam HPC Award, young researcher category, India 2025
    - Best Poster Award, IEEE HiPC Student Research Symposium 2023, 2024
- Dr Phani Motamarri
    - ACM Gordon Bell Prize SC 2023.
    - Dr. APJ Abdul Kalam HPC Award, young researcher category, India 2025
- Prof. Abhishek Singh's Lab
    - Subhendu Mishra – Best Poster Award ("60 Years of DFT" conference, July 2024, IIT Mandi)
    - Ashutosh Srivastava – Best Poster Award ("National Physicists Conclave 2024" conference, February 2024, SRM Institute of Science and Technology, Kattankulathur)

- Prof. Animesh Kuley
    - Received one DAE-BRNS and one SERB/ARF projects
    - Member of International Tokamak Physics Activity (ITPA) ITER: Energetic Particle Physics Topical Group.

5. Access to External Users

SERC also provides access to its high-end resources to researchers of Academic organizations and Government-funded R&D laboratories for cutting-edge research. Users of the following Institutes have utilized more than 1.5 million CPU core hours in 2024.

1. BITS Pilani, Hyderabad
2. BITS Pilani, Pilani
3. C-DAC, Pune
4. IISER, Thiruvananthapuram
5. IIIT Delhi
6. IIIT Hyderabad
7. IIT Bombay
8. IIT Dhanbad
9. IIT Dharwad
10. IIT Palakkad
11. IIT Hyderabad
12. IIT Madras
13. IIT Patna
14. Jawaharlal Nehru University, Delhi
15. Mahindra University, AP
16. Savitri Bhai Phule Pune University
17. SRM Institute of Science and Technology, Chennai
18. SRM University, AP
19. VIT Chennai

6. Publications in 2022-2024 using SERC HPC Resources

6.1 2024

6.1.1 Journals

1. Anand, A., Diwan, S. S., & Swaminathan, N. (2024). A comparative study of bandpass-filter-based multi-scale methods for turbulence energy cascade. Journal of Turbulence, 1–10.
2. Harpreet Kaur, G. Bala & Ashwin Seshadri (2024). *Climate response to interhemispheric differences in radiative forcing governed by shortwave cloud feedbacks*. Environmental Research: Climate. **https://iopscience.iop.org/article/10.1088/2752-5295/ad8df6**
3. Anu Xavier, **G. Bala**, Shinto Roose and KH Usha; 2024: An investigation of the relationship between tropical monsoon precipitation changes and stratospheric sulfate aerosol optical depth, Oxford open climate change, https://academic.oup.com/oocc/article/4/1/kgae016/7737801)
4. Usha, KH, **G. Bala,** A. Xavier, 2024: Sensitivity of the global hydrological cycle to the altitude of stratospheric sulphate aerosol layer, Environmental Research Letters, https://doi.org/10.1088/1748-9326/ad5e9d)
5. Jayakrishnan, KU, **G. Bala**, K Caldeira, 2024: Dependence of climate and carbon cycle response in net zero emission pathways on the magnitude and duration of positive and negative emission pulses, Earth's Future, https://doi.org/10.1029/2024EF004891.
6. A.B.S Thakur and J. Sukhatme, Changes in the tropical upper tropospheric zonal momentum balance due to global warming, Weather and Climate Dynamics, 10.5194/wcd-5-839-2024, 2024.
7. A.B.S Thakur, J. Sukhatme and N. Harnik, The role of Tropical and Extra-tropical Waves in the Hadley Circulation, Quarterly Journal of the Royal Meteorological Society, 10.1002/qj.4784, 2024.
8. P. Kushwaha, J. Sukhatme and R.S. Nanjundiah, Role of Bay of Bengal Low Pressure Systems in the Formation of Mid-Tropospheric Cyclones over the Arabian Sea and Western India, Quarterly Journal of the Royal Meteorological Society, 10.1002/qj.4726, 2024.
9. Singh U, P.N. Vinayachandran, V. Natarajan, (2024), Advection-Based Tracking and Analysis of SalinityMovement in the Ocean, Computers & Geosciences, https://doi.org/10.1016/j.cageo.2023.105493.
10. Goswami, S.K., Aditya, K., 2024. An asynchronous discontinuous Galerkin method for massively parallel PDE solvers. Computer Methods in Applied Mechanics and Engineering.

11. Nayak, D., Jonnalagadda, A., Balakrishnan, U., Kolla, H., Aditya, K., 2024. A co-kurtosis PCA based dimensionality reduction with nonlinear reconstruction using neural networks. Combustion and Flame.
12. Rodhiya, A., Gruber, A., Bothien, M.R., Chen, J.H. and Aditya, K., 2024. Spontaneous ignition and flame propagation in hydrogen/methane wrinkled laminar flames at reheat conditions: Effect of pressure and hydrogen fraction. Combustion and Flame.
13. Gopalakrishnan, H.S., Maddipati, R., Gruber, A., Bothien, M.R. and Aditya, K., 2024. A Reactor-Network Framework to Model Performance and Emissions of a Longitudinally Staged Combustion System for Carbon-Free Fuels. Journal of Engineering for Gas Turbines and Power.
14. G. Panigrahi, N.Kodali, D. Panda, P. Motamarri. Fast hardware-aware matrix-free algorithms for higher-order finite- element discretized matrix multivector products on distributed systems. Journal of Parallel and Distributed Computing. Vol. 192, pp 104925, 2024.
15. Sharma, P., Thomas, S., Nair, M., Govind Rajan, A.* Machine Learnable Language for the Chemical Space of Nanopores Enables Structure-Property Relationships in Nanoporous 2D Materials. J. Am. Chem. Soc. 2024, 146, 44, pp 30126–30138.
16. Paliwal, S., Li, W., Liu, P.*, Govind Rajan, A.* Generalized Model for Inhibitor-Modulated 2D Polymer Growth to Understand the Controlled Synthesis of Covalent Organic Frameworks. JACS Au 2024, 4, 8, pp 2862–2873.
17. Govind Rajan, A.*, Martirez, J. M. P., Carter, E. A.* Strongly Facet-Dependent Activity of Iron-Doped β-Nickel Oxyhydroxide for the Oxygen Evolution Reaction. Phys. Chem. Chem. Phys. 2024, 26, pp 14721–14733. (Invited article for the special issue “25th PCCP Anniversary Issue”.).
18. Kumar, S., Govind Rajan, A.* Predicting Quantum-Mechanical Partial Charges in Arbitrarily Long Boron Nitride Nanotubes to Accurately Simulate Nanoscale Water Transport. J. Chem. Theor. Comput. 2024, 20, 8, pp 3298–3307.
19. Ghorai, S., Govind Rajan, A.* From Molecular Precursors to MoS2 Monolayers: Nanoscale Mechanism of Organometallic Chemical Vapor Deposition. Chem. Mater. 2024, 36, 6, pp 2698–2710.
20. D. Pal, A. Ghosh, Present day mantle structure from global mantle convection models since the Cre taceous, Geophysical Journal International, 238, p. 1651-1675, 2024.
21. D. Majumder, B. Sreenivasan and G. Maurya, Self-similarity of the dipole–multipole transition in rapidly rotating dynamos, J. Fluid Mech., 980, A30, 2024.
22. M. Arandhara and S. G. Ramesh, "Nuclear quantum effects in gas-phase ethylene glycol", Phys. Chem. Chem. Phys. 26, 19529 (2024).
23. M. Arandhara and S. G. Ramesh, "Nuclear quantum effects in hydroxide hydrate along the H-bond bifurcation pathway", J. Phys. Chem. A 128, 1600 (2024).
24. M. Arandhara and S. G. Ramesh, "Nuclear quantum effects in gas-phase 2-fluoroethanol", Phys. Chem. Chem. Phys. 26, 6885 (2024).
25. (2024) Krishnakanth Baratam and Anand Srivastava*, "SOP-MULTI: A self-organized polymer based coarse-grained model for multi-domain and intrinsically disordered

proteins with conformation ensemble consistent with experimental scattering data (Accepted, JCTC)", https://doi.org/10.1021/acs.jctc.4c00579

26. (2024) Chandramouli Natarajan and Anand Srivastava*, " Efficiently determining membrane-bound conformations of peripheral membrane proteins using replica exchange with hybrid tempering, submitted", The European Physical Journal Special Topics, https://doi.org/10.1140/epjs/s11734-024-01386-x
27. (2024) Oishika Jash, Anand Srivastava, and Sundaram Balasubramanian*, "HP35 Protein in the Mesopore of MIL-101(Cr) MOF: A Model to Study Cotranslocational Unfolding" ACS Omega (https://doi.org/10.1021/acsomega.4c05452)
28. (2024) Sahithya Iyer and Anand Srivastava*, "Membrane lateral organization from potential energy disconnectivity graph", Review article, Biophysical Chemistry, Special Issue on Biomolecular Energy Landscapes (https://doi.org/10.1016/j.bpc.2024.107284)
29. (2024) Madhusmita Tripathy* and Anand Srivastava*, "Non-affine deformation analysis and 3D packing defects: A new way to probe membrane heterogeneity in molecular simulations", Invited contribution to Methods in Enzymology book series (Biophysical Approaches for the Study of Membrane Structure), Editors: Tobais Baumgart and Markus Deserno) (https://linkinghub.elsevier.com/retrieve/pii/S0076687924000958)
30. (2024) Poonam Pandey and Anand Srivastava*, "sAMP-VGG16: Drude polarizable force-field assisted image-based deep neural network prediction model for short antimicrobial peptides", PROTEINS: Structure, Function, and Bioinformatics, https://onlinelibrary.wiley.com/doi/10.1002/prot.26681
31. (2024) Rajlaxmi Saha, Prathyush Poduval, Krishnakanth Baratam, Jayashree Nagesh, Anand Srivastava*, “Membrane catalysed formation of nucleotide clusters and its role in the origins of life”, JPCB, https://pubs.acs.org/doi/10.1021/acs.jpcb.3c08061
32. Valley-Polarized Topological Phases with In-Plane Magnetization, Nano Lett., 24, 42, 13213–13218 (2024) R. K. Barik, S. Mishra, M. Khazaei, S. Wang, Y. Liang, Y. Sun, A. Ranjbar, T. L. Tan, J. Wang, S. Yunoki, K. Ohno, Y. Kawazoe, and A. K. Singh
33. Symmetry-assisted anomalous Hall conductivity in a CrS2−CrBr3 heterostructure, Phys. Rev. B, 110, 125406 (2024), S. Mishra, N. Maity, and A. K. Singh
34. Moisture-Sensitive Fe2O3 Nanoparticle-Based Magnetic Soft Actuators, ACS Appl. Nano Mater, 7, 17, 21200-21208, 2024, S. Narendhiran, S. Meher, S. Midya, S. Mishra, S. P. Prusti, M. Balachandran, A. K. Singh, and P. Kumbhakar
35. Utilization of High Entropy Alloy (Co–Cu–Fe–Mn–Ni) and Support (CeO2) Interaction for CO2 Conversion into Syngas, Adv. Sustain. Syst. , 8, 11, 2400219 (2024), B. P. Gangwar, R. Mitra, A. Parui, P. Gakhad, P. K. Yadav, A. K. Singh, C. S. Tiwary, K. Biswas, S. Sharma
36. Low-temperature dry reforming using high entropy alloy (Co-Fe-Ga-Ni-Zn)-cerium oxide (CeO_2) hybrid nanostructure, Chem. Eng. J., 495, 153291, (2024), B. P. Gangwar, P. Tripathi, R. Das, S. Sarkar, A. K. Singh, C. S. Tiwary, and S. Sharma
37. Chemistry and Local Environment Adaptive Representation Graphs as Material Descriptors, Acta Mater., 276, 120122 (2024), S. Swetlana and A. K. Singh
38. Green Synthesis of Magnesium Single Atom Catalyst from Spinacia oleracea-Chlorophyll Extracts for Sustainable Electrocatalytic Nitrate Reduction to Ammonia, Green Chem., Just Accepted, (2024), K. Kumar , P. Tripathi , G. Raj , D. Kalyan , D. B. Gorle , N. G. Mohan , S. K. Makineni , K. Ramanujam , A. K. Singh and K. K. Nanda

39. Strain-Induced Tribocatalytic Activity of 2D ZnO Quantum Dots, J. Phys. Chem. C, Just Accepted (2024), P. Kumbhakar, S. Mishra, P. Kumbhakar, R. K. Barik, C. S. Tiwary, and A. K. Singh
40. Combined approach to capture the evolution of oxidation of Nickel based superalloys using data driven approaches, Phys. Rev. Materials, 8, 053601 (2024), N. Khatavkar, and A. K. Singh
41. Combinatorial modulation to augment all-round HER activity of Ru-CrN catalyst, J. Mater. Chem. A, 12, 8291-8301 (2024), B. Sarkar , B. K. Barman , A. Parui , A. K. Singh and K. K. Nanda
42. Probing Interlayer Interactions and Commensurate–Incommensurate Transition in Twisted Bilayer Graphene through Raman Spectroscopy, ACS Nano, 18, 4756–4764 (2024), V. Pandey, S. Mishra, N. Maity, S. Paul, Abhijith M. B, A. K. Roy, N. R. Glavin, K. Watanabe, T. Taniguchi, A. K. Singh, and V. Kochat
43. Nickle Telluride Quantum Dots as a Counter Electrode for an Efficient Dye-Sensitized Solar Cell, ACS Appl. Electron. Mater., 6, 487–495 (2024), S. Narendhiran, S. Midya, P. L. Mahapatra, M. Balachandran, C. S. Tiwary, A. K. Singh, and P. Kumbhakar
44. Gyrokinetic simulations of electrostatic microturbulence in ADITYA-U tokamak with argon impurity, Tajinder Singh, Kajal Shah, Deepti Sharma, Joydeep Ghosh, Kumarpalsinh A. Jadeja, Rakesh L. Tanna, M. B. Chowdhuri, Zhihong Lin, Abhijit Sen, Sarveshwar Sharma, Animesh Kuley, Nuclear Fusion 64, 086038 (2024).
45. Global gyrokinetic simulations of electrostatic microturbulent transport in LHD stellarator with boron impurity, Tajinder Singh, Javier H Nicolau, Federico Nespoli, Gen Motojima, Zhihong Lin, Abhijit Sen, Sarveshwar Sharma, Animesh Kuley, Nuclear Fusion 64, 016007 (2024).
46. Shinjan Mandal, Indrajit Maity, H. R. Krishnamurthy, and Manish Jain, Phonon linewidths in twisted bilayer graphene near the magic angle, Physical Review B 110, 125421 (2024).
47. Krishna Prasad Bera, Darshit Solanki, Shinjan Mandal, Rabindra Biswas, Takashi Taniguchi, Kenji Watanabe, Varun Raghunathan, Manish Jain, A. K. Sood, and Anindya Das, Twist Angle-Dependent Phonon Hybridization in WSe2/WSe2 Homobilayer, ACS Nano 18, 24379 (2024).
48. Shaili Sett, Rahul Debnath, Arup Singha, Shinjan Mandal, K. M. Jyothsna, Monika Bhakar, Kenji Watanabe, Takashi Taniguchi, Varun Raghunathan, Goutam Sheet, Manish Jain, and Arindam Ghosh, Emergent Inhomogeneity and Nonlocality in a Graphene Field-Effect Transistor on a Near-Parallel Moiré Superlattice of Transition Metal Dichalcogenides, Nano Letters 24, 9245 (2024).
49. Robin Bajaj, Seung-Cheol Lee, H. R. Krishnamurthy, Satadeep Bhattacharjee, and Manish Jain, Calculation of Gilbert damping and magnetic moment of inertia using the torque-torque correlation model within an ab initio Wannier framework, Physical Review B 109, 214432 (2024)
50. Shashank Kumar Ojha, Sankalpa Hazra, Surajit Bera, Sanat Kumar Gogoi, Prithwijit Mandal, Jyotirmay Maity, Andrei Gloskovskii, Christoph Schlueter, Smarajit Karmakar, Manish Jain, Sumilan Banerjee, Venkatraman Gopalan, and Srimanta Middey, Quantum fluctuations lead to glassy electron dynamics in the good metal regime of electron doped KTaO3, Nature Communications 15, 3830 (2024).
51. Mohit Kumar Jat, Priya Tiwari, Robin Bajaj, Ishita Shitut, Shinjan Mandal, Kenji Watanabe, Takashi Taniguchi, H. R. Krishnamurthy, Manish Jain, and Aveek Bid,

Higher order gaps in the renormalized band structure of doubly aligned hBN/bilayer graphene moiré superlattice, Nature Communications 15, 2335 (2024).

52. Prasanna, K. M. Usha, Manish Jain, and M. S. Hegde, Lattice oxygen and feed oxygen exchange for the high rate of H2+O2 recombination on Ti1−xPdxO2−x catalyst at room temperature, Catalysis Letters 154, 868 (2024).
53. Mohit Kumar Jat, Shubhankar Mishra, Harsimran Kaur Mann, Robin Bajaj, Kenji Watanabe, Takashi Taniguchi, H. R. Krishnamurthy, Manish Jain, and Aveek Bid, Controlling Umklapp Scattering in a Bilayer Graphene Moiré Superlattice, Nano Letters 24, 2203 (2024).
54. Bhaskar Ghawri, Phanibhusan S Mahapatra, Manjari Garg, Shinjan Mandal, Aditya Jayaraman, Kenji Watanabe, Takashi Taniguchi, Manish Jain, U Chandni, and Arindam Ghosh, Non-Boltzmann thermoelectric transport in minimally twisted bilayer graphene, Physical Review B 109, 045436 (2024).
55. Dutta et al., *Dissipation of AGN jets in a clumpy ISM*, ApJ 973, 148 (2024).
56. Ghosh, Dutta & Sharma, *Ram pressure stripping in clusters*, MNRAS 531, 3445 (2024).

6.1.2 Conferences and Workshops

1. Jyoti Ranjan Majhi, Magan Singh, and Kartik Venkatraman (2024). Prediction of transonic buffet in a finite span wing using global stability analysis. In Second Buffet Workshop. JAXA Chofu Aerospace Center. August 30, 2024.
2. Jyoti Ranjan Majhi and Kartik Venkatraman (2024). Prediction of transonic buffet in an axial flow fan using global stability analysis. In International Forum on Aeroelasticity and Structural Dynamics 2024 (IFASD 2024). Den Haag, Netherlands. June 18-20, 2024.
3. Magan Singh and Kartik Venkatraman (2024). Transonic shock oscillations in an oscillating finite span wing. In International Forum on Aeroelasticity and Structural Dynamics 2024 (IFASD 2024). Den Haag, Netherlands. June 18-20, 2024.
4. Pawel Chwalowski, Garrett McHugh, Steven Massey, Lior Poplingher, Daniella E. Raveh, Adam Jirasek, Nicholas F. Giannelis, Kartik Venkatraman, Magan Singh, Behzad Ahrabi and Moeljo Hong (2023). Shock-Buffet Prediction Report in Support of the High Angle Working Group at the Third Aeroelastic Prediction Workshop. In: 2024 AIAA SciTech Forum, Orlando, FL, USA, January 8-12, 2024.
5. Vempati, C., Thazhathattil, V., Das, R., & Hemchandra, S. (2024). Identifying noise source regions in a supersonic jet using information flux methods. In *30th AIAA/CEAS Aeroacoustics Conference (2024)* (p. 3259).
6. Dash, P., Mallik, T., Verma, N., Roy Choudhury, A., Ravikrishna, R.V. and Aditya, K., 2024, June. A Deep Learning Based Model for Identifying Recirculation Zones From Experimental Images of Trapped Vortex Combustors. In Turbo Expo: Power for Land, Sea, and Air. American Society of Mechanical Engineers.
7. Structure of the Bacterial Cell Envelope and Interactions with Antimicrobials: Insights from Molecular Dynamics Simulations, Pradyumn Sharma, Rakesh Vaiwala, Amar

Krishna Gopinath, Rajalakshmi Chockalingam, K. Ganapathy Ayappa, Langmuir, 40, 7791-7811 (2024). 10.1021/acs.langmuir.3c03474.

8. Martini-3 Coarse-Grained Models for the Bacterial Lipopolysaccharide Outer Membrane of Escherichia coli, Rakesh Vaiwala, K. Ganapathy Ayappa, Journal of Chemical Theory and Computation, 20, 1704-1716 (2024). https://doi.org/10.1021/acs.jctc.3c00471

6.2 2023

6.2.1 Journals

1. Jyoti Ranjan Majhi and Kartik Venkatraman (2023). On the nature of transonic shock buffet in an axial flow fan. In: *AIAA Journal,* 2023.
2. Muthichur, N., Vempati, C., Hemchandra, S., & Samanta, A. (2023). Reduced-order models of aeroacoustic sources for sound radiated in twin subsonic jets. *Journal of Fluid Mechanics*, *972*, A33.
3. Eddy-freshwater interaction using regional ocean modeling system in the Bay of Bengal N Paul, J Sukhatme, Gayen, B., Sengupta, D. Journal of Geophysical Research: Oceans 128 (4), e2022JC019439, 2023
4. N. Paul, J. Sukhatme, B. Gayen and D. Sengupta, Eddy-Freshwater Interaction Using Regional Ocean Modeling System in the Bay of Bengal, Journal of Geophysical Research, 10.1029/2022JC019439, 2023.
5. Goswami, S.K., Matthew, V.J., Aditya, K., 2023. Implementation of low-storage Runge-Kutta time integration schemes in scalable asynchronous partial differential equation solvers. Journal of Computational Physics.
6. Jonnalagadda, A., Kulkarni, S., Rodhiya, A., Kolla, H., Aditya, K., 2023. A co-kurtosis based dimensionality reduction method for combustion datasets. Combustion and Flame.
7. S. Das, B. Kanungo, V. Subramanian, G. Panigrahi, P. Motamarri, D. M Rogers, P. Zimmerman, V. Gavini. Large-scale materials modeling at quantum accuracy: Ab initio simulations of quasicrystals and interacting extended defects in metallic alloys **(ACM Gordon Bell Prize).** Proceedings of SC23, The International Conference for High Performance Computing, Networking, Storage, and Analysis. 2023.
8. S. Khadatkar, P. Motamarri. Subspace recursive Fermi-operator expansion strategies for large-scale DFT eigenvalue problems on HPC architectures. Journal of Chemical Physics. Vol. 159, pp 031102, 2023.
9. K. Ramakrishnan, S. K. K. Nori, S. Lee, G. P Das, S. Bhattacharjee, P. Motamarri. Chemical Bonding in Large Systems Using Projected Population Analysis from Real- Space Density Functional Theory Calculations. Journal of Chemical Theory and Computation. Vol. 19, pp 4216, 2023.
10. Lal, D., Konnur, T., Verma, A. M., Shaneeth, M., Govind Rajan, A.* Unraveling Low Overpotential Pathways for Electrochemical CO2 Reduction to CH4 on Pure and Doped MoS2 Edges. Ind. Eng. Chem. Res. 2023, 62, 49, pp 21191–21207. (Invited article for the special issue “2023 Class of Influential Researchers”.)
11. Seal, A., Tiwari, U., Gupta, A., Govind Rajan, A.* Incorporating Ion-Specific van der Waals and Soft Repulsive Interactions in the Poisson-Boltzmann Theory of Electrical Double Layers. Phys. Chem. Chem. Phys. 2023, 25, pp 21708–21722.

12. John, A., Verma, A. M., Shaneeth, M., Govind Rajan, A.* Discovering a Single-Atom Catalyst for CO2 Electroreduction to C1 Hydrocarbons: Thermodynamics and Kinetics on Aluminum-Doped Copper. ChemCatChem 2023, 15 (14), e202300188.
13. Bhowmik, S., Warner, J. H., Govind Rajan, A.* Role of Chemical Etching in the Nucleation of Nanopores in 2D MoS2: Insights from First-Principles Calculations. J. Phys. Chem. C 2023, 127 (14), pp 6873–6883. (Invited article for the special issue "Early-Career and Emerging Researchers in Physical Chemistry Volume 2".)
14. Thomas, S., Silmore, K., Sharma, P., Govind Rajan, A.* Enumerating Stable Nanopores in Graphene and their Geometrical Properties Using the Combinatorics of Hexagonal Lattices. J. Chem. Inf. Model. 2023, 63 (3), pp 870–881.
15. Implementing Trajectory Extending Kinetic Monte Carlo Simulations to Evaluate Pure and Gas Mixture Diffusivities through Dense Polymeric Membrane, Subhadeep Dasgupta, K. S. Arun, K. Ganapathy Ayappa and Prabal K. Maiti, Journal of Physical Chemistry B, 127, 9841-9849 (2023). https://doi.org/10.1021/acs.jpcb.3c05661
16. Selective Photonic Gasification of Strained Oxygen Clusters on Graphene for Tuning Pore Size in Å-Regime, Bondaz, Luc; Ronghe, Anshaj; Li, Shaoxian; Cernevics, Kristians; Hao, Jian; Yazyev, Oleg; Ayappa, K. Ganapathy; Agrawal, Kumar Varoon, JACS Au 3, 10, 2844-2854 (2023). https://doi.org/10.1021/jacsau.3c00395
17. Cholesterol Catalyzes Unfolding in Membrane Inserted Motifs of the Pore Forming Protein Cytolysin A, Avijeet Kulshrestha, Rahul Roy, Sudeep Punnathanam, K. Ganapathy Ayappa, Biophysical Journal, 122, 4068-4081 (2023) https://doi.org/10.1016/j.bpj.2023.09.005
18. Graphene Nanopores Enhance Water Evaporation from Salt Solutions: Exploring the Effects of Ions and Concentration, Anshaj Ronghe and K. Ganapathy Ayappa, Langmuir, 39, 8787–8800 (2023). https://doi.org/10.1021/acs.langmuir.3c00797
19. Conformational Flexibility is a Key Determinant for the Lytic Activity of the Pore-Forming Protein, Cytolysin A: Kulshrestha, Avijeet; Maurya, Satyaghosh; Gupta, Twinkle; Roy, Rahul; Punnathanam, Sudeep; Ayappa, K. Ganapathy, Journal of Physical Chemistry B 127, 69-84 (2023). https://doi.org/10.1021/acs.jpcb.2c05785
20. D.Pal, A. Ghosh, How the Indian Ocean Geoid Low Was Formed, Geophysical Research Letters, 50, e2022GL102694, doi:10.1029/2022GL102694, 2023.
21. J. Paul, C. P. Conrad, T. W. Becker, A. Ghosh, Convective Self-Compression of Cratons and the Stabi lization of Old Lithosphere, Geophysical Research Letters, 50, e2022GL101842, doi:10.1029/2022GL101842, 2023.
22. D. Majumder and B. Sreenivasan, The role of magnetic waves in tangent cylinder convection, Phys. Earth Planet. Inter., 344, 107105, 2023.
23. Alexander, D. N. Kumar, W. J. Knoben, and M. Clark, "Evaluating the parameter sensitivity and impact of hydrologic modeling decisions on flood simulations," Advances in Water Resources, p. 104 560, 2023, issn: 03091708. doi: https://doi.org/10.1016/j.advwatres.2023.104560.
24. (2023) Harini SureshKumar, Rajeswari Appadurai and Anand Srivastava*, "Glycans modulate lipid binding in Lili-Mip lipocalin protein", Glycobiology Journal, https://doi.org/10.1093/glycob/cwad094
25. (2023) Sangeetha Balasubramanian, Shovamayee Maharana, and Anand Srivastava*, "Boundary residues" between the folded RNA recognition motif and disordered RGG domains are critical for FUS–RNA binding" , Journal of Biological Chemistry, https://doi.org/10.1016/j.jbc.2023.105392 (In Press,)

26. (2023) Rajeswari Appadurai, Jaya Krishna, Massimiliano Bonomi, Paul Robustelli* and Anand Srivastava*, "Clustering Heterogeneous Conformational Ensembles of Intrinsically Disordered Proteins with t-Distributed Stochastic Neighbor Embedding" Journal of Chemical Theory And Computation, https://doi.org/10.1021/acs.jctc.3c00224
27. (2023) Madhusmita Tripathy* and Anand Srivastava*, "Lipid packing in biological membranes governs protein localization and membrane permeability", Biophysical Journal, https://doi.org/10.1016/j.bpj.2023.05.028
28. (2023) Himani Khurana, Krishnakanth Baratam, Soumya Bhattacharyya, Anand Srivastava, Thomas J Pucadyil*, "Mechanistic analysis of a novel membrane-interacting variable loop in the pleckstrin-homology domain critical for dynamin function." PNAS, https://doi.org/10.1073/pnas.2215250120
29. Shape Change of Cu Thin Films on Nonreacting Metal Substrates and the Effects of Oxidation during Vacuum Annealing, J. Phys. Chem. C., 127, 49, 23862-23869 (2023), Y. Yamada, S. Swetlana, A. K. Singh, Y. Kawazoe, M. Yahagi, and J. Koike
30. Acetylene Semi-hydrogenation at Room Temperature over Pd-Zn Nanocatalyst, Chem. Eur. J., 29, e202301932 (2023), G. Tiwari, G. Sharma, R. Verma, P. Gakhad, A. K. Singh, V. Polshettiwar and B. R. Jagirdar.
31. Utilization of structural high entropy alloy for CO oxidation to CO_2, Mater. Today Energy, 37, 101386 (2023), S. Dhakar, A. Sharma, N. K. Katiyar, A. Parui, R. Das, A. K. Singh, C. S. Tiwary, S. Sharma, K. Biswas
32. Broad photoluminescence from large Frank-Condon relaxation dynamics of hole polarons in $LiGaO_2$, Phys. Rev. B 108, L041201 (2023) M. Dey and A. K. Singh
33. Gyrokinetic simulation of electrostatic microturbulence in ADITYA-U tokamak, Tajinder Singh, Deepti Sharma, Tanmay Macwan, Sarveshwar Sharma, Joydeep Ghosh, Abhijit Sen, Zhihong Lin, and Animesh Kuley, Nuclear Fusion 63, 056008 (2023).
34. Sudipta Kundu, Tomer Amit, HR Krishnamurthy, Manish Jain, and Sivan Refaely-Abramson, Exciton fine structure in twisted transition metal dichalcogenide heterostructures, npj Computational Materials 9, 186 (2023).
35. Mitta Divya, Nikhil Cherukupally, Sanat Kumar Gogoi, Jyoti Ranjan Pradhan, Sandeep Kumar Mondal, Manish Jain, Anatoliy Senyshyn, and Subho Dasgupta, Super Flexible and High Mobility Inorganic/Organic Composite Semiconductors for Printed Electronics on Polymer Substrates, Advanced Materials Technologies 8, 2300256 (2023).
36. Mohapatra, Sharma et al., *Multiphase condensation in cluster haloes*, MNRAS 525, 3831 (2023).
37. Sarkar, Mondal, Sharma & Piran, *Misaligned jets from Sgr A* and Fermi/eROSITA bubbles*, ApJ 951, 36 (2023).

6.2.2 Conferences and Workshops

1. Jyoti Ranjan Majhi and Kartik Venkatraman (2023). Numerical simulation of transonic buffet in an axial flow fan. In: *2023 AIAA Aviation Forum and Exposition*, San Diego, USA, June 12-16, 2023.
2. Jyoti Ranjan Majhi and Kartik Venkatraman (2023). Prediction and characterization of transonic buffet in an axial flow fan. In: 57th 3AF International Conference (AERO2023), Bordeaux, France, March 29-31, 2023.
3. Magan Singh and Kartik Venkatraman (2023). The influence of angle of attack on the nature of transonic shock buffet in a finite span wing. In: 57th 3AF International Conference (AERO2023), Bordeaux, France, March 29-31, 2023.

4. Magan Singh and Kartik Venkatraman (2023). Transonic buffet in the Benchmark Supercritical Wing. In: 2023 AIAA SciTech Forum, National Harbor, MD, USA, January 23-27, 2023.
5. Arif Md, Magan Singh, Tumkur Pradeepa Karnick and Kartik Venkatraman (2023). Two-dimensional transonic buffet in a supercritical wing section. In: 2023 AIAA SciTech Forum, National Harbor, MD, USA, January 23-27, 2023.
6. Adithya Mayya, Magan Singh, and Kartik Venkatraman (2023). Transonic shock vortex shock boundary layer interactions over a delta wing. In: 57th 3AF International Conference (AERO2023), Bordeaux, France, March 29-31, 2023.
7. O.N, Ramesh et al. RANS Predictions of Transonic Shock-Induced Flow Separation over Sandia Axisymmetric Hump, 57th 3AF International Conference on Applied Aerodynamics, March 29–31, 2023, Bordeaux, France.
8. O.N. Ramesh et al. RANS and DES Predictions of Transonic Shock-Induced Flow Separation over Sandia Axisymmetric Hump, Asian Computational Fluid Dynamics Conference, Nov 2023, HAL Management Academy, Bengaluru, India.
9. Gupta, S., Datta, A., Hemchandra, S., & Boxx, I. (2023, June). Precessing vortex core suppression in a swirl stabilized combustor with hydrogen addition. In *Turbo Expo: Power for Land, Sea, and Air* (Vol. 86953, p. V03AT04A002). American Society of Mechanical Engineers.
10. Hemchandra, S., Datta, A., & Juniper, M. P. (2023, June). Learning RANS model parameters from LES using bayesian inference. In *Turbo Expo: Power for Land, Sea, and Air* (Vol. 86953, p. V03AT04A051). American Society of Mechanical Engineers.
11. Anand, A., Diwan, S., & Swaminathan, N. (2023). Intermittent structures of intense inter-scale energy fluxes in turbulent channel flow, Bulletin of the 76th Annual Meeting of Division of Fluid Dynamics of American Physical Society.
12. Anand, A., Swaminathan, N., & Diwan, S. (2023). Dissipation structures in a turbulent channel flow. In 14th Asian Computational Fluid Dynamics Conference.
13. S. Dasika & R. K. Shukla, “Simulations of shock induced bubble collapse in a Newtonian fluid,”10th International and 50th National Conference on Fluid Mechanics and Fluid Power, Indian Institute of Technology, Jodhpur, India, December 20 – 22, 2023.
14. M. Sawardekar & R.K. Shukla, “A Sharp Interface Immersed Boundary Method for Three-Dimensional Flow Past Moving Boundaries”, Proceedings of the 10th International and 50th National Conference on Fluid Mechanics and Fluid Power (FMFP) December 20-22, 2023.

6.3 2022

6.3.1 Journals

1. Singhal R, Ravichandran S, Govindarajan R, Diwan SS. Virus transmission by aerosol transport during short conversations. Flow. 2022;2:E13. doi:10.1017/flo.2022.7.
2. Verma, A. K., Govind Rajan, A.* Surface Roughness Explains the Observed Water Contact Angle and Slip Length on 2D Hexagonal Boron Nitride. Langmuir 2022, 38 (30), pp 9210–9220. (This article was amongst the most-read ones in Langmuir a month after its publication.)
3. Sheshanarayana, R., Govind Rajan, A.* Tailoring Nanoporous Graphene Via Machine Learning: Predicting Probabilities and Formation Times of Arbitrary Nanopore Shapes. J. Chem. Phys. 2022, 156, 204703. (This article is a part of the "Emerging Investigators Special Collection" and was selected as an "Editor's Pick".)
4. Sharma, B. B., Govind Rajan, A.* How Grain Boundaries and Interfacial Electrostatic Interactions Modulate Water Desalination Via Nanoporous Hexagonal Boron Nitride. J. Phys. Chem. B 2022, 126 (6), pp 1284–1300.
5. Interactions of Surfactants with the Bacterial Cell Wall and Inner Membrane: Revealing the Link Between Aggregation and Antimicrobial Activity, Pradyumn Sharma, Rakesh Vaiwala, Srividhya Parthasarathi, Nivedita Patil, Anant Verma, Morris Waskar, Janhavi Raut, Jaydeep K. Basu and K. Ganapathy Ayappa, Langmuir, 38, 15714-15728 (2022). https://doi.org/10.1021/acs.langmuir.2c02520
6. Finite Temperature String Method with Umbrella Sampling using Path Collective Variables: Application to Secondary Structure Change in a Protein, Avijeet Kulshrestha, Sudeep N. Punnathanam and K. Ganapathy Ayappa, Soft Matter, 18, 7593-7603 (2022). https://doi.org/10.1039/D2SM00888B
7. Influence of Chain Length on Structural Properties of Carbon Molecular Sieving Membranes and their Effects on CO2, CH4 and N2 adsorption: A Molecular Simulation Study, Subhadeep Dasgupta, Rajasekaran M., Projesh K.Roy, Foram M.Thakkar, Amar Deep Pathak, K. Ganapathy Ayappa and Prabal K.Maiti, Journal of Membrane Science, 664, 121044 (2022). https://doi.org/10.1016/j.memsci.2022.121044
8. Differentiating Interactions of Antimicrobials with Gram-negative and Gram-positive Bacteria using Molecular Dynamics Simulations, Rakesh Vaiwala, Pradyumn Sharma and K. G. Ayappa, Biointerphases, 17, 061008 (2022).https://doi.org/10.1116/6.0002087
9. A Molecular Dynamics Study of Antimicrobial Peptide Translocation Across the Outer Membrane of Gram-negative Bacteria, Pradyumn Sharma, K. G. Ayappa, Journal of Membrane Biology, 255, 665–675 (2022). https://doi.org/10.1007/s00232-022-00258-6
10. Microtubule Dynamics and the Coupling to Mitochondrial Population Evolution in Fission Yeast Cells: A Kinetic Monte Carlo Study, Samlesh Choudhary, Vaishnavi Ananthanarayanan and Ganapathy Ayappa, Soft Matter, 18, 4483-4492 (2022). https://doi.org/10.1039/D2SM00155A
11. Enhanced Water Evaporation from Å-scale Graphene Nanopores, Wan-Chi Lee1, Anshaj Ronghe, Luis Francisco Villalobos, Shiqi Huang, Mostapha Dakhchoune, Mounir Mensi, Kuang-Jung Hsu, K. Ganapathy Ayappa and Kumar Varoon Agrawal, ACS Nano 16, 9, 15382–15396 (2022). https://doi.org/10.1021/acsnano.2c07193
12. Influence of the Extent of Hydrophobicity on Water Organization and Dynamics on 2D Graphene Oxide Surfaces,M. Rajasekaran and K. Ganapathy Ayappa, Physical Chemistry Chemical Physics (PCCP) 24, 14909-14923 (2022). https://doi.org/10.1039/D1CP03962H

13. A. Ghosh, D. Pal, Do lower mantle slabs contribute in generating the Indian Ocean Geoid Low? Tectonophysics, 822, doi:10.1016/j.tecto.2022.229176, 2022.
14. Varma and B. Sreenivasan, The role of slow magnetostrophic waves in the formation of the axial dipole in planetary dynamos, Phys. Earth Planet. Inter., 106944, 2022.
15. (2022) Tripathy, M., Srivastava, A., Sastry, and Madan Rao*, "Protein as evolvable functionally constrained amorphous matter". Journal of Biosciences . https://doi.org/10.1007/s12038-022-00313-3
16. (2022) Kumar, G., Duggisetty, S.C. & Srivastava, A. A Review of Mechanics-Based Mesoscopic Membrane Remodeling Methods: Capturing Both the Physics and the Chemical Diversity. J Membrane Biol (2022). https://doi.org/10.1007/s00232-022-00268-4
17. (2022) Gaurav Kumar and Anand Srivastava,"Membrane Remodeling Due to a Mixture of Multiple Types of Curvature Proteins",J. Chem. Theory Comput. 2022, 18, 9, 5659–5671(2022) https://doi.org/10.1021/acs.jctc.2c00126
18. (2022) Akshara Sharma, Aniruddha Seal, Sahithya S. Iyer, and Anand Srivastava,"Enthalpic and entropic contributions to interleaflet coupling drive domain registration and antiregistration in biological membrane",Phys. Rev. E 105, 044408 (2022) https://doi.org/10.1103/PhysRevE.105.044408
19. (2022) Prakash Kulkarni, Vitor B. P. Leite, Susmita Roy, Supriyo Bhattacharyya, Atish Mohanty, Srisairam Achuthan, Divyoj Singh, Rajeswari Appadurai, Govindan Rangarajan, Keith Weninger, John Orban, Anand Srivastava, Mohit Kumar Jolly, Jose N. Onuchic, Vladimir N. Uversky, and Ravi Salgia , "Intrinsically disordered proteins: Ensembles at the limits of Anfinsen's dogma", Biophysics Rev. 3, 011306 (2022) https://doi.org/10.1063/5.0080512.
20. S. Dasika, D. Vaghani, & R. K. Shukla, “Constrained least-squares based adaptive-order finite-volume WENO scheme for the simulation of viscous compressible flows on unstructured grids,” Journal of Computational Physics, 470, 111534, 2022.
21. Das, R. K. Shukla & R. N. Govardhan, “Universal scaling laws for propulsive performance of thrust producing foils undergoing continuous or intermittent pitching, Fluids, 7(4), 142, 2022.
22. P. Giri & R. K. Shukla, “Optimal transport of surface-actuated microswimmers,” Physics of fluids, 34, 043604, 2022.
23. Das, R. K. Shukla & R. N. Govardhan, “Contrasting thrust generation mechanics and energetics of flapping foil locomotory states characterized by a unified St-Re scaling,” Journal of Fluid Mechanics, 930, A27, 2022.
24. Intrinsic Charge Polarization in $Bi_{19}S_{27}Cl_3$ Nano Roads Promotes Selective C-C Coupling Reaction During Photoreduction of CO_2 to Ethanol, Adv. Mater., 35, 2205994 (2022), K. Das, R. Das, M. Riyaz, A. Parui, D. Bagchi, A. K. Singh, A. K. Singh, C. P. Vinod, S. C. Peter
25. Machine Learning Assisted Interpretation of Creep and Fatigue Life in Titanium Alloys, APL Machine Learning, 1, 016102 (2023), S. Swetlana, A. Rout, A. K. Singh
26. Highly interpretable machine learning framework for prediction of mechanical properties of nickel based superalloys, Phys. Rev. Materials, 6, 123603 (2022), N. Khatavkar, and A. K. Singh
27. Selective Reduction of CO_2 on $Ti_2C(OH)_2$ MXene through Spontaneous Crossing of Transition States, ACS Appl. Mater. Interfaces, 14, 40913-40920 (2022), A.Parui, P. Srivastava, and A. K. Singh

28. Growth of Highly Crystalline Ultrathin Two-dimensional Selenene, 2D Mater., 9, 045004 (2022), P. V. Sarma, R. Nadarajan, R. Kumar, R. M. Patinharayil, N. Biju, S. Narayanan, G. Gao, C. S. Tiwary, M. Thalakulam, R. Kini, A. K. Singh, P. M Ajayan and M. Shaijumon
29. Quantum Confinement Effect on Defect Level of Hydrogen Doped Rutile VO_2 Nanowires, J. Appl. Phys., 131, 235702 (2022), M. Dey, S. Chowdhury, S. Kumar, and A. K. Singh
30. Origin of layer-dependent electrical conductivity of transition metal dichalcogenides, Phys. Rev. B, 105, 165430 (2022), Singh, M. Dey, and A. K. Singh
31. Electroreduction of CO_2 with Tunable Selectivity on Au-Pd Bimetallic Catalyst: A First Principle Study, ACS Appl. Mater. Interfaces, 14, 11313-11321 (2022), S. Agarwal, A. K. Singh
32. Interfacial electron transfer strategy to improve the hydrogen evolution catalysis of CrP heterostructure, Small, 18, 2106139 (2022), B. Sarkar, A. Parui, D. Das, A. K. Singh and K. K. Nanda
33. Enhanced Covalency and Nanostructured Phonon Scattering Lead to High Thermoelectric Performance in n-type PbS, Mater. Today Energy, 24, 100953 (2022), E. Rathore, R. Juneja, D. Sarkar, S. Roychowdhury, M. Kofu, K. Nakajima, A. K. Singh, and K. Biswas
34. Feature Blending: An Approach Towards Generalized Machine Learning Models for Property Prediction, ACS Phys. Chem Au, 2, 16-22 (2022), S. Satsangi, A. Mishra, and A. K. Singh.
35. Global gyrokinetic simulations of electrostatic microturbulent transport using kinetic electrons in LHD stellarator, Tajinder Singh, Javier H Nicolau, Zhihong Lin, Sarveshwar Sharma, Abhijit Sen, and Animesh Kuley, Nuclear Fusion 62, 126006 (2022).
36. Rahul Debnath, Shaili Sett, Sudipta Kundu, Rabindra Biswas, Varun Raghunathan, Manish Jain, Arindam Ghosh, and Akshay Singh, Tuning exciton complexes in twisted bilayer WSe2 at intermediate misorientation, Physical Review B 106, 125409 (2022).
37. Anjali Lalithambika, V Kranthi Kumar, Manish Jain, and Srinivasan Raghavan, Molybdenum and Tungsten Di-sulfides: First Principles Investigation of Adatom Attachment and Diffusion on c-plane Alpha Sapphire and Correlation with Growth, Crystal Growth & Design 22, 4708 (2022).
38. Bhaskar Ghawri, Phanibhusan S Mahapatra, Manjari Garg, Shinjan Mandal, Saisab Bhowmik, Aditya Jayaraman, Radhika Soni, Kenji Watanabe, Takashi Taniguchi, H R Krishnamurthy, Manish Jain, Sumilan Banerjee, U Chandni, and Arindam Ghosh, Breakdown of semiclassical description of thermoelectricity in near-magic angle twisted bilayer graphene, Nature Communications 13, 1 (2022).
39. Saismit Naik, Mit H. Naik, Indrajit Maity, and Manish Jain, Twister: Construction and structural relaxation of commensurate moiré superlattices, Computer Physics Communications 271, 108184 (2022).
40. Sudipta Kundu, Mit H. Naik, H. R. Krishnamurthy, and Manish Jain, Moiré induced topology and flat bands in twisted bilayer WSe2: A first-principles study, Physical Review B 105, L081108 (2022).
41. Mohapatra, Federrath & Sharma, *Multiphase turbulence in galactic haloes*, MNRAS 514, 3139 (2022).

6.3.2 Conferences and Workshops

1. Balakrishna, N., Mathew, J., & Samanta, A. On late stages of transition in round jets, 12th International Symposium on Turbulence and Shear Flow Phenomena (TSFP12), July 19–22, 2022; Osaka, Japan.
2. Magan Singh, Tumkur Pradeepa Karnick and Kartik Venkatraman (2022). Transonic buffet in the finite span Benchmark Supercritical Wing (BSCW). In: 2022 AIAA Aviation Forum, Chicago, IL, June 27 - July 1, 2022.
3. Adithya Mayya, Tumkur Pradeepa Karnick and Kartik Venkatraman (2022). Shock vortex interactions and transonic buffet over a flexible delta wing. In: 2022 AIAA Aviation Forum, Chicago, IL, June 27-July 1, 2022.
4. O.N.Ramesh et al. Computational Predictions of Transonic Shock-Induced Flow Separation over Sandia Axisymmetric Hump, Symposium on Applied Aerodynamics and Design of Aerospace Vehicles (SAROD 2022), Dec 15–17, 2022, Hyderabad, India.
5. Datta, A., Mathew, J. and Hemchandra, S., "The explicit filtering method for large eddy simulations of a turbulent premixed flame", *Combustion and flame,* 2022, vol. 237, https://doi.org/10.1016/j.combustflame.2021.111862.
6. R. K. Shukla, P. Das & J. B. Freund, "A least-squares constrained sharp-interface method for bubble dynamics," Cavitation & Bubble Dynamics Mini symposium, 19th US National Congress on Theoretical and Applied Mechanics, Austin, Texas, US, June 19 – 24, 2022.
7. R. K. Shukla, M. Sawardekar, P. Das & J. B. Freund, "Adaptive high-resolution interface capturing simulations of bubble growth and collapse dynamics in generalized Newtonian fluids," Cavitation meets Data Science: Advances, applications, and challenges at the interfaces of nonlinear physics, data processing, and machine learning, Göttingen, Germany, June 10 –11, 2022.
8. M. Sawardekar & R.K. Shukla, "An Adaptive Sharp Interface Immersed Boundary Technique for coupled Fluid-Rigid body dynamics", Proceedings of the 9th International and 49th National Conference on Fluid Mechanics and Fluid Power (FMFP) December 14-16, 2022, IIT Roorkee.